IDENTIFICATION OF THE HEDGEHOG PATHWAY AS A NOVEL THERAPEUTIC TARGET IN MALIGNANT GLIOMAS

By

Anuraag Sarangi

Dissertation

Submitted to the Faculty of the

Graduate School of Vanderbilt University

In partial fulfillment of the requirements

for the degree of

DOCTOR OF PHILOSOPHY

in

Neuroscience

December, 2009

Nashville, Tennessee

Approved:

Professor Michael K. Cooper

Professor Chin Chiang

Professor Bruce Appel

Professor Harold L. Moses

Professor Mark deCaestecker

To my wife, Kavitha, and son, Shrey, my eternal sources of love and support,

and

To my parents, Geetanjali and Mrutyunjay, and sister, Ankita,

always smiling, always inspiring

ACKNOWLEDGEMENTS

I would like to thank my advisor, Dr. Michael Cooper, for his guidance, support and encouragement throughout these years of my graduate studies. Working with him has enabled me to learn invaluable skills that will always help me throughout my career – perseverance, keen observation, attention to detail, constant pursuit of ideas, succinct and effective communication.

My dissertation committee members, Dr. Chin Chiang, Dr. Bruce Appel, Dr. Hal Moses and Dr. Mark deCaestecker, were extremely helpful in generating ideas and providing direction towards the completion of my project. I thank them for their constructive feedback and support.

I would like to thank the wonderful colleagues in my lab, especially Gerardo Valadez, Vandana Grover and Sarah Z. Rush, who provided a nurturing and friendly environment where I could carry out my research. My most memorable experiences at Vanderbilt consist of working with such a wonderful team of colleagues. In addition, I want to thank collaborators in the Departments of Neuropathology, Neurosurgery, and Infinity Pharmaceuticals for their discussions and technical support. I would also like to thank the faculty and staff of the Vanderbilt Neuroscience Program who have always been supportive of my decisions and encouraged me to pursue my individual research interests.

And foremost, I would like to thank my family, especially my wife, Kavitha, my son, Shrey, and my parents. Their constant encouragement and support has enabled me to accomplish this goal. They are the source of my inspiration, motivation and strength. I will always be grateful that I have them by my side.

TABLE OF CONTENTS

Page

LIST OF TABLES

LIST OF FIGURES

Figure Page

LIST OF ABBREVIATIONS

AA	Anaplastic Astrocytoma
BMP	Bone morphogenetic protein
CNS	Central nervous system
CSC	Cancer stem cells
EGF	Epidermal growth factor
EGL	External granular layer
FGF	Fibroblast growth factor
GEMM	Genetic engineered mouse models
GBM	Glioblastoma multiforme
HGG	High grade glioma
Hh	Hedgehog
H&E	Hematoxylin and Eosin
IGL	Internal granular layer
NOD/SCID	Non obese diabetic / severe combined immuno-deficiency
PK/PD	Pharmacokinetics / Pharmacodynamics
PL	Purkinje layer
SAG	Smoothened agonist
SANT	Smoothened antagonist
Shh	Sonic hedgehog
SGZ	Sub granular zone
SVZ	Sub ventricular zone
VNT	Ventral neural tube

INTRODUCTION

Gliomas are the predominant type of primary tumor found in the central nervous system (CNS). These tumors are highly invasive and notoriously refractory to current therapies. Patients diagnosed with a malignant glioma face a dismal prognosis that has remained relatively unchanged in the last three decades. A dire need exists to discover more effective therapies. A promising novel approach to glioma therapy is based upon modulating molecular mechanisms that regulate cell types critical for tumor growth. Recent identification of cancer stem cells that initiate and maintain tumor growth in gliomas has prompted investigation into the molecular signaling pathways that regulate this unique cell type. The Hedgehog (Hh) signaling pathway regulates stem cells and is activated in several cancer types. Prompted by the role of Hh signaling in regulating neural stem cell self-renewal, we investigated the potential role of the pathway in glioma growth. To address this question, we evaluated the status of Hh signaling in primary gliomas. Furthermore, we tested our hypothesis that Hh signaling regulates glioma growth in a relevant preclinical model.

CHAPTER I

REGULATORY MECHANISMS IN GLIOMA BIOLOGY

Gliomas

Primary gliomas account for more than 40% of tumors of the central nervous system (Kleihues et al 1995). World Health Organization (WHO) classification of gliomas is based on two factors, (i) the predominant cell type found in the tumor, or phenotype, and (ii) grade of malignancy (I to IV) that is assigned based on extent of aggressive, proliferative, and necrotic features within the tumor (Kleihues et al 1995). Table 1.1 summarizes the classification of gliomas based on these two factors along with pathological features. For example, a glioma that primarily consists of cells resembling astrocytic morphology and demonstrates a moderate level of proliferation in the tumor could receive a WHO classification of a Grade II Astrocytoma. This type of classification serves as a prognostic indicator and aids treatment strategies. Grade I pilocytic astrocytomas can consist of diffuse cells arranged in a fibrillary pattern amidst extensive endothelial proliferation. Grade II oligodendroglioma displaying the characteristic “fried-egg” appearance. Grade III anaplastic astrocytoma tend to show cellular atypia and poorly differentiated cells. A grade IV GBM typically contains heterogenous groups highly proliferative cells that are seen surrounding regions of neo-vasculature and necrosis. In less than 5% of GBM cases, grades II or III astrocytomas progress to form grade IV GBM. These tumors are hence classified

as secondary GBM, but are molecularly and clinically distinct from primary GBMs.

Molecular biology of gliomas

Distinct molecular profiles differentiate gliomas from one another (Holland 2001). For example, a characteristic feature of oligodendrogliomas is chromosomal 1p/19q loss-of-heterozygosity (LOH) that leads to deletion of putative tumor suppressor genes (Reifenberger et al 1994). Oncogenic amplifications of genes, such as EGFR and PDGFR-A, are a rare occurrence in oligodendrogliomas. However, these genes are frequently found amplified in astrocytomas. PDGFR-A overexpression and p53 deletion are early oncogenic events in low-grade astrocytomas. Further loss of Rb gene and CDK4 amplification can lead to anaplastic changes in astrocytomas (Mason and Cairncross 2008). Several gene alterations are commonly found in GBMs including EGFR and EGF ligand amplification, loss of chromosome 10q and mutations in the tumor suppressor gene PTEN. Primary GBM rarely present with a p53 mutation - a hallmark feature that distinguishes them from secondary GBM (Ohgaki et al 2004). Another important distinction between primary and secondary GBMs that has recently emerged is the presence of mutations in the isocitrate dehydrogenase 1 (IDH1) and IDH2 genes (Yan et al 2009). The mutant form of IDH1 gene is found in more than 70% of grades II and III astrocytomas, oligodendrogliomas, and secondary GBMs, and is considered to be an early tumorigenic event (Watanabe et al 2009). Primary GBMs rarely (5%) expressed the mutant form. This evidence

further reinforced the notion of disparity between primary and secondary GBM at a genetic and clinical level.

Therapies

Current therapies include surgical intervention followed by a regimen of radiotherapy and/or chemotherapy. Surgery is the first option for most gliomas, although pilocytic astrocytomas are the only group that is cured by surgical intervention alone. In the case of malignant gliomas (grades III and IV), surgical resection does not seem to provide any increased survival benefit for patients (Sanai and Berger 2008). The highly infiltrative nature of malignant gliomas renders surgery ineffective in removing all tumor cells. Even total resection of malignant gliomas, sometimes by way of a cerebral hemispherectomy (Hillier 1954), has proven futile in preventing recurrence of disease (Lacroix et al 2001). Thus, surgical intervention provides limited benefits for patients, such as global symptomatic relief due to release of local compression at the site of the tumor (Pang et al 2007). Additionally, surgery allows inspection of the resected tissue by a pathologist to identify phenotypic features that can aid more accurate diagnosis and treatment strategies.

Radiation therapy (Laperriere et al 2002) and chemotherapeutic agents (Kreisl 2009), such as the alkylating agent Temozolomide (TMZ), provide only palliative benefits that are short-lived. Post-operative radiotherapy is commonly used in newly diagnosed malignant gliomas (Keime-Guibert et al 2007, Kristiansen et al 1981, Walker et al 1980) since it shows a small statistically

significant survival benefit compared with no radiotherapy alone. The survival benefits depend on the method and dosage of radiation. No significant survival benefit differences were observed between whole brain radiation and local field radiation (Kita et al 1989). However, increasing the dose of radiation to 60 Gy in 30 fractions over 45 Gy in 20 fractions did provide a small improvement in survival for the higher dose (Bleehen and Stenning 1991), albeit at a cost of increased detrimental quality-of-life especially for older patients.

The use of chemotherapeutic agents as adjuvant to radiotherapy has yielded the most promising results for aggressive treatment of glioblastomas thus far (Nieder et al 2009). For example, a recent study demonstrated that the combination of TMZ and radiation treatment resulted in a marginal increase in survival of about 3 months for patients suffering from a grade IV GBM (Stupp et al 2005, Stupp et al 2009). Temozolomide (*Temodar/Temodol*) is an oral alkylating agent that damages DNA and triggers death of tumor cells (Villano et al 2009). Some tumor cells, however, synthesize MGMT enzyme that repairs this type of DNA damage. Thus, tumors treated with MGMT inhibitors or that demonstrate epigenetic silencing of MGMT gene are more responsive to Temozolomide treatment (Hegi et al 2005). Conversely, presence of MGMT can predict poor response to Temozolomide (El-Jawahri et al 2008, Friedman et al 1998).

Treatment benefits against gliomas vary based on several factors. As illustrated in Table 1.1, grade I gliomas are generally curable with surgical resection, while median survival time for a patient with a grade II glioma is

between 10-15 years. Grade III glioma patients have a median survival time of 5-10 years even after aggressive treatment. However, grade IV glioma patients contend with a dismal prognosis of less than 12 months from surgical resection. These statistics have remained relatively unchanged in the past three decades. Novel treatment modalities that could provide greater benefit to patients are actively investigated and include VEGF inhibitors such as Genentech's Bevacizumab (Avastin) to inhibit new blood vessel growth (Norden et al 2008), EGFR inhibitors that modulate an often-overexpressed tyrosine kinase receptor pathway in gliomas (Karpel-Massler et al 2009), and Gliadel wafers to provide localized and controlled release of chemotherapeutic agents to the tumor site (McGirt et al 2009). Extent of efficacy achieved by these treatments is still under investigation in clinical trials.

Table 1.1. Phenotypic, pathological and prognostic features of gliomas

Phenotype	*Grade*	*Pathological Features*	*Median Survival*
Pilocytic Astrocytoma	I	Few mitotic figures; endothelial proliferation	Curable
Astrocytoma, Oligodendroglioma	II	Well differentiated cells; low to moderate mitotic activity; generally infiltrative	10-15 years
Astrocytoma, Oligodendroglioma	III	Anaplastic features; poorly differentiated cells; histological evidence of malignancy in the form of increased mitotic activity	2-5 years
Glioblastoma Multiforme (GBM)	IV	High mitotic index; vascular proliferation; necrotic areas	1 year

Cancer stem cell hypothesis

Conventionally used treatment modalities however aim to eliminate the highly proliferative component of the tumor mass with multiple rounds of cytotoxic treatments. These approaches do not take into consideration the heterogeneity of cell types in gliomas or the efficacy of selectively targeting specific cells with greater propensity for tumorigenesis and resistance (Frosina 2009).

In recent years, an alternate view of tumorigenesis has emerged which incorporates concepts from stem cell biology and developmental biology discipline. This paradigm, as illustrated in Figure 1.1, contrasts with the aforementioned stochastic model of gliomas and suggests that cells within a tumor are part of a hierarchy: multi-potent cancer stem cells that give rise to transit-amplifying progenitor cells that propagate and become differentiated tumor cells (Jordan et al 2006). Cancer stem cells (CSC) are characterized by two unique properties: (i) the ability to initiate and propagate tumor, and (ii) the ability to self-renew and give rise to transit-amplifying progenitors and differentiated tumor cells.

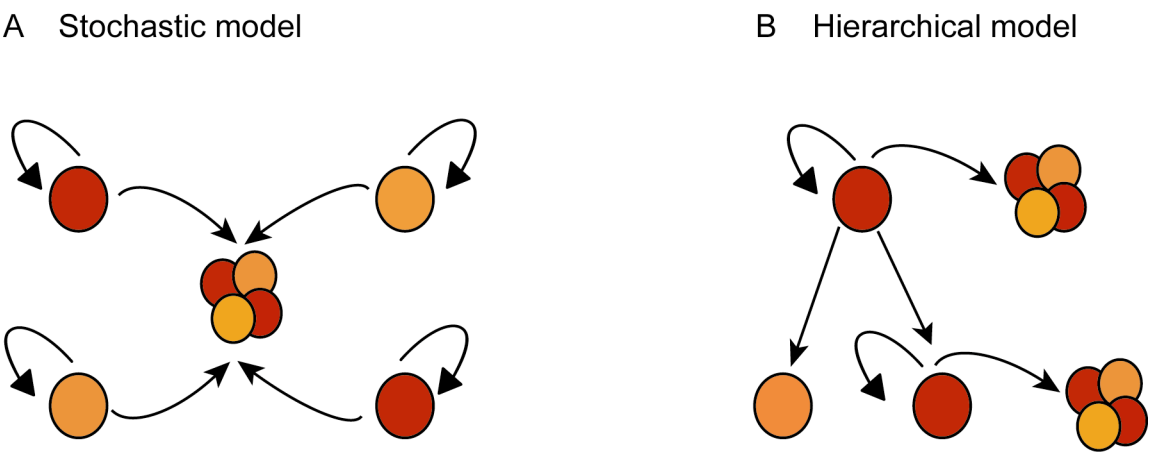

Figure 2.1. Stochastic and hierarchical models of tumor growth. (A) A stochastic model assumes that even in a heterogenous tumor, each cell within the tumor has equal ability to initiate tumor formation. (B) Conversely, the hierarchical model proposes that only a small subpopulation of cancer stem cells possess the ability to self-renew, initiate tumor formation and give rise to differentiated tumor cells.

This CSC hypothesis provides a framework to develop new treatment paradigms. The implications of this framework are enormous. Theoretically, CSC possess the ability to initiate and maintain growth of a tumor. CSC have been found in the tumor core and invasive cell populations of many solid tumors (Hermann et al 2007, Puglisi et al 2009. Empirically, CSC have been shown to express elevated levels of multi-drug transporter proteins that can efflux out chemotherapeutic agents {Donnenberg, 2005 #206). CSC also resist radiotherapy by employing DNA repair mechanisms more effectively (Bao et al 2006a). Therefore, CSC are likely candidates that escape conventional treatment modalities and contribute to patient relapse. Thus, it is possible that eliminating CSC from the tumor can achieve maximum benefit from treatment (Park et al 2009).

The first step towards developing targeted therapy against CSC is to isolate these cells and study their molecular characteristics. Since these cells share many characteristics with embryonic and adult stem cells, their isolation has relied on methodologies used to isolate embryonic and adult stem cells. In the case of CSC from brain tumors, two primary methods have been utilized: (i) culturing cells in conditions favorable to the maintenance of stem cells, and (ii) using unique cell surface markers to sort for stem cells. Borrowing from neural stem cell literature, growing tumor cells in culture conditions favorable for stem cell maintenance, i.e. without the addition of serum and in the presence of growth factors, allows stem cells to cluster together as spheres and proliferate. These spheres consist of multi-potent stem cells, lineage restricted progenitor cells and differentiated cells (Deleyrolle and Reynolds 2009, Reynolds and Weiss 1992).

Similarly, glioma cells cultured in stem cell medium are termed *gliomaspheres* (GS) (Ehtesham et al 2007). Prospective isolation of stem cells in this manner allows the cells to be maintained in culture medium for subsequent *in vitro* experiments. The second method for stem cell isolation relies on separating cells that express specific stem cell markers. Ideally, these markers should be restricted to the stem cell only and should be present on the cell surface to allow for magnetic or fluorescence based separation. Borrowing from the hematopoeitic literature, CD133 is the best-known cell surface marker that has been used to isolate cancer stem cell from gliomas (Singh et al 2003). CD133 (also known as Prominin 1 or AC133) is a novel five transmembrane domain protein (Yin et al 1997). In seminal studies conducted by Peter Dirk's group (Singh et al 2004b), putative CSC were isolated using CD133 expression from gliomas and medulloblastomas. These cells demonstrated properties of tumor-initiation, self-renewal, propagation and multipotency. CD133+ cells isolated from primary human gliomas xenotransplanted in immunocompromised mice initiated tumor formation and faithful recapitulation of patient disease. In contrast, cultured cell lines maintained over long passages are immortalized and lose their ability to faithfully recapitulate cardinal features of the disease (Lee et al 2006).

Using these techniques to isolate putative CSC has allowed investigation into their behavior at a molecular level and devise treatment paradigms specifically targeting these cells. Two approaches that have been reported with success include (i) affecting CSC ability to draw nutrients from new blood vessels

by eliminating neo-angiogenesis (Bao et al 2006b), and (ii) terminally differentiating these cells to curb their tumorigenic potential (Piccirillo et al 2006).

Rich's group demonstrated that administration of VEGF inhibitor, Avastin, led to significant decrease in the development of new blood vessels affecting CSC viability and tumorigenic potential (Bao et al 2006b). As a corollary, Gilbertson and colleagues presented evidence to show that CSC preferentially reside near tumor blood vessels that form a supportive niche (Calabrese et al 2007). Thus, inhibiting new blood vessel growth may be one effective measure for eliminating CSC.

Vescovi's group (Piccirillo et al 2006) presented one of the most compelling pieces of evidence to illustrate the efficacy of a treatment strategy against CSC. This strategy relied on exposing CSC to a pro-differentiating signal – bone morphogenetic protein (BMP). Upon exposure to BMP, CSC were induced to differentiate and lost their ability to initiate tumor in xenotransplanted mice. BMP is a signaling molecule crucial during embryonic development and implicated in cancer (Blanco Calvo et al 2009). The success of this strategy prompts investigation into other developmental signaling pathways that may also be required for stem cell maintenance and tumor growth. The Hedgehog (Hh) signaling pathway is one such pathway.

Hedgehog signaling pathway during development and disease

The Hh pathway is a crucial cell signaling mechanism with widespread roles during embryogenesis. The Hh gene was first discovered by (Nusslein-Volhard

and Wieschaus 1980) while conducting functional gene mutation analysis in the Drosophila. Later, three mammalian orthologs of the Hh protein were discovered: Sonic hedgehog (Shh), Indian hedgehog (Ihh) and Desert hedgehog (Dhh) (Bitgood et al 1996, Echelard et al 1993, Ingham and McMahon 2001, Pathi et al 2001, St-Jacques et al 1999). In the CNS, the Hh pathway regulates some of the critical functions of during development and tissue homeostasis, including the self-renewal mechanisms of quiescent stem cells, the proliferation of the external granule neuron precursors in the developing cerebellum in a time and position dependent manner, and the patterning of the ventral neural tube (Rubin and de Sauvage 2006).

In the adult neurogenic regions of the mammalian brain, namely the sub-ventricular zone (SVZ) and the sub-granular zone (SGZ), the Hh pathway has been demonstrated to be important in self-renewal and proliferation of precursor neural stem cells (Ahn and Joyner 2005, Lai et al 2003, Machold et al 2003, Palma et al 2005) as illustrated in Figure 1.2c. Hh regulates the B-type stem cells and C-type transit-amplifying cells eventually giving rise to A-type neuroblast cells which migrate towards the olfactory bulb following the rostral migratory stream.

During late embryogenesis and early postnatal life, Hh signal is secreted from Purkinje neurons in the developing cerebellum. Hh induces the proliferation of external granule neuron precursors (Figure 1.2b) that migrate across the Purkinje neuron layer and establish the internal granular layer (Dahmane and Ruiz i Altaba 1999, Wechsler-Reya and Scott 1999).

Hh signal secreted from the notochord acts as a morphogen and patterns the lower ventral neural tube in a distinct, gradient specific mechanism as shown in Figure 1.2A. The distance separating a Hh generating cell from a receiving cell during this process of cell non-autonomous signaling determines the amount of Hh binding and subsequent activation of the pathway. The activated pathway induces segmental expression of specific combinations of transcription factors that determine cell fate throughout the neural tube. For example, in the ventral neural tube, the cells closest to the source of Hh signaling express NKX2.2 and differentiate to become p3-domain interneurons. The cells slightly further away from the source express Olig2 and give rise to pMN-domain motor neurons (Rowitch 2004). This coordinated emergence of multiple cell types in the neural tube is partly determined by the extent of Hh signaling. Thus, Hh signaling serves as a critical regulator of cell function and fate in mammalian embryonic development and adult tissue maintenance.

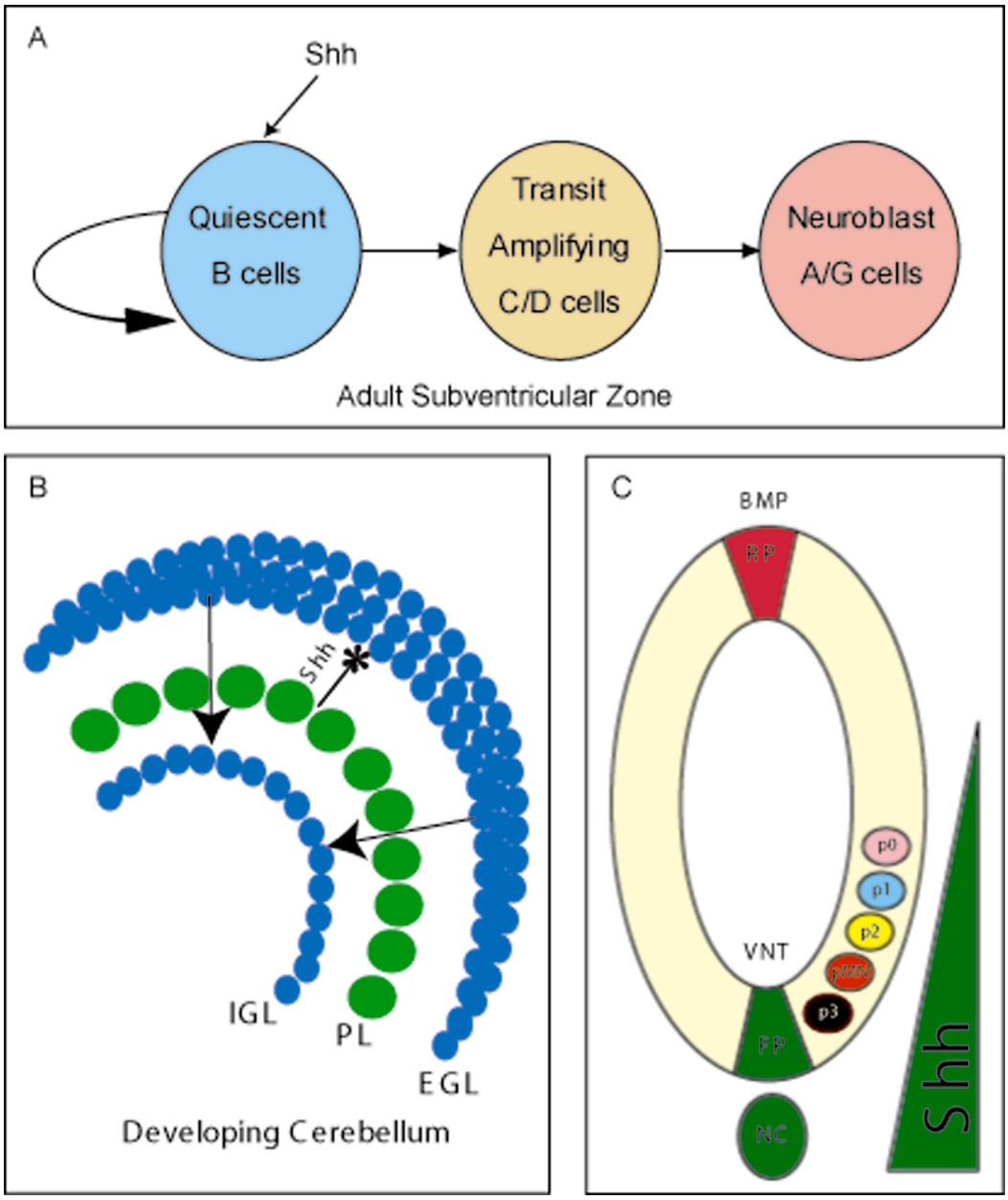

Figure 1.2. Roles of Hedgehog signaling in mammalian CNS. (A) Sonic hedgehog (Shh) signaling regulates the self-renewal properties of quiescent stem cells present in the adult subventricular zone that give rise to rapidly dividing transit amplifying cells and subsequently migrating neuroblasts. (B) During late embryogenesis and early postnatal development, secretion of Shh by purkinje neurons aids the proliferation of granule cell precursors in the external granular layer that subsequently migrate inwards to form the internal granular layer. (C) Shh plays a significant role in patterning the developing neural tube. Shh secreted from the notochord and floor plate diffuses in a gradient to determine the fate of cells at various domains of the ventral neural tube. p3, p2, p1, and p0 domains give rise to interneuron populations while pMN domain gives rise to motor neurons and oligodendrocytes. Abb. IGL internal granular layer, EGL, external granular layer, PL, purkinje layer, VNT, ventral neural tube, NC, notochord, FP, floor plate, RP, roof plate, BMP, bone morphogenetic protein, Shh, sonic hedgehog.

Hh signal transduction cascade induces the expression of several important genes. The full length Hh protein in the generating cell undergoes auto-cleavage to produce a signaling domain that is dual-lipid modified and secreted from the cell surface (Pepinsky et al 1998, Porter et al 1996a, Porter et al 1996b, Wendler et al 2006). Secreted Hh protein binds to its 12-transmembrane receptor Patched (PTCH) to release its inhibition on Smoothened (SMOH), a 7-transmembrane protein also on the cell surface. This loss of inhibition on SMOH induces activation of downstream signal transduction proteins and repression of negative regulators of the pathway, such as Suppressor of Fused (SUFU). Eventual activation of the GLI transcription factors initiate transcription of Hh gene targets including, Nmyc and CyclinD1, along with PTCH and GLI1 themselves. The resulting increase in PTCH protein expression on the cell surface allows sequestration of Hh protein near the source of the signal and acts as a gradient regulator in a negative-feedback loop (Chen and Struhl 1996). Several small molecule modulators have been synthesized to act at the level of Smoothened to activate or inhibit the Hh pathway (Chen et al 2002a, Chen et al 2002b, Taipale et al 2000) (see (Rubin and de Sauvage 2006) Nature Reviews for a summary). The best-characterized inhibitor of the pathway is Cyclopamine, a plant alkyloid compound that acts at the level of SMOH and is thought to compete for the endogenous binding site regulated by PTCH (Chen et al 2002a, Cooper et al 1998).

Aberrant regulation of the Hh pathway is implicated in many disease states including holoprosencephaly (Chiang et al 1996, Roessler et al 1996),

diabetic neuropathy (Calcutt et al 2003) and many types of cancers in the body (Beachy et al 2004). Interestingly, both ligand-independent and ligand-dependent mechanisms of Hh pathway activation have been demonstrated. The pathway is known to play a key role in the growth of about 30% of sporadic medulloblastomas, a pediatric brain tumor commonly found in the posterior fossa. Loss-of-function mutations in PTCH (Berman et al 2002, Chidambaram et al 1996, Johnson et al 1996, Unden et al 1996) and SUFU (Taylor et al 2002), or gain-of-function mutations in SMOH (Reifenberger et al 1998) result in constitutive ligand-independent activation of the pathway in medulloblastoma cells. Ligand-dependent pathway activation has been demonstrated in lung (Watkins et al 2003), foregut (Berman et al 2003), pancreatic (Thayer et al 2003) and metastatic prostate tumors (Fan et al 2004, Karhadkar et al 2004, Sanchez et al 2004). Production of the ligand in the tumor cells induces pathway activity and proliferative response. More recently, Fred de Sauvage's group provided evidence to suggest that in several epithelial cancers, ligand-dependent Hh pathway activity is seen in the stromal component of the tumor and not within tumor cells. Hh signal generated by the tumor cells serves to activate pathway response in the stroma that in turn secretes tumor support factors such as VEGF and IGF (Theunissen and de Sauvage 2009, Yauch et al 2008). Thus, aberrant Hh pathway activity can take many forms leading to the development of or supporting the growth of cancer in several tissue types.

Hedgehog pathway in gliomas

Several studies have presented evidence for Hh pathway activation in a broad range of glioma subtypes (Bar et al 2007, Clement et al 2007, Dahmane et al 2001, Ehtesham et al 2007, Katayam et al 2002, Sarangi et al 2009, Xu et al 2008). Contrary to other reports however, our studies indicate that the Hh pathway is activated in only distinct glioma subtypes, namely grades II and III astrocytomas and oligodendrogliomas but not in grade IV *de novo* GBM (Ehtesham et al 2007, Sarangi et al 2009). This distinction is important to note when developing clinical trials based on using Hh inhibitors to treat gliomas. Evaluating targeted intervention of the Hh pathway in grades II and III gliomas will ensure that maximum therapeutic benefit is achieved in those tumor types where pathway activity has been shown to be involved in tumor growth. On the other hand, a failed clinical trial based on Hh pathway inhibition in GBM can be misinterpreted as a lack of therapeutic efficacy in gliomas in general.

Moreover, although other reports demonstrated survival benefit of pathway inhibition in mouse models of gliomas, they suffer from several caveats. The earliest studies (Dahmane et al 2001, Katayam et al 2002) only provided suggestive evidence based on gene and protein expression that the Hh pathway could be activated in gliomas, but did not elaborate on the biological role of Hh signaling in gliomas. One recent study xenografted a GBM cell line that had been transduced with a lentiviral vector to suppress Smoothened expression, and reported increased survival that did not reach statistical significance (Clement et al 2007). Another study utilized a GBM cell line transfected with GLI1 siRNA prior

to transplantation and reported decreased tumor volume, but did not measure survival (Xu et al 2008). A third study demonstrated that a GBM cell line treated with 10 uM cyclopamine failed to engraft in athymic nude mice (Bar et al 2007). However, at this dose, cyclopamine also inhibits cholesterol synthesis and thus cell growth in culture independent of pathway status (Beachy et al 1997). These studies suggest that Hh signaling may regulate GBM growth, but suffer from several major limitations: (i) cultured cells were manipulated prior to transplantation, and thus it is not known whether Hh pathway inhibition in an established glioma would modulate growth and survival; (ii) cultured glioma cell lines are known to undergo genetic changes during culture, particularly in the presence of serum but also using stem-cell culture techniques (Lee et al 2006); and (iii) a single glioma cell line was assayed in each study and thus it is not clear to what degree these data would apply to the broader array of malignant gliomas. Thus, it is imperative to have a clear understanding of which specific glioma subtypes possess an operational Hh pathway and establish the biological roles of Hh signaling in glioma tumorigenesis. Chapter II in this dissertation explores Hh pathway activation within a broad range of gliomas (data published in Ehtesham et al 2007) and demonstrates the mechanism of pathway activation. Chapter III demonstrates the establishment of a relevant pre-clinical xenotransplantation mouse model for gliomas that are used for subsequent studies illustrated in Chapter IV to address in the biological role of Hh signaling in gliomas (data published in Sarangi et al 2009). Chapter V reflects on the implications of our work and presents directions for future research.

CHAPTER II

LIGAND-DEPENDENT ACTIVATION OF THE HEDGEHOG PATHWAY IN DISTINCT GLIOMA SUBTYPES

Abstract

The Hedgehog (Hh) signaling pathway regulates progenitor cell fate in embryogenesis and tumorigenesis of multiple organ systems. We have investigated the activity of this pathway in adult gliomas, and demonstrate that the Hh pathway is operational and activated within grades II (GII) and III (GIII), but not IV (GIV) gliomas. Furthermore, our studies reveal that pathway activity and responsiveness is confined to progenitor cells within these tumors. Additionally, we demonstrate that Hh signaling in glioma progenitor cells is ligand-dependent and provide evidence documenting the in vivo production of Sonic hedgehog (Shh) protein at the tumor margin. These findings suggest a regulatory role for the Hh pathway in progenitor cells within GII and GIII gliomas, and the potential clinical utility of monitoring and targeting this pathway in these primary brain tumors.

Introduction

Gliomas are the most common primary brain tumors and are divided into four clinical grades. World Health Organization (WHO) grades II–IV are intractable to current therapies and the 5-year survival rate is 33% (American Cancer Society, (2004)). Recently, progenitor or stem-like cells have been isolated from primary

brain tumors (Galli et al 2004, Hemmati et al 2003, Lee et al 2006, Singh et al 2003, Singh et al 2004b), and termed 'cancer stem cells' (CSC) (Singh et al 2004a). The CSC hypothesis suggests that stem cells constitute a small fraction of the tumor and give rise to partially or fully differentiated cell types comprising the majority of the tumor. The activation and operational status of signaling pathways in brain tumor CSC remain unknown, and their identification and characterization could yield critical targets for new therapeutic avenues. One such mechanism may be the Hedgehog (Hh) pathway, whose activity is required for the growth and maintenance of tumors of the cerebellum, skin, lung, foregut and prostate (Beachy et al 2004). The Hh pathway regulates progenitor cell proliferation within these tissues, and in this context, its activity has been linked to tumorigenesis. Prior reports concerning Hh signaling and gliomas have yielded conflicting results (Dahmane et al 2001, Katayam et al 2002), and thus the operational status of the pathway in gliomas remains to be determined.

Prompted by a requirement for Hh signaling in the regulation of cerebral neural progenitor cells (Ahn and Joyner 2005, Lai et al 2003), we investigated the activity of this pathway in gliomas. Our studies indicate that the Hh pathway is activated within a significant portion of grade II (GII) and grade III (GIII) gliomas, but not in grade IV (GIV) de novo glioblastoma multiforme (GBM). We provide evidence that the pathway is activated within tumor cells that express the proliferation marker Ki67 and progenitor cell related proteins Bmi-1 and Olig2. In primary glioma cell lines, we demonstrate that Hh pathway activity is ligand-

dependent and that pathway responsiveness can be measured under culture conditions that favor progenitor cell maintenance but not differentiation.

Taken together, these mechanistic data provide evidence that the Hh pathway is activated in progenitor cells within GII and GIII gliomas, and support a role for Hh signaling in these tumors.

Materials and methods

Tissue procurement

Brain tissues were obtained at Vanderbilt Medical Center in accordance with an institutional review board approved protocol. A portion of each tumor was sent to pathology for diagnoses and remaining tissue to a tumor bank for analyses. Primary brain tumors were phenotyped and graded as described (Kleihues et al 1995, Kleihues et al 2002).

Immunohistochemical analysis of tumors

Immunodetection was performed with the following antibodies: PTCH-1 (1:200; Santa Cruz Biotechnologies, Santa Cruz, CA, USA, G19 Lot No. J2505), Shh (1:200; Santa Cruz Biotechnologies, H160), Ki67 (1:10; Chemicon, Temecula, CA, USA), Bmi-1 (1:50; Serological Corporations, Billerica, MA, USA), Olig2 (1:250; Chemicon), GFAP (1:1000; Chemicon) and NeuN (1:500; Chemicon). Sequential double-antibody labeling was performed as described (Becher et al 1998). In situ hybridization for Shh was performed as described (Oh et al 2005), with digoxigenin-labeled riboprobe synthesized from Shh cDNA (forward

5’-GCGGCACCAAGCTGGTGAAG-3’ and reverse

5’-GGTGAGCAGCAGGCGCTCGC-3’).

Western immunoblot analysis of tumors

PTCH (G19, 1:200) or human a-actinin (1:200; Chemicon) immunoblotting in snap-frozen tumor samples was performed as described (Chen et al 2002a).

RNA extraction, cDNA synthesis and QRT–PCR

Total RNA was extracted from brain tissue with the RNeasy Mini Kit (QIAGEN), and Shh-LIGHT Z3 cells with the RNAqueous 4-PCR kit (Ambion). Genomic DNA was removed (RNase-Free DNase Set, QIAGEN) and purified RNA quantified (RiboGreen RNA Quantitation Kit, Molecular Probes). Single-stranded cDNA was synthesized with oligo(dT) and random hexamer primers (iScript cDNA Synthesis Kit, Bio-Rad). For negative controls, reverse transcriptase was omitted from the synthesis reaction (-RT). QRT-PCR was performed in triplicate for each sample and on the corresponding -RT control with SYBR Green Supermix (Bio-Rad), cDNA template, and primers for PTCH, GLI1, and GAPDH. For standard curves, QRT-PCR was performed on serial dilutions of a cDNA mixture; 40% Universal Human Reference RNA (Stratagene), 40% Total Brain RNA (Clontech), and 10% total RNA each from BT16, and BT17. PTCH, GLI1 and GAPDH quantities were determined according to the standard curve method (User Bulletin #2, PE Applied Biosystems). Calibrator cDNA (Universal Human Reference RNA, Stratagene) was included in every reaction, for comparisons among experiments.

PTCH expression levels in each tumor grade were analyzed using one-way ANOVA of log-transformed data, followed by post hoc comparisons to control samples by the least significant difference method.

Primary glioma-derived cell culture

Tumor samples were dissociated (Accutase, ICT), and purified with a discontinuous Percoll (Sigma) gradient (35% and 65%). For standard cultures, cells were plated in DMEM/F12, 10% FBS, and 1X Penicillin-Streptomycin (Invitrogen). For GS, cells were plated in non-tissue culture treated polystyrene flasks (BD-Falcon) in Neurobasal medium (Invitrogen) with B-27 supplement (Invitrogen), 2 µg/mL heparin (Sigma), 2 mM L-Gln (Invitrogen), 20 ng/mL LIF (Chemicon), 20 ng/mL EGF (ProSpec TechnoGene), 20 ng/mL FGFb (ProSpec TechnoGene), and 1X Penicillin-Streptomycin (Invitrogen). Cells were plated at densities of 3-5 x 104 viable cells/cm^2.

Reverse transcriptase (RT)–PCR

cDNA was amplified with intron-spanning primers specific for nestin, Bmi-1, Musashi-1, Sox-2, CD133 and GAPDH (Supplementary Table 1) for 40 PCR cycles and visualized in 2% agarose/TAE gels stained with ethidium bromide. The identity of each amplification product was confirmed by sequencing.

Hh-signaling assays in primary glioma cell cultures

Standard cell lines or GS were cultured in triplicate for 36–42 h either alone, with 5 mM cyclopamine, 100 nM SANT1, 5 nM ShhNp (purified, fully lipid-modified Shh protein) (Taipale et al 2000) or varying doses (5–500 nM) of SAG. Confluent standard cell lines were cultured in Dulbecco's modified Eagle's medium/F12 with 0.5% fetal bovine serum and GS in neurobasal medium with B-27 supplement, 2 mg/ml heparin, 2mM L-Gln, 20 ng/ml LIF, 20 ng/ml EGF, and 20 ng/ml FGFb. PTCH, GLI1 and GAPDH levels were measured by QRT–PCR as described above.

Results

Characterization of Patched protein expression in gliomas

To identify Hh-responsive cells in gliomas, we assayed for expression of the Hh receptor Patched (PTCH; Figure 1). Immunohistochemical staining of 13 gliomas revealed scattered PTCH-positive cells within three GII oligodendrogliomas, one GII astrocytoma and three GIII anaplastic astrocytomas, but not in any of three GIV de novo GBM (Figure 2.2d–l and Supplementary Figure 2.S1A and C). Rare PTCH-positive cells could be seen in only one of three pilocytic astrocytomas (Figure 2.2a–c). Histopathological examination revealed anisokaryosis within PTCH-expressing cells, indicating their malignant phenotype. PTCH protein expression in GII and GIII gliomas was further corroborated by Western immunoblot (Figure 2.2m, lanes 3–6). Conversely, PTCH protein expression was lower in GI and GIV gliomas (Figure 2.2m, lanes 1, 2, 7 and 8).

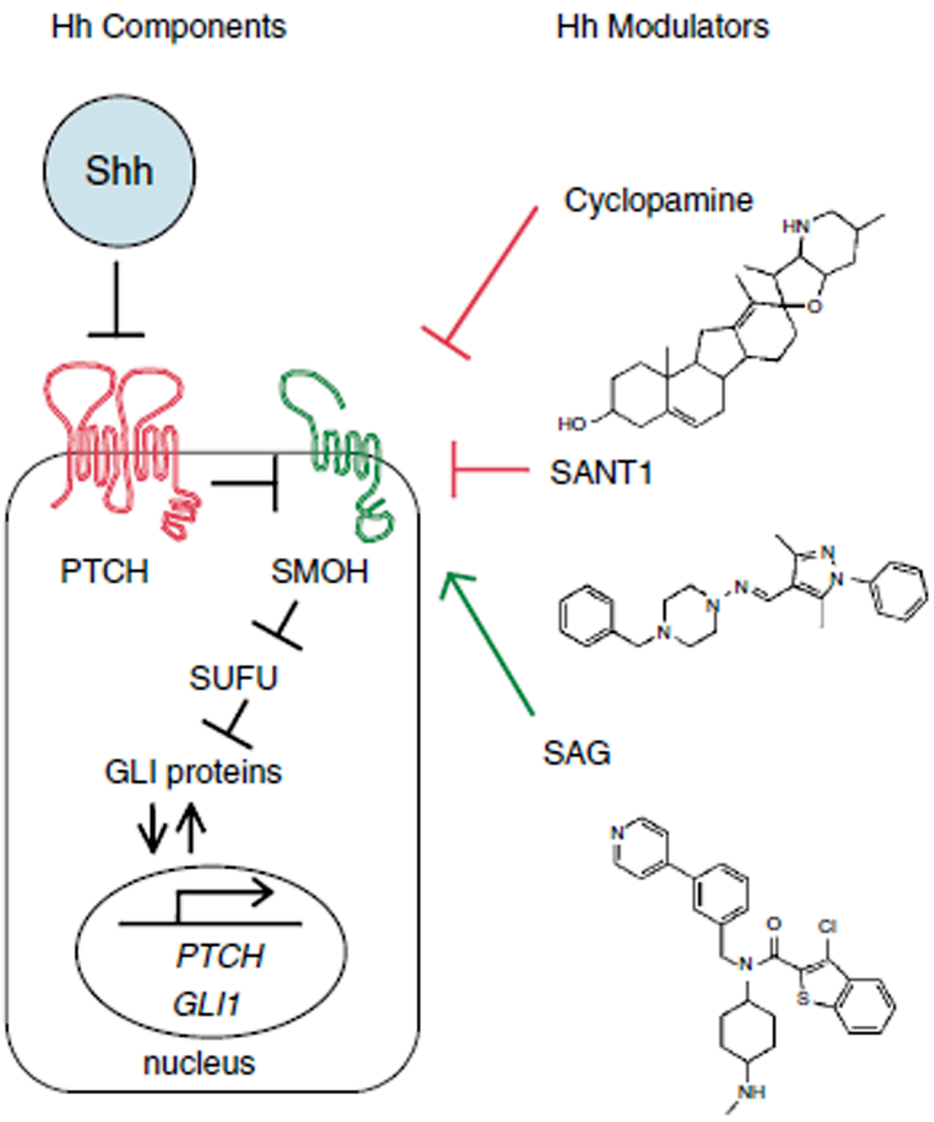

Figure 2.1. Schematic of the Hh pathway and pharmacological modulators. Depicted are Hh pathway components and gene targets PTCH and GLI1. Also shown are small molecule antagonists (cyclopamine and SANT1) and agonist (SAG) that modulate SMOH activity.

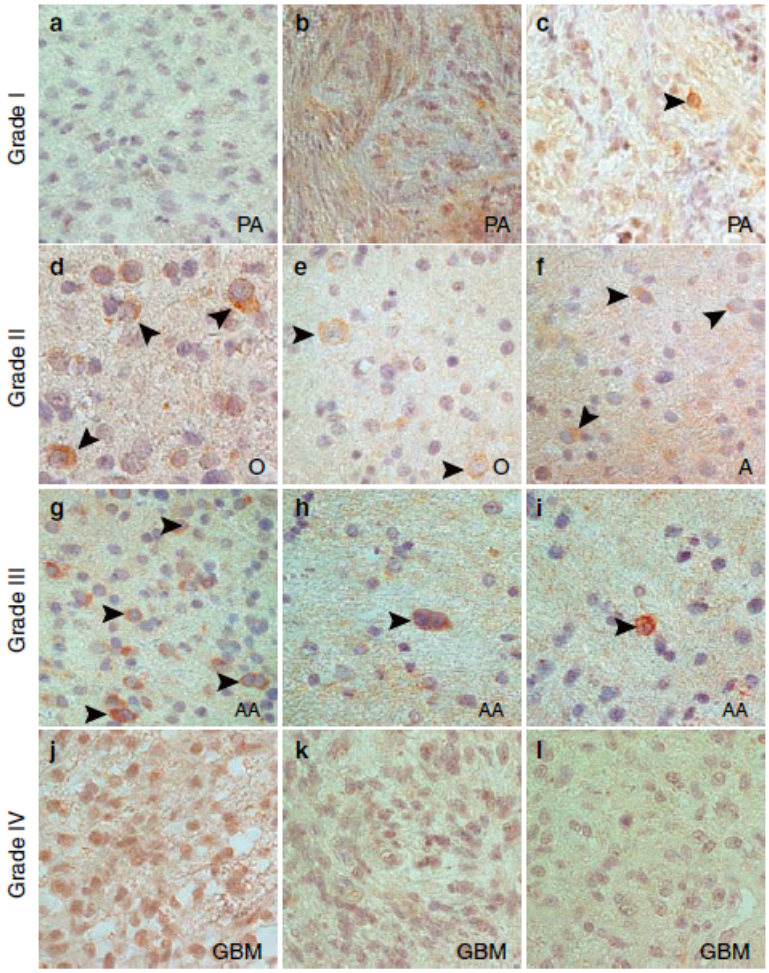

m

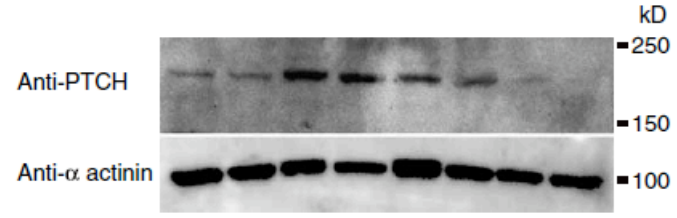

Lane	1	2	3	4	5	6	7	8
WHO Grade	I	I	II	II	III	III	IV	IV
Pathology	PA	PA	O	O	AA	AO	GBM	GBM
PTCH Level	1.1	3.3	6.9	11.0	19.4	10.1	1.0	0.2

Figure 2.2. PTCH protein expression in gliomas. (a–l) Immunostaining revealed PTCH expression (arrow heads) within a subset of neoplastic cells predominantly in GII and GIII gliomas, rarely in PA, and not in GBM. (m) Analysis of PTCH expression levels by immunoblotting and QRT–PCR (PTCH level in bottom row of table) demonstrated the highest levels in GII and GIII gliomas. PA, pilocytic astrocytoma; O, oligodendroglioma; A, astrocytoma; AA, anaplastic astrocytoma; GBM, glioblastoma multiforme.

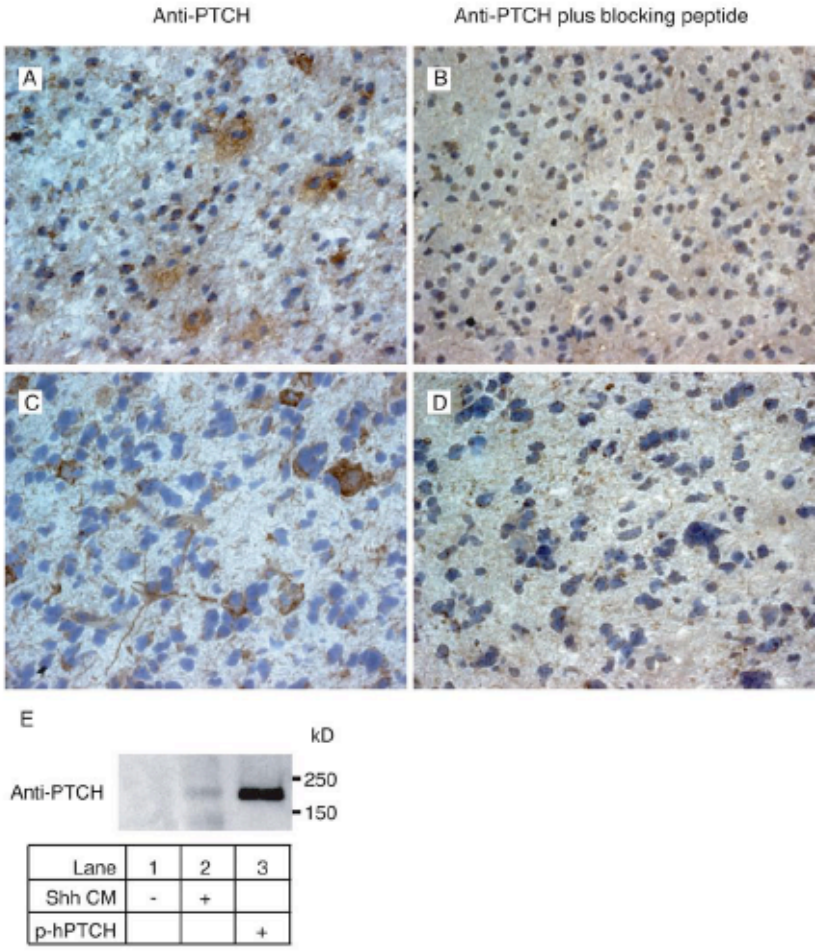

Figure 2.S1. PTCH protein expression in a GII oligodenroglioma andGIII anaplastic astrocytoma. A-D, PTCH immunostaining in frozen tissue sections of a GII oligodendroglioma (A and B) and a GIII anaplastic astrocytoma (C and D) revealed PTCH expression within a subset of cells (A and C). Specificity of PTCH staining is demonstrated by the elimination of signal following pre-incubation of G19 primary antibody was pre-incubated with a 5-fold excess (wt/wt) of blocking peptide (Santa Cruz Biotechnologies, B and D). E, Specificity of PTCH antibodies is further demonstrated by PTCH immunoblotting (H267 antibody) of immunoprecipitates (G19 antibody) from NIH3T3 cells induced with Shh-CM (lanes 1 and 2) and HEK293 cells transfected with a human PTCH expression construct (lane 3). Note, PTCH staining for the anaplastic astrocytoma in C and D is also shown in paraffin section in Figure 2I.

The expression of PTCH within a subset of tumor cells suggests that Hh pathway activity may be confined to a specific population of glioma cell types. To characterize PTCH-expressing cells, we analysed a GII astrocytoma for coexpression of the proliferation marker Ki67 (Figure 2.3a and b) and the stem cell-related marker Bmi-1 (Figure 2.3c and d). By sequential double-antibody labeling, PTCH expression was detected in 23.1±0.5% of the cells (n=13 high-powered microscopic fields; average±s.e.m.). Ki67 staining was observed only in PTCH-expressing cells and was coexpressed in 9.3705% of the PTCH-positive cells (n=8). Bmi-1 was coexpressed in 87.3±2.4% of PTCH positive cells (n=5). These findings suggest that proliferation is confined to PTCH-expressing cells with progenitor features.

PTCH expression is significantly elevated within GII and GIII gliomas

To quantify the differences observed by Western blot analysis of PTCH protein expression in eight gliomas of varying grades, we measured PTCH mRNA levels in these (Figure 2.2m) and 50 other primary brain tumors (Table 2.1). As PTCH is a transcriptional target of the Hh pathway (Figure 2.1), quantitative real-time–polymerase chain reaction (QRT–PCR) measurement of PTCH mRNA levels provides a sensitive method for assessing the degree of Hh pathway activity in tumor-derived tissues and cell cultures (Berman et al 2003, Karhadkar et al 2004). For all samples, PTCH levels were normalized to endogenous glyceraldehyde-3-phosphate dehydrogenase (GAPDH) levels and expressed as the fold-difference relative to a control temporal lobe sample resected from a

patient with epilepsy (sample 1 in Table 2.1). In contrast to control samples, the relative PTCH mRNA levels were 2.09±0.64 in GI (P¼0.346), 6.66±1.31 in GII (P=0.002), 9.26±3.09 in GIII (P=0.003) and 1.15±0.18 in GIV (P=0.808) gliomas (average±s.e.m.), indicating significant elevation of PTCH mRNA levels only within GII (n=12) and GIII (n=12) gliomas. With the exception of a medulloblastoma, low PTCH levels were measured in the other primary brain tumors (samples 56–62 in Table 2.1), and these were not included in our statistical analyses.

Within GII and GIII tumors, elevated PTCH expression was detected in oligodendrogliomas and astrocytomas (Table 2.1 and Figure 2.4). The variability of PTCH levels in GII and GIII glioma samples may indicate that the Hh pathway is activated only in a subset of these tumors, or reflect inherent limitations of the sampling method (see Materials and methods section).

Notably, 21 of the 22 GBM samples in this analysis were clinically de novo, and low PTCH levels in these tumors suggest the following possibilities: (i) the Hh pathway might be activated in de novo GBM as a consequence of PTCH inactivation, (ii) PTCH expression in a CSC population represents a small, and therefore, difficult to measure portion of GBM, or (iii) the pathway is not activated in de novo GBM. To test the first possibility, we measured expression of the Hh gene-target GLI1 (Figure 2.1) by QRT–PCR in an additional set of tissues (Supplementary Figure 2.S2, samples 63–77). In all 11 de novo GBM samples analysed, GLI1 levels were uniformly low and not elevated above those found in control samples. These data suggest that the Hh pathway is not activated within

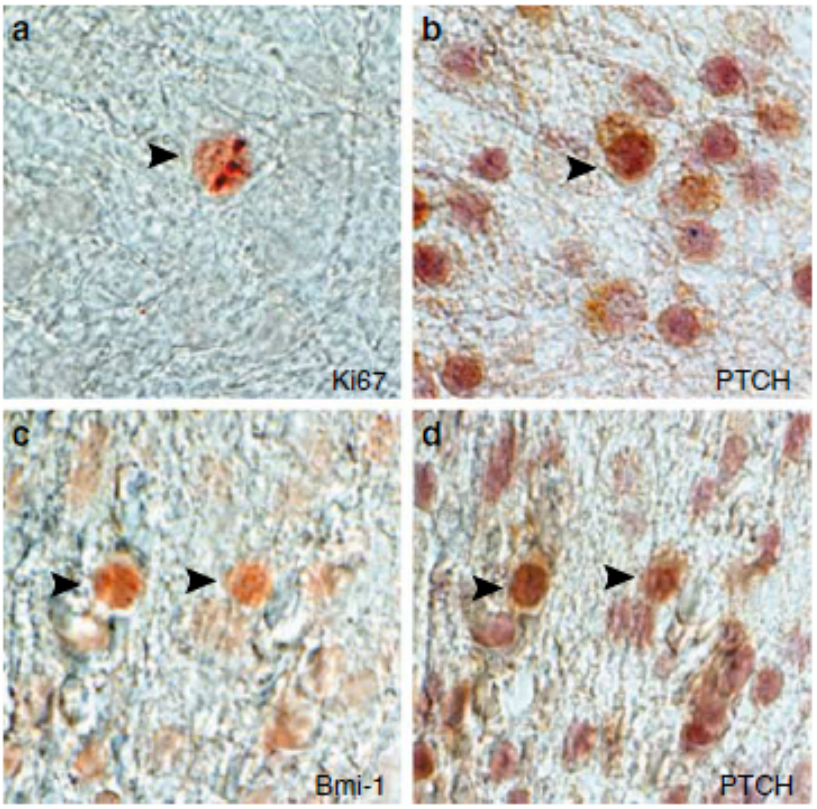

Figure 2.3. Expression of proliferation and stem cell markers within PTCH-positive cells in a GII astrocytoma. Sequential doubleantibody-labeling demonstrated coexpression of Ki67 and Bmi-1 (red, a and c, respectively) with PTCH (brown, arrowheads in b and d).

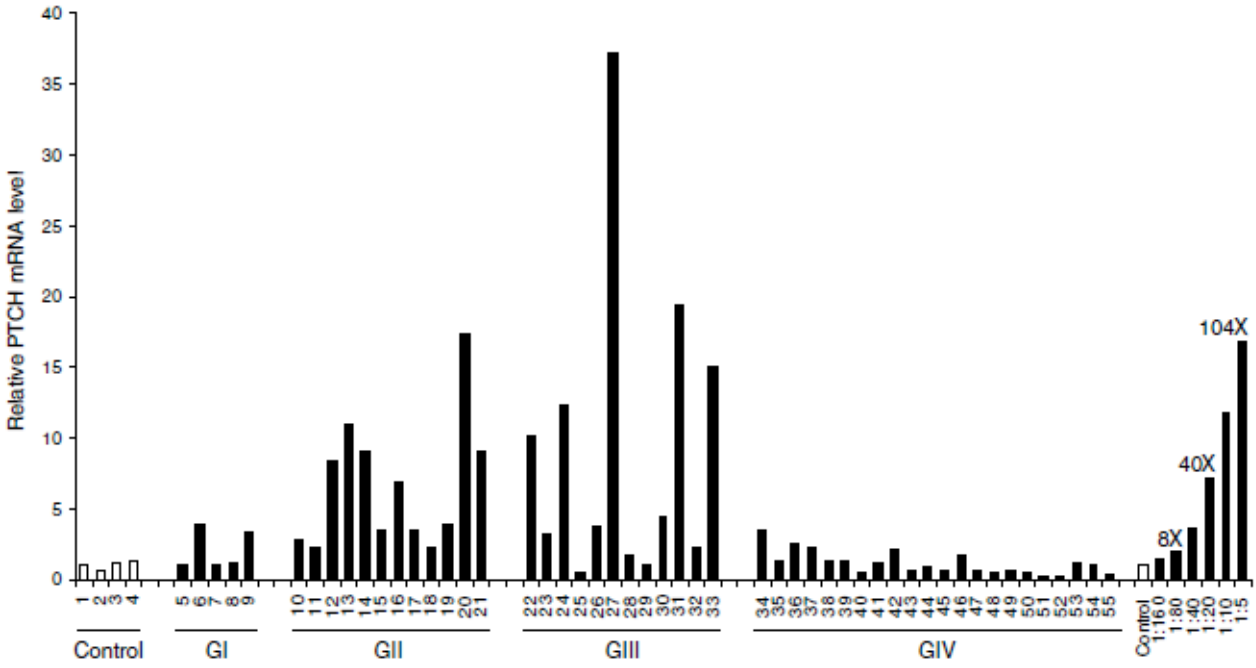

Figure 2.4. PTCH mRNA expression in gliomas. Graphic illustration of the relative PTCH expression levels from samples listed in Table 1 revealed significant elevation within GII and GIII gliomas only (see text for statistical analyses). Also shown are PTCH levels and corresponding Shh-reporter activity (104-fold with maximal stimulation) in NIH3T3 cells induced with serial dilutions of Shh-CM.

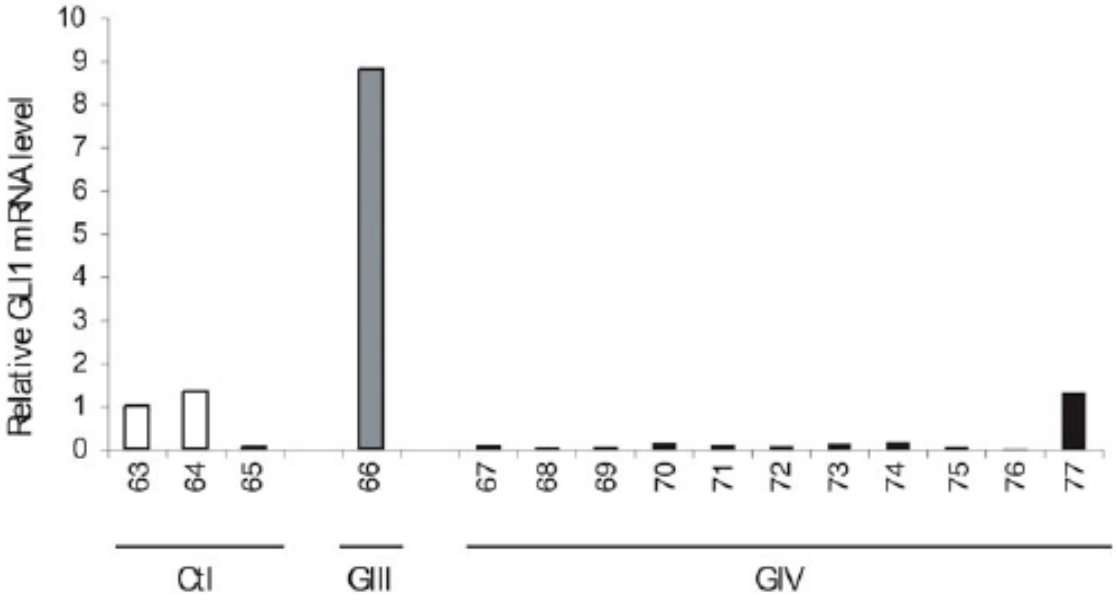

Figure 2.S2. GLI1 mRNA expression in gliomas. Graphic illustration of relative GLI1 expression levels (normalized to control sample 63) revealed no elevation within 11 *de novo* GBM (BT67-77). A GIII anaplastic oligodendroglioma (BT 66) was included as a positive control.

Table 2.1. Quantitative real-time PCR measurements of PTCH mRNA levels in human control brain and primary brain tumors

Sample	*Pathology*	*PTCH*
1	Non-neoplastic temporal lobe sample	1.00
2	Non-neoplastic temporal lobe sample	0.63
3	Non-neoplastic temporal lobe sample	1.17
4	Non-neoplastic cortex	1.30
5	Pilocytic astrocytoma	1.05
6	Pilocytic astrocytoma	3.97
7	Pilocytic astrocytoma	1.03
8	Pilocytic astrocytoma	1.11
9	Pilocytic astrocytoma	3.27
10	Oligodendroglioma	2.87
11	Oligodendroglioma	2.33
12	Oligodendroglioma	8.42
13	Oligodendroglioma	10.97
14	Oligodendroglioma	9.01
15	Oligodendroglioma	3.54
16	Oligodendroglioma	6.86
17	Astrocytoma	3.45
18	Astrocytoma	2.22
19	Astrocytoma	3.98
20	Astrocytoma	17.27
21	Astrocytoma	9.04
22	Anaplastic oligodendroglioma	10.09
23	Anaplastic oligodendroglioma	3.20
24	Anaplastic astrocytoma	12.37
25	Anaplastic astrocytoma	0.45
26	Anaplastic astrocytoma	3.82
27	Anaplastic astrocytoma	37.16
28	Anaplastic astrocytoma	1.80
29	Anaplastic astrocytoma	1.05
30	Anaplastic astrocytoma	4.46
31	Anaplastic astrocytoma	19.35
32	Anaplastic astrocytoma	2.29
33	Anaplastic astrocytoma	15.03
34	GBM	3.59
35	GBM	1.35
36	GBM	2.54
37	GBM	2.30
38	GBM	1.40
39	GBM	1.29
40	GBM	0.52
41	GBM	1.17
42	GBM	2.13
43	GBM	0.62
44	GBM	0.83
45	GBM	0.64
46	GBM	1.80
47	GBM	0.57
48	GBM	0.47
49	GBM	0.67
50	GBM	0.46
51	GBM	0.17
52	GBM	0.22
53	GBM	1.24
54	GBM	0.97
55	Secondary GBM	0.42
56	Subependymoma	1.29
57	Ependymoma	1.86
58	Ependymoma	0.59
59	Anaplastic ependymoma	0.45
60	Anaplastic ependymoma	0.26
61	Medulloblastoma	7.40
62	Meningioma	0.22

Abbreviations: GBM, glioblastoma multiforme; GAPDH, glyceraldehyde- 3-phosphate dehydrogenase; PTCH, Patched; PCR, polymerase chain reaction. PTCH mRNA expression was normalized to that of GAPDH and is expressed as the fold-difference relative to control brain tissue sample number 1.

de novo GBM by loss of PTCH-mediated suppression, and that while GLI1 and PTCH transcripts can be detected in GBM (Dahmane et al 2001), by quantitative measurement their expression levels are low (Katayam et al 2002).

Hh pathway responsiveness is maintained in primary progenitor cells cultured from GII and GIII gliomas

To assess the operational status of the Hh pathway in GII–GIV gliomas, primary cell cultures were generated from freshly resected brain tumors. To obtain standard adherent cultures, dissociated tumor cells were plated in serum-containing medium. For culture conditions favoring the maintenance of glioma progenitor cells (Galli et al 2004, Hemmati et al 2003, Lee et al 2006, Singh et al 2003, Singh et al 2004b), dissociated cells from the same tumors were plated in serum-free medium supplemented with epidermal growth factor (EGF), fibroblast growth factor (FGF) and leukemia inhibitory factor (LIF). Under these conditions, spheres of cells were derived (termed glioma spheres (GS)), which expressed the neural precursor markers nestin, Bmi-1, Musashi-1 and Sox-2 (Supplementary Figure 2.S3). Secondary and tertiary spheres were generated from dissociated GII and GIII GS plated at clonal density (data not shown).

However, serial passage of bulk cultures did not produce expanding cell numbers. In contrast to the exponential growth reported for GS from GBM (Galli et al 2004, Lee et al 2006), the failure to generate long-term

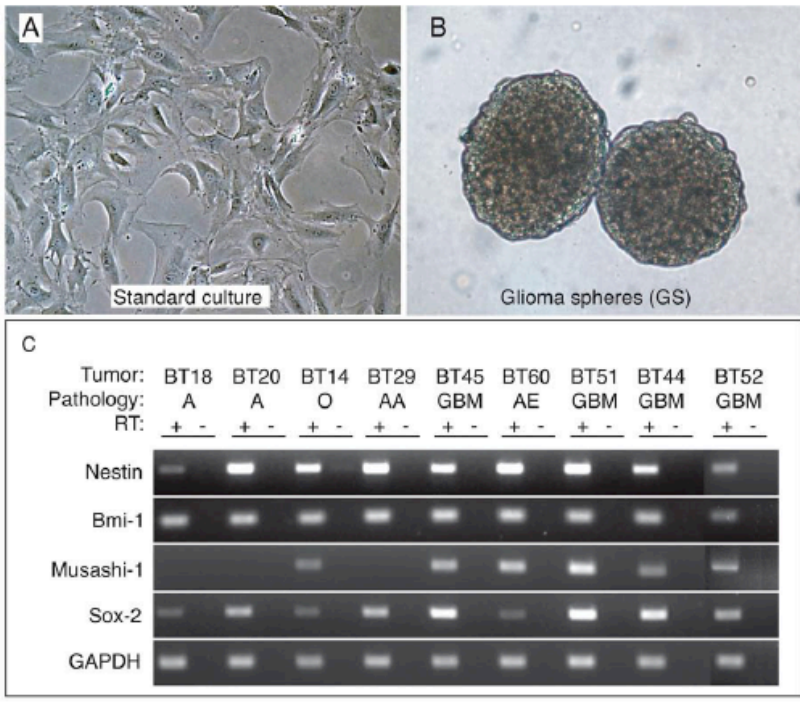

Figure 2.S3. Glioma spheres (GS) express neural progenitor cell markers. A-B, Phase-contrast images of a standard culture (A) and GS (B) from a GII astrocytoma (BT20). C, GS from two astrocytomas (BT18 and BT20), one oligodendroglioma (BT14) and one anaplastic astrocytoma (BT29), four GBM (BT44, BT45, BT51, and BT52), and an anaplastic ependymoma (BT60) were characterized using RT-PCR for expression of a panel of neural progenitor cell markers. For each sample, products of reactions containing reverse transcriptase (RT, +) and those in which the enzyme was omitted (-) are shown. A = astrocytoma, O = oligodendroglioma, AA = anaplastic astrocytoma, GBM = glioblastoma multiforme, AE = anaplastic ependymoma.

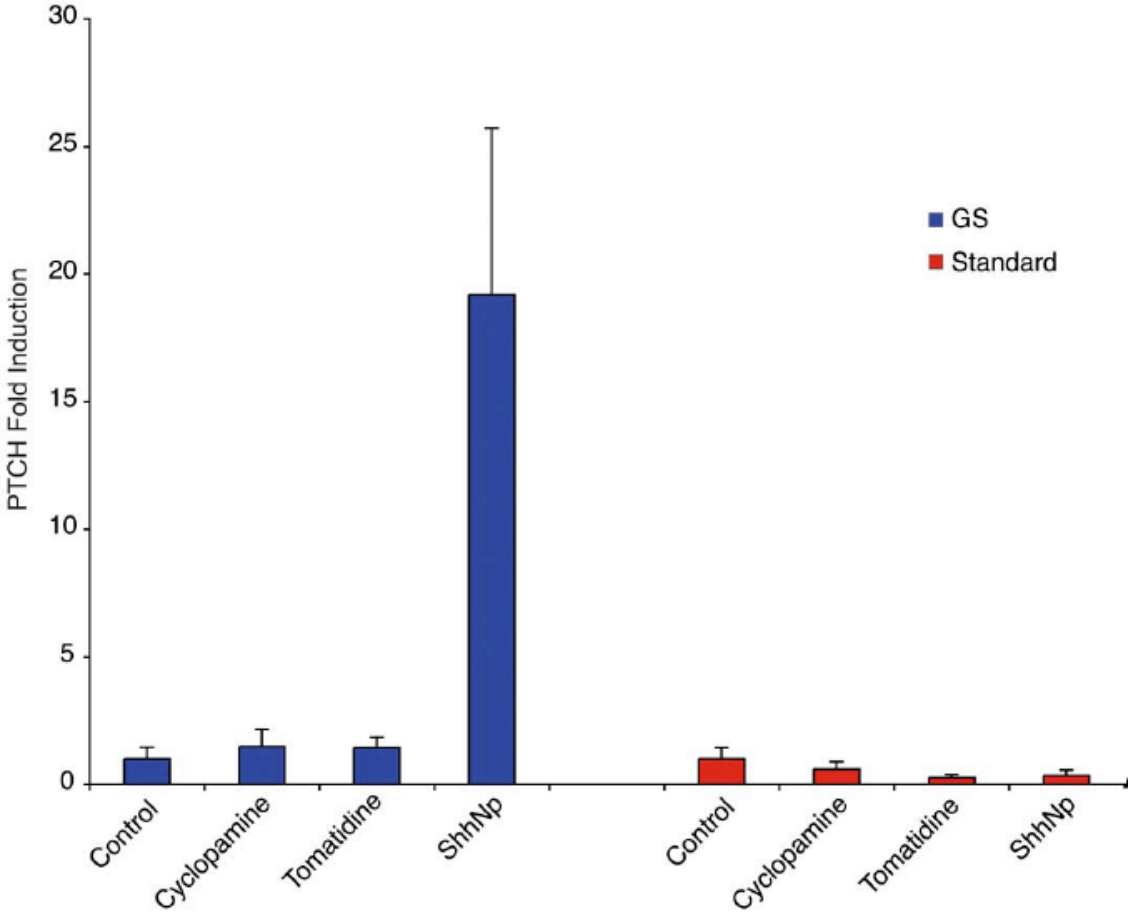

Figure 2.S4. Absence of PTCH induction in glioma standard cultures. GS or standard cultures from a GII oligodendroglioma (BT14) were cultured in triplicate for 36 hours either alone (control) or with 5 μM cyclopamine, 5μM tomatidine, or 5 nM ShhNp. The fold induction of PTCH levels observed in GS was absent in the corresponding standard cultures. PTCH levels in cultures treated with either cyclopamine or tomatidine did not differ significantly from those in corresponding controls.

GS cultures from GII and GIII gliomas may represent the requirement for alternative culture methods or reflect differences in growth kinetics.

To directly assay Hh pathway activity in these primary glioma cell lines, PTCH and GLI1 mRNA levels were measured following culture in the presence or absence of purified Shh protein (ShhNp) (Taipale et al 2000), or cyclopamine, a specific inhibitor of Hh signaling (Figure 2.1) (Chen et al 2002a, Cooper et al 1998). The addition of ShhNp resulted in elevations of both PTCH and GLI1 expression in short-term GS cultures derived from GII and GIII astrocytomas and oligodendrogliomas, but not from any of the GBM or an anaplastic ependymoma (Figure 2.5a). Conversely, treatment of GS with cyclopamine did not reduce PTCH or GLI mRNA. Additionally, pathway responsiveness to ShhNp was absent in standard serum-containing primary glioma cultures (Supplementary Figure 2.S4 and data not shown). These findings provide evidence that the Hh pathway is operationally intact within GII and GIII oligodendrogliomas and astrocytomas under culture conditions that favor progenitor cell maintenance, but not differentiation.

Our results indicate that the Hh pathway is at a basal level in GII and GIII GS and that exogenous ligand is required to activate signaling. To further confirm the ability to modulate Hh signaling in GS, we sought to establish whether, once activated, the pathway could then be inhibited. For this purpose, additional GS from a GII astrocytoma and a GIII anaplastic oligodendroglioma were generated in the presence or absence of a Smoothened (SMOH) agonist (SAG; see Figure 2.1) (Chen et al 2002b, Frank-Kamenetsky et al 2002). After 7

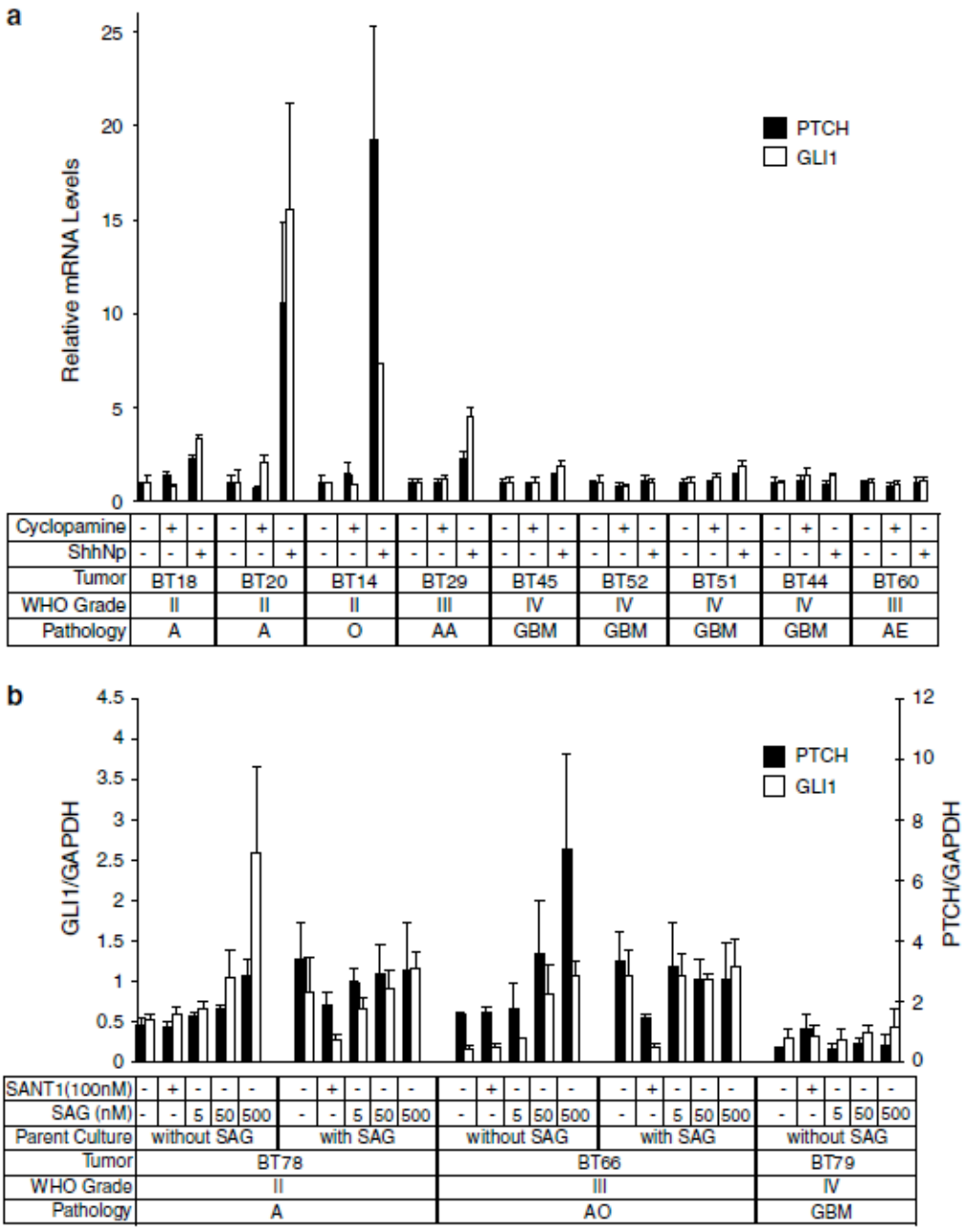

Figure 2.5. Characterization of Hh pathway responsiveness in glioma spheres (GS). (a) GS from two astrocytomas (BT18 and BT20), one oligodendroglioma (BT14), one anaplastic astrocytoma (BT29), four GBM (BT44, BT45, BT51 and BT52) and an anaplastic ependymoma (BT60) were cultured for 36 h either alone (control), with 5 mM cyclopamine or 5 nM ShhNp. In triplicate cultures for each cell line and culture condition, PTCH and GLI1 levels were normalized to GAPDH and expressed relative to the untreated control GS. For BT14, cDNAs from triplicate samples were pooled to measure relative GLI1 values due to insufficient starting material. (b) GS from a GII astrocytoma (BT78), a GIII anaplastic oligodendroglioma (BT66) and a GBM (BT79) were generated in the presence or absence of SAG, removed from the corresponding parent culture and subsequently cultured either alone, in the presence of SANT1 or increasing doses of SAG. PTCH and GLI1 levels are expressed relative to GAPDH. A, astrocytoma; O, oligodendroglioma,; AO, anaplastic oligodendroglioma; AA, anaplastic astrocytoma; GBM, glioblastoma multiforme; AE, anaplastic ependymoma.

days, GS from the corresponding parent culture were re-plated either alone in the presence of SANT1 (a SMOH antagonist; see Figure 2.1) (Chen et al 2002a) or in increasing doses of SAG. PTCH and GLI1 levels in GS derived from parent cultures grown in the absence of SAG were not further suppressed with SANT1 and demonstrated dose-responsive elevations with SAG (Figure 2.5b). Conversely, PTCH and GLI1 levels were elevated in GS from parent cultures derived in the presence of SAG, and could be reduced to basal levels by SANT1 treatment. These data demonstrate that Hh signaling in GII and GIII GS can be modulated by either activation or inhibition, thereby confirming the operational status of the pathway in these tumors.

On the basis of our survey of 12 GII–GIV GS, we find that the ability to modulate a Hh pathway response in cell lines derived from oligodendroglial and astrocytic GII and GIII tumors, but not from GBM or an ependymoma, correlates well with our PTCH and GLI1 mRNA measurements in gliomas (Table 2.1, Figure 2.4 and Supplementary Figure 2.S2). Furthermore, the inability to modulate basal PTCH and GLI1 levels in GBM GS with cyclopamine, SANT1, ShhNp or SAG (Figure 2.5a and b) suggests that the Hh pathway is unlikely to be activated or operationally intact in a CSC population within de novo GBM.

PTCH expression is found in an Olig2-positive glial fibrillary acidic protein (GFAP)-negative cell population common to GII and GIII oligodendrogliomas and astrocytomas, but not GBM

The heterogeneity of astrocytic and oligodendroglial tumor cells within diffuse gliomas is well recognized, and their classification is based on the proportion and spatial clustering of these two phenotypic populations. For example, as in our

study, tumors may be classified as astrocytoma when the two populations are intermingled with astrocytic predominance, and as oligoastrocytoma when the two populations are separated into distinct areas (Kleihues et al 1995). These two cell types have been shown to display mutually exclusive expression of Olig transcription factors and glial fibrillary acidic protein (GFAP) (Azzarelli et al 2004, Mokhtari et al 2005). Therefore, to evaluate in which cellular components the Hh pathway might be activated, we analysed PTCH expression in conjunction with that of Olig2 and GFAP. Within oligodendrogliomas and astrocytomas, PTCH expression was most readily detected within a subset of Olig2-positive and GFAP-negative cells (Figure 2.6a–d). However, PTCH expression was not confined to this population, as we also observed PTCH-positive Olig2-negative GFAP-negative cells within the same oligodendroglioma and astrocytoma samples (Figure 2.6e–h). Notably, we did not observe PTCH expression in GFAP-positive cells (Figure 2.6i and j). Rare Olig-2-positive GFAP-negative cells could be identified in de novo GBM, and these cells did not express PTCH (Figure 2.6k and l). These findings suggest that the Hh pathway may be activated within a shared population of Olig2-positive GFAP-negative cells in GII and GIII oligodendrogliomas and astrocytomas.

Characterization of Shh expression in gliomas

The induction of PTCH and GLI1 in GII and GIII GS by ShhNp is consistent with a mechanism of ligand dependent Hh pathway activation. To determine the source of Hh ligand in gliomas, we assayed for Sonic, Indian and Desert Hh

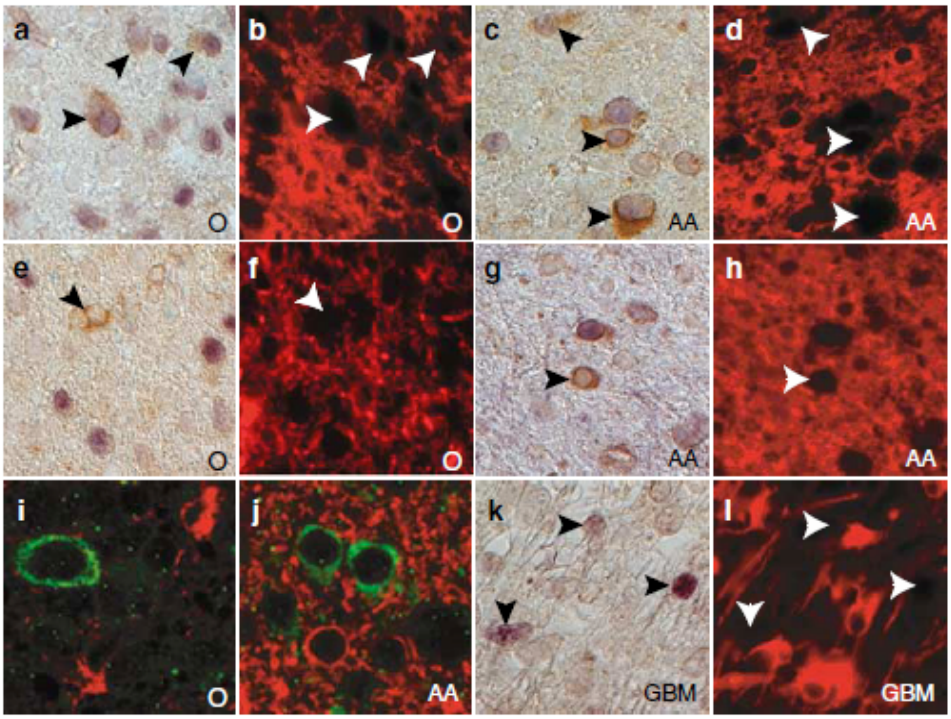

Figure 2.6. Expression of PTCH in Olig2-positive GFAP-negative cells within oligodendrogliomas and astrocytomas. (a–d) Immunohistochemical (a and c) and immunofluorescent (b and d) staining revealed the presence of PTCH (brown) expression within Olig2 (blue)-positive, GFAP (red)-negative cells in a GII oligodendroglioma (O, a and b) and a GIII anaplastic astrocytoma (AA, c and d). (k and l) In contrast, rare Olig2-positive GFAP-negative cells identified in GBM did not express PTCH. (e–h). Within GII and GIII gliomas, PTCH expression was also detected in Olig2-negative GFAP-negative cells. (i and j) The absence of GFAP (red) expression in PTCH (green)-positive cells was confirmed using laser scanning confocal microscopy.

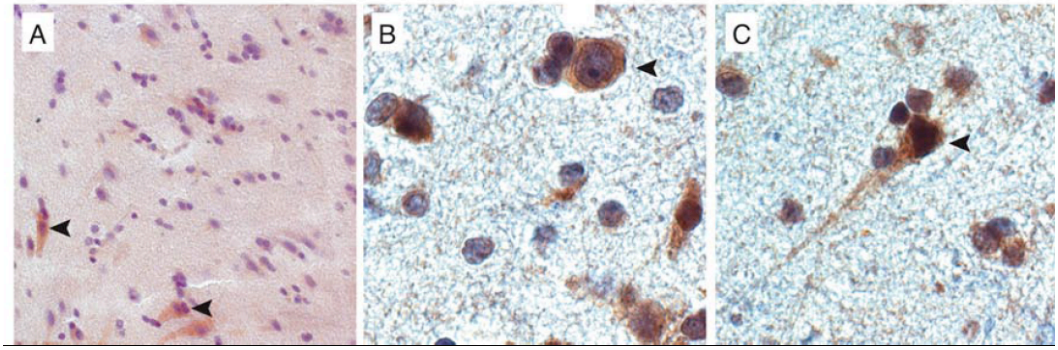

Figure 2.S5. Expression of Shh at glioma margin. A-C, Immunostaining of a GII astrocytoma revealed Shh expresion within adjacent brain parenchyma in cells with large nuclei lightly stained with hematoxylin and pyramidal morphology (A, arrowheads). At higher magnification (B and C), clusters of invading tumor cells can be visualized in close proximity to Shh-expressing cells (arrowheads).

expression in GS. Shh transcript could be detected in one GIII and two GIV GS (Figure 2.7a), demonstrating no correlation between Shh expression and pathway responsiveness (Figure 2.5). These data are consistent with our observations that the pathway is not inhibited by cyclopamine or SANT1 treatment and that exogenous Shh ligand or SAG are required to obtain a Hh response in GS (Figure 2.5).

Corroborating these results, immunohistochemical staining for Shh in GII–GIV gliomas revealed no discernable staining within tumor cells (Figure 2.7b–d). However, Shh staining was observed at the tumor margin in parenchymal cells with neuronal morphology adjacent to clusters of invading tumor cells (Supplementary Figure 2.S5) and within the tumor in cells with prominent nucleoli and the appearance of overrun neurons (Figure 2.7b–d). To better determine the cellular source of secreted ligand, we performed in situ hybridization with an Shh RNA probe. Signal was detected only in cells that expressed the neuronal marker NeuN (Figure 2.7e–g). These findings suggest that neurons may serve as an in vivo source of Shh ligand.

Discussion

Our studies define the glioma subtypes in which the Hh pathway is activated, namely WHO grades II and III astrocytomas and oligodendrogliomas. We have explored the culture conditions under which pathway modulation can be achieved, and demonstrate that the pathway is not operational in standard serum-containing cultures that induce cell differentiation, but rather in cultures that maintain glioma progenitor cells. Finally, we provide evidence that the Hh

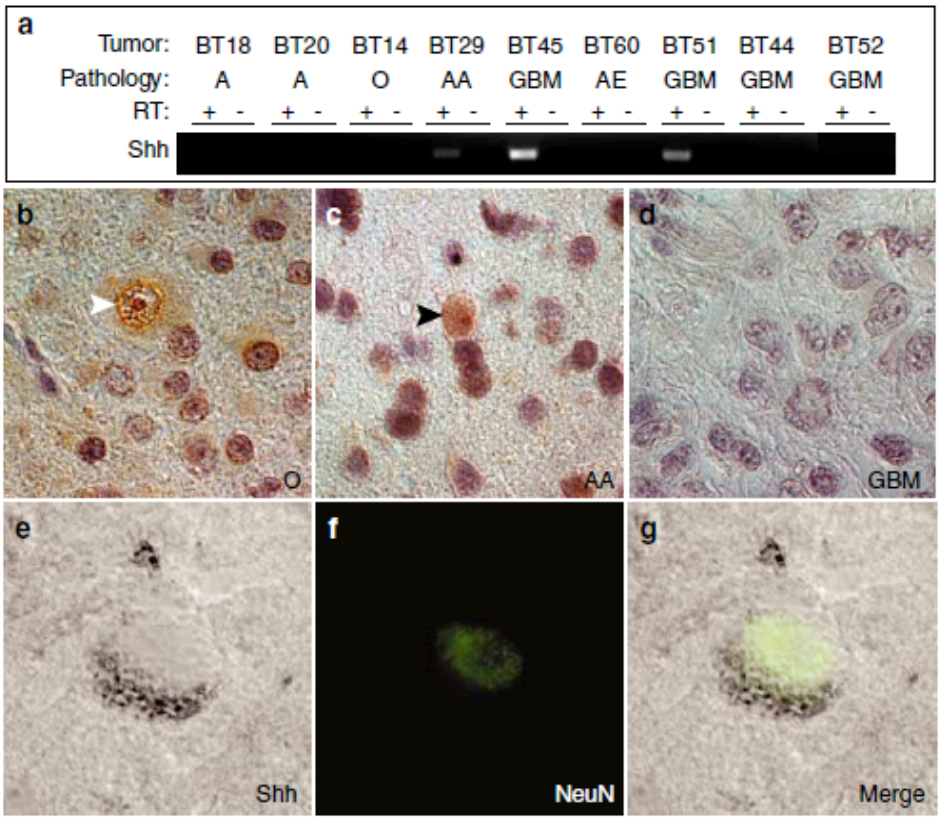

Figure 2.7. Expression of Shh in gliomas. (a) Shh expression in GS by RT–PCR revealed a lack of correlation with Hh-responsiveness (see Figure 5). For each sample, reactions containing RT (þ) and those in which the enzyme was omitted (_) are shown. (b and c) Immunostaining demonstrated expression of Shh within overrun neurons (arrow heads) in a GII ologodendroglioma (O) and a GIII anaplastic astrocytoma (AA). (d) Shh staining was not detected within GBM. (e–g) In situ hybridization confirmed the expression of Shh (black) message in NeuN (green)-positive neurons.

pathway is activated in a ligand-dependent manner, with a strict requirement for exogenous ligand.

The cellular origin of gliomas is unknown, and in this context it remains to be determined whether the striking absence of Hh pathway activity in the clinically de novo GBMs we analysed indicates that many GII and GIII gliomas may arise from Hh-responsive cell types whereas de novo GBM do not. This concept is reinforced by our observation that GIV GS expressed CD133, a stem cell marker used to identify CSC in GBM (Bao et al 2006b, Singh et al 2003, Singh et al 2004b), and did not demonstrate Hh pathway modulability, whereas GII and GIII GS were CD133-negative and Hh-responsive (data not shown). The WHO classification of malignant gliomas is based on histological appearance and malignancy grade, with a spectrum of progression of oligodendroglioma (GII) to anaplastic oligodendroglioma (GIII) and of diffuse astrocytoma (GII) to anaplastic astrocytoma (GIII) and GBM (GIV) (Kleihues et al., 2002). Two clinical GBM entities have been defined, primary or de novo GBM, occurring without evidence of antecedent disease, and secondary GBM, resulting from progression of a previously diagnosed lower grade glioma. Molecular analysis supports the divergent evolution of de novo and secondary GBM subtypes (Maher et al 2006, Ohgaki et al 2004). Our data raise the possibility that the Hh pathway might be activated in secondary GBM. However, we were unable to address this issue as our series contained only one secondary GBM. Nonetheless, our determination that the Hh pathway is activated within GII and GIII gliomas, but not in de novo GBM represents an important distinction for the formulation of clinical studies to

investigate the use of Hh modulators as therapeutic agents. This is an important aspect of our findings as earlier work reporting the detection of PTCH and GLI transcripts in GBM tumor samples and standard glioma cell lines by nonquantitative methods (Dahmane et al 2001) has formed the basis for advocating the clinical testing of Hh inhibitors in patients with GBM (Sanai et al 2005).

Our demonstration of Hh-pathway responsiveness in both oligodendrogliomas and astrocytomas, is attributable in part, to the presence of PTCH expression in an Olig2-positive GFAP-negative cell population identified as common to classic oligodendrogliomas, pure astrocytomas and oligoastrocytomas (Mokhtari et al 2005). However, our identification of PTCH expression in Olig2-negative GFAP-negative cells suggests that Hh pathway activity may not be exclusive to an oligodendroglial compartment in these tumors. The absence of PTCH staining in GFAP-positive cells indicates that Hh pathway activity may not be present within later stages of astrocytic differentiation, and further lineage marker analysis will be required to assess its presence within astrocytic precursors.

The strict requirement for Hh ligand or agonist to activate the pathway in cell culture, the lack of correlation between Hh ligand expression and pathway-responsive in GS, and the neuronal expression of Shh are consistent with a mechanism of ligand dependent pathway activation in GII and GIII gliomas. This is distinct from both the ligand-independent activation in medulloblastoma and the ligand-dependent mechanism identified in lung (Watkins et al 2003), foregut

(Berman et al 2003) and metastatic prostate (Fan et al 2004, Karhadkar et al 2004, Sanchez et al 2004) tumors. Studies from these latter tumor types demonstrate endogenous Shh ligand production in tumor cells (Berman et al 2003, Fan et al 2004, Karhadkar et al 2004, Sanchez et al 2004, Watkins et al 2003). In contrast, our findings indicate the need for exogenous ligand to activate the pathway. This is an important mechanistic concept for future studies to determine the functional role of Hh signaling in gliomas. Hh pathway activity is known to contribute to the growth and maintenance of multiple tumor types (Beachy et al 2004). Although functional roles for Hh signaling in GII and GIII gliomas are yet to be determined, this study does provide relevant observations. For example, we report that the pathway is activated in glioma cells with proliferative and progenitor cell features, and that tumor cells can be visualized clustered around Shh expressing cells at the tumor margin. These findings suggest that Hh signaling may regulate glioma cell growth and invasion. Furthermore, given the known role of Shh signaling in initiating Olig2-mediated oligodendrogliogenesis during embryonic development (Ligon et al 2006), our data suggest an analogous function in GII and GIII gliomagenesis. As such, our findings point to the potential clinical utility of monitoring and targeting the Hh pathway in GII and GIII gliomas.

CHAPTER III

ESTABLISHING DIRECT ORTHOTOPIC XENOGRAFT MODELS OF GLIOMAS

Abstract

A critical mechanism for studying the role of Hedgehog signaling in gliomas *in vivo* is the development of an animal model that faithfully recapitulates patient disease. Existing animal models rely on germ-line mutations, and heterotopic xenotransplantation of cell lines or primary tumor cells as secondary xenografts. However, these approaches are known to suffer from several limitations, including the inability to model the diverse genetic and phenotypic characteristics of gliomas, and the ectopic growth of tumors in sites that do not mirror the native host environment. We have utilized a direct orthotopic primary xenograft approach by transplanting CD133+ tumor-initiating cells from patient tumors samples to create models of malignant gliomas that represent patient disease. These xenografted tumors displayed the characteristic infiltrative and aggressive properties of malignant gliomas. Interestingly, low grade (grades I and II) gliomas demonstrated atypical features in xenografted mice, including uncharacteristically aggressive behavior and metastasis to lymph nodes outside the CNS. Our set of malignant glioma xenografts forms a panel of useful resource for pre-clinical studies to determine the therapeutic effects of Hh pathway inhibition on gliomas.

Introduction

To test the efficacy of new treatments, it is imperative to create an animal model that accurately represents the patient disease. Exclusive use of *in vitro* assays to test novel compounds suffers from several limitations: (i) cultured cell lines do not fully recapitulate the genetic makeup and cellular heterogeneity of tumors (Lee et al 2006), (ii) maintaining cell lines through several passages selects for specific immortalized cells with the capacity to grow across multiple passages, (iii) cell lines do not reflect the complex 3-dimensional tumor-stroma interaction (Park et al 2009). Pre-clinical testing in animal models, on the other hand, enables us to draw reasonable inferences in a relevant setting about the possible success of the treatment strategy in clinical trials. Many techniques have been utilized to create such glioma models including, genetically engineered mouse models (GEMMs) (Huse and Holland 2009), syngeneic mouse models (Mikheev et al 2009), heterotopic subcutaneous xenografts of primary tissue (Zhou et al 2009), orthotopic xenografts of cultured cell lines and primary cells (Shapiro et al 1979, Shu et al 2008) into immunocompromised mice. Each of these methodologies provides certain advantages and disadvantages over the other methods.

Several GEMM models of gliomas are commonly used that utilize the mutation or deletion of critical cell cycle control and/or receptor tyrosine kinase (RTK) genes. For example, driving overexpression of Ras and Akt genes in Nestin-positive cells results in a tumor that morphologically is similar to a GBM (Holland 2001). Viral expression using the RCAS system is a popular techinique that can induce tumorigenesis in mice by driving the overexpression of relevant

oncogenes, such as Ras and Akt (Holland et al 2000). A mutation in the EGFR gene can constitutively activate the EGF pathway. This mutant form, EGFRvIII, when combined with Ras gain-of-function mutation driven by a GFAP-specific promoter, can lead to the development of low-grade oligodendroglioma (Ding et al 2003). Loss of p53 expression in $PTCH^{+/-}$ heterozygous mice leads to sporadic medulloblastoma formation (Wetmore et al 2001). These GEMM models have the advantage of modeling certain oncogenic events in mice that replicate the mutations commonly seen in subsets of gliomas. The mice also present with greater tumor formation and mortality rates thus allowing for consistency in designing pre-clinical studies. However, their accuracy to represent patient disease is debatable since they attempt to model a combination of certain oncogenic events that may not fully represent the complexity of genetic changes present in patient disease.

Subcutaneous xenotransplantion of cell lines and primary tumor cells in immunocompromised mice has been another extensively used methodology for pre-clinical testing (Johnson et al 2001, Maruo et al 1990). This methodology generally serves as a first-line of *in vivo* testing mechanism for novel therapeutic compounds. The main advantages of using subcutaneous xenografts are the relative ease of designing and implementing PK/PD studies on a regular basis. Abundant access to cell lines and mice allows greater number of mice to be used and shorter periods of time-to-growth for implanted tumors. Subcutaneous implantation, often in the flank of mice, allows for easy quantification of palpable tumor volume and growth measurements. However, recent studies have

established the ability of tumor cells to undergo genotypic and phenotypic transformation in culture (De Witt Hamer et al 2008, Lee et al 2006, Pandita et al 2004) prior to implantation. These changes do not reflect characteristics of the patient sample and cannot be restored in secondary xenografts (Daniel et al 2009). Furthermore, distinct stem cell populations (Vescovi et al 2006) and dependency on key signaling pathways (Sasai et al 2006) can be lost in cancer cell cultures. Genomic profiles can be maintained to a better extent in cancer sphere culture, though they still fail to mirror the genotype of primary tumors (De Witt Hamer et al 2008, Lee et al 2006). In a secondary subcutaneous xenograft, since the cells are grown in an ectopic environment devoid of their natural niche support factors, phenotypic similarity to patient sample has been hard to maintain across several passages and has demonstrated limited value in predicting clinical efficacy (Klement et al 2000, Sharpless and Depinho 2006, Takimoto 2001).

To circumvent these limitations, direct orthotopic xenotransplantion of primary tumor cells can be utilized that negate the influences of in vitro culture, provide a native microenvironment, and preserve the integrity of tumor-initiating cell (Sarangi et al 2009, Shu et al 2008, Suggitt and Bibby 2005). This mechanism has been suggested as a vast improvement in predictive PK/PD modeling compared to subcutaneous xenografts (Daniel et al 2009, Kerbel 2003, Park et al 2009). This methodology preserves many of the cardinal features of patient tumor characteristics. Moreover, in the case of non-CNS tumor types, this mechanism can recapitulate distal metastasis phenotype upon surgical resection

of the parent transplanted tumor, thus reflecting the clinical course of patients who undergo surgical treatment and develop advanced metastatic disease (Horowitz et al 1988). Treating mice that demonstrate similar advanced disease phenotype can provide more relevant therapeutic efficacy data (Kerbel 2003). A few limitations of this methodology include: (i) depending upon the orthotopic site where tumor cells need to be implanted, tumor growth can be difficult to measure and monitor (e.g. brain), (ii) such transplantations are performed on immunocompromised mice to prevent rejection of foreign tissue thus limiting the modeling of the immunological response to tumorigenesis.

Nevertheless, direct orthotopic xenotransplantation strategy remains one that closely recapitulates patient disease and maintains its characteristics upon serial transplantation. Moreover, one can select for specific tumor-initiating cell populations from gliomas, e.g. by using cell surface markers such as CD133. This approach has been used recently by several groups (Bao et al 2006b, Clement et al 2007, Sarangi et al 2009, Singh et al 2004b) to establish glioma xenografts in the brains of immunocompromised mice.

Materials and Methods

Tissue procurement

Excess brain tumor specimens were obtained for research purposes from patients in accordance with a protocol approved by Vanderbilt Medical Center Institutional Review Board. Primary brain tumors were phenotyped and graded as described (Kleihues et al 1995, Kleihues et al 2002).

CD133 cell selection and flow cytometry

Tumor samples were minced mechanically, dissociated with papain (Worthington Biochemical Corporation), and passed through a 40 μm filter. Cells were labeled with a CD133/1 (15 ug/ml; Miltenyi Biotec) antibody crosslinked to magnetic nanoparticles and subjected to immunomagnetic cell separation using the EasySep Magnetic Selection Kit (Stem Cell Technologies). Purity of the CD133-enriched population was assessed by flow cytometry after labeling enriched cells with CD133/2-APC (Miltenyi Biotec) antibody. Isotype-matched controls were included in the analysis to determine background signal levels. Gates thresholds were set relative to the CD133 negative-selection samples.

Xenotransplantation, monitoring mice, and survival analysis

CD133-enriched cells were transplanted into the striatum of NOD/SCID mice according to a protocol approved by the Vanderbilt Medical Center Institutional Animal Care and Use Committee. Mice were anesthetized with ketamine and xylazine, and securely placed on a stereotactic frame. Using aseptic surgical procedures, an incision was made in the scalp and a small burr-hole was drilled 2.5 mm lateral to the bregma. CD133-enriched cells were implanted 2.5 mm into the right striatum using a Hamilton syringe. Mice were maintained until development of neurological symptoms, significant weight loss or signs of distress (piloerection and/or hunched posture).

Histology and immunohistochemistry

Immunodetection was performed for Ki67 (1:50; Dako) and GFAP (1:500; Chemicon) on paraffin-embedded sections and for anti-human nuclear epitope (1:50; Chemicon) on frozen sections as described (Ehtesham et al 2007). Routine histological analysis was performed using Hematoxylin and Eosin (H&E) staining.

Results

CD133 enrichment

We established several xenograft mouse lines using orthotopic implantation of CD133-enriched tumor initiating cells from primary brain tumor specimens (Table 3.1). The specimens used in this study were freshly resected patient glioma samples. All four grades of gliomas ranging from WHO Grade I (4 specimens), Grade II (6 specimens), Grade III (4 specimens) and Grade IV (7 specimens) were represented in our study. On the day of resection, and without passaging cells in culture, primary brain tumor specimens were subjected to immunomagnetic selection for CD133 cell surface expression using magnetic nanoparticle-coupled antibody. As shown in Figure 3.1, CD133+ yield ranged between 2-35%. The figure also illustrates the number of cells transplanted per mouse per tumor. A striking observation from our dataset suggests that there is

Table 3.1. Pathological features of gliomas used in our xenograft panel and details of implantation parameters. Table also indicates which tumors successfully engrafted in mice and which ones demonstrated atypical features.

Tumor #	*Tumor ID*	*Age/ Gender*	*Pathology*	*Grade*	*No. of cells injected per mouse*	*No. of mice implanted*	*Xenograft Success*	*Atypical Features*
0115	115-GG	18y M	Ganglioglioma	I	20000	6		
0117	117-GG	14y F	Ganglioglioma	I	1250	6		
0125	125-JPA	6y F	J. Pilo. Astrocytoma	I	11000	3	+	+
0429	129-JPA		J. Pilo. Astrocytoma	I	20000	10		
0121	221-GG	14y F	Ganglioglioma	II	1125	6	+	+
0214A	214A-O	30y M	Oligodendroglioma	II	2250	10		
0219	219-RO	46y F	R. Oligodendroglioma	II	8000	3		
0610	210-O		Oligodendroglioma	II	30000	9	+	+
0611	211-O		Oligodendroglioma	II	40000	9	+	+
0612	212-A		Astrocytoma	II	12000	5	+	+
0304B	304B-AA	50y M	A. Astrocytoma	III	29000	4		
0404	304-AOA	44y F	A. Oligoastrocytoma	III	20000	13	+	
1212	312-HGA	54y M	H.G. Astrocytoma	III	30000	10	+	
0402	302-AG	28y M	A. Ganglioglioma	III	20000	10	+	
1206	406-GBM	83y F	Glioblastoma Multiforme	IV	90000	3	+	
0122B	422B-GS	39y F	Gliosarcoma	IV	6480	9	+	
0208	408-GBM	33y M	Glioblastoma Multiforme	IV	4000	3		
0212A	412A-GBM	45y M	Glioblastoma Multiforme	IV	5000	7	+	
0214B	414B-GBM	67y F	Glioblastoma Multiforme	IV	4600	9		
0408A	408A-GBM	71y F	Glioblastoma Multiforme	IV	30000	1		
0408B	408B-GC	16y M	Gliomatosis Cerebri	IV	30000	1		
0414	414-MB	39y M	Medulloblastoma	IV	100000	9	+	
0416	416-MB	42y M	Medulloblastoma	IV	50000	10	+	

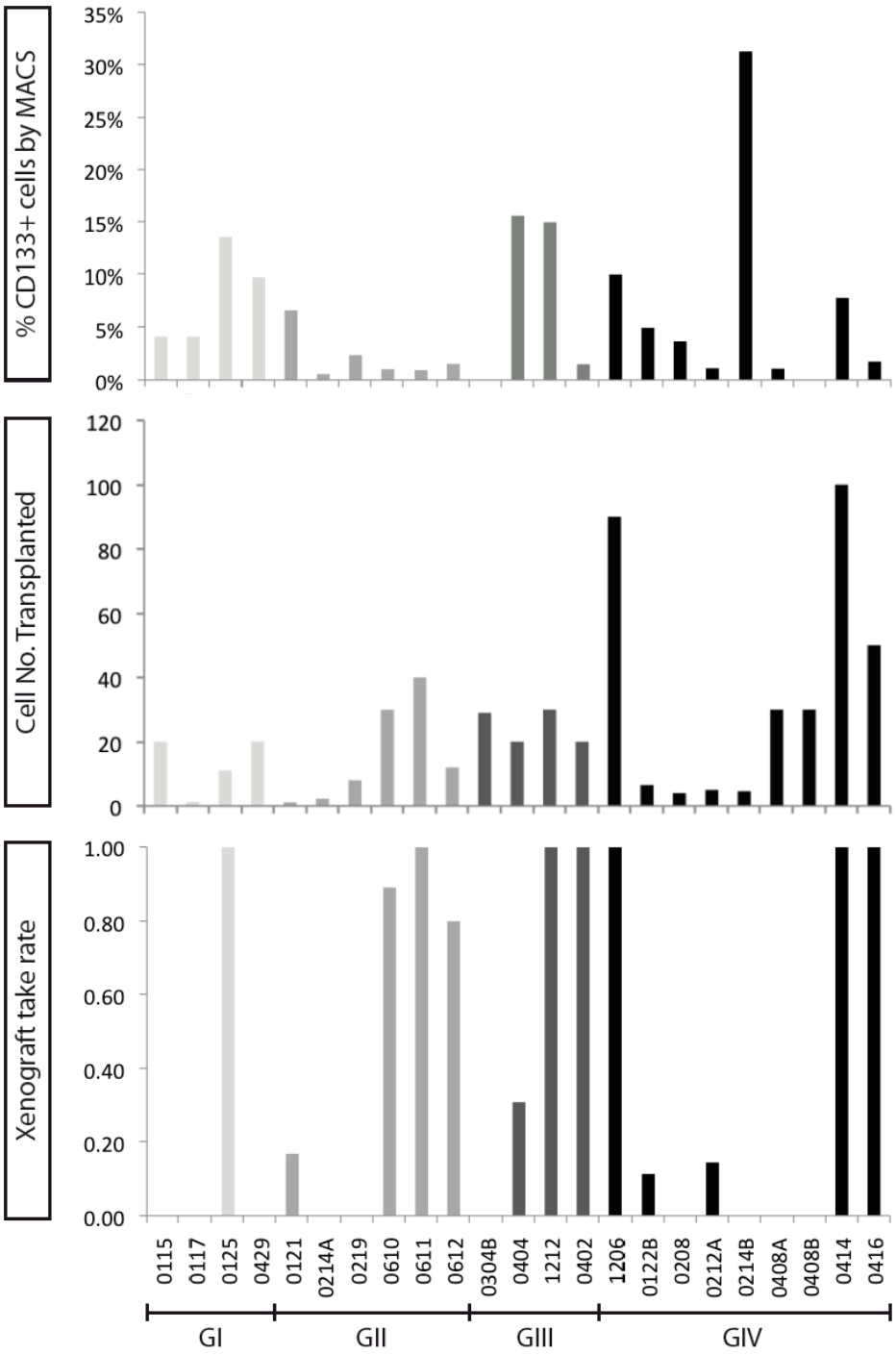

Figure 3.1. Graphic illustration of percentage of CD133 positive cells, number of cells transplanted per mouse and xenograft take rate. Data is shown on a linear scale from GI to GIV tumors identified by their tumor number (see Table 3.1 for details). Immediate following surgical resection each patient tumor sample was subjected to immunomagnetic selection using magnetic nanoparticle coupled CD133/1 antibody. Top graph plots the percentage of CD133+ cells sorted from total cell number. Depending upon the availability of sufficient cell numbers, a group of mice were implanted with CD133+ cells ranging from a 1000-100,000 cells per mouse as shown in the middle graph. The bottom graph displays the ratio of mice (expressed as a fraction of 1.0) that developed neurological symptoms indicating tumor engraftment.

no clear correlation between percent CD133+ cells, number of cells transplanted, and the grade of glioma or xenograft take rate. A fraction of CD133+ cells were analyzed for purity by flow cytometry using a separate fluorescent molecule conjugated CD133/2 antibody that recognizes a different epitope of CD133. Enrichment of CD133+ cells in the positive-selection ranged from 2-36% (Figure 3.2).

Direct orthotopic xenotransplantation

CD133 enriched cells were orthotopically xenotransplanted into NOD/SCID mice. Once the mice started losing weight or developed neurological symptoms due to the tumor burden, the CD133-based magnetic selection procedure was repeated on harvested xenograft tumor tissue for serial passaging of CD133-enriched cells to the next set of mice. In contrast to patient tissue, purity of CD133-enriched samples from xenograft tissue was higher, ranging from 50-80% by flow cytometry analysis. For example, in the case of the PT-312-HGA tumor, we obtained a purity of 36.5% relatively in the CD133-positive selection from the patient sample. The corresponding xenograft tissue (X-312-HGA) yielded much greater CD133-enrichement (54.01%) in the positive selection (Figure 3.2). One possible explanation for this disparity could be due to the cleaner sample preparation obtained from a mouse brain tissue compared to the human patient sample which contain calcified and necrotic regions rendering the creation of a single cell suspension technically unfeasible. Xenograft take rate was determined based on the fraction of mice that developed neurological symptoms and died or

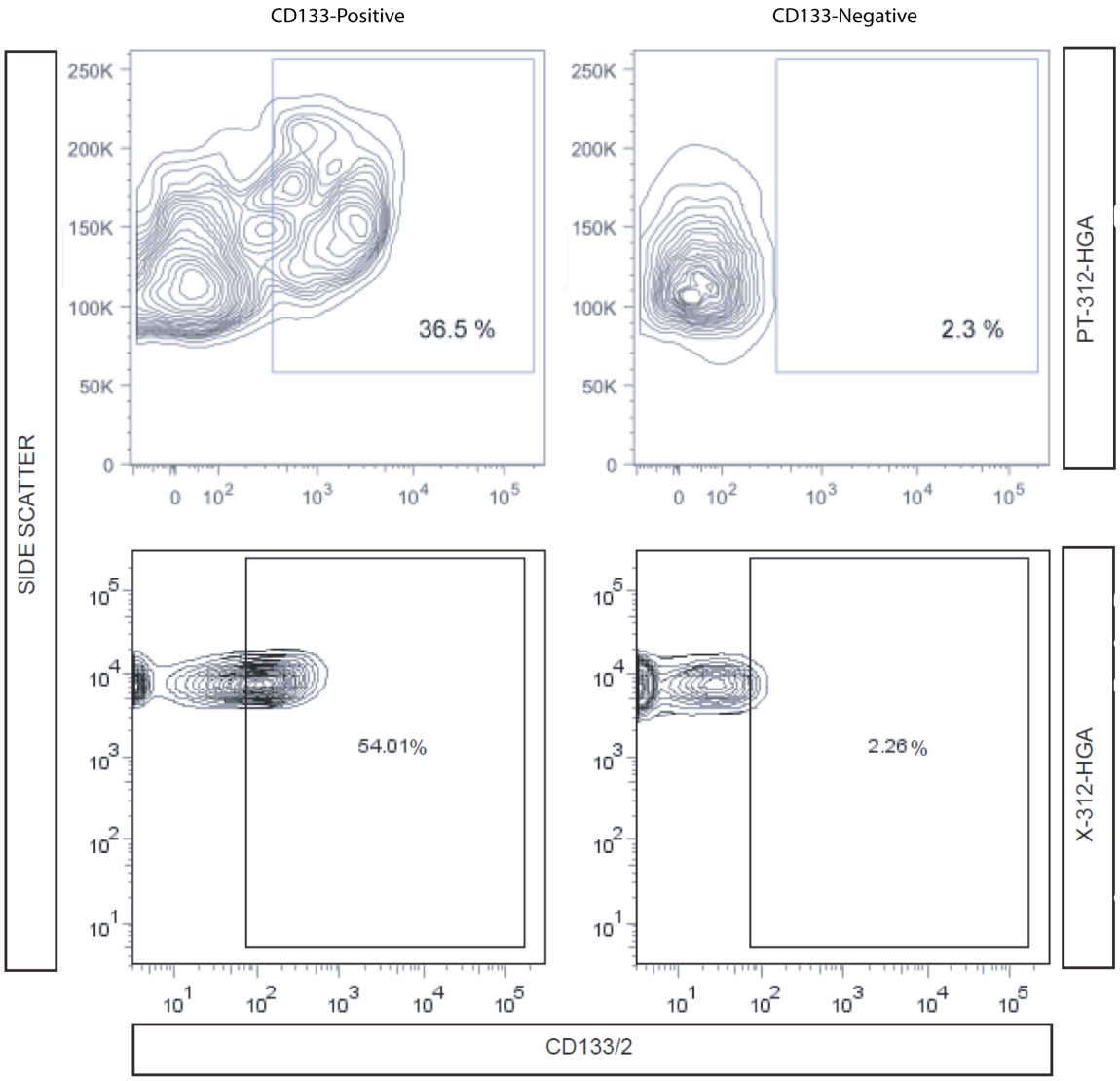

Figure 3.2. Purity analysis of CD133 sorted fraction from patient and xenograft tissue. A fraction of PT-312-HGA sorted cells were analyzed by flow cytometry using the CD133/2 antibody. The CD133-positive fraction consisted of 36.5% pure CD133 cells that were completely absent in the negative fraction. The immunomagnetic selection procedure, however, yielded better purity of sample from xenograft tissue. Bottom panel illustrates the purity of the CD133 selection from the corresponding X-312-HGA sample. The CD133-positive fraction from the xenograft tissue contained at least 54.01% pure CD133+ cells when compared to the negative fraction. X-axis indicates CD133/2 mean fluorescence intensity, Y-axis indicates side scatter profile of cells.

were sacrificed. By this method, 50% of transplanted primary malignant gliomas (WHO grades III and IV) engrafted in 69-100% of NOD/SCID mice recipients.

Faithful recapitulation of patient disease in high grade gliomas

Consistent with corresponding tumor behavior in patients, high grade brain tumor xenografts faithfully recapitulated patient tumor characterisitcs. Our high grade brain tumor panel consisted of four Grade III gliomas and seven Grade IV gliomas (Table 3.1). Percent CD133 yield ranged from 2 – 30%. H&E and Ki67 staining revealed that the high grade tumor xenografts were histologically identical to the patient tumor samples (Figures 3.3 and 3.4). As shown in Figure 3.3a, invasive tumor cells expressed Ki67 abundantly and were marked by a human-specific antibody (HuNu). Figure 3.3b provides an example of a tumor developed after transplantation of a GL26 glioma cell line. The tumor develops into a well-circumscribed mass with sharp borders (arrow). This type of growth does not reflect inherent tumor characteristics of gliomas as in a patient. Orthotopically xenotransplanted tumors directly from the patient sample exhibited classic characteristics of leptomeningeal spread (Figure 3.4c), parenchymal invasion (Figure 3.4d), corpus callosum migration (Figure 3.4e) and seeding the contralateral hemisphere (Figure 3.4f). Figure 3.5 provides additional examples of high grade gliomas that display phenotypically similar characteristics as patient gliomas. Notably, high-power magnification of xenografted tumor and patient tissue shows very similar morphological and histological features including, high MIB-index, cellular atypia and neo-vasculature.

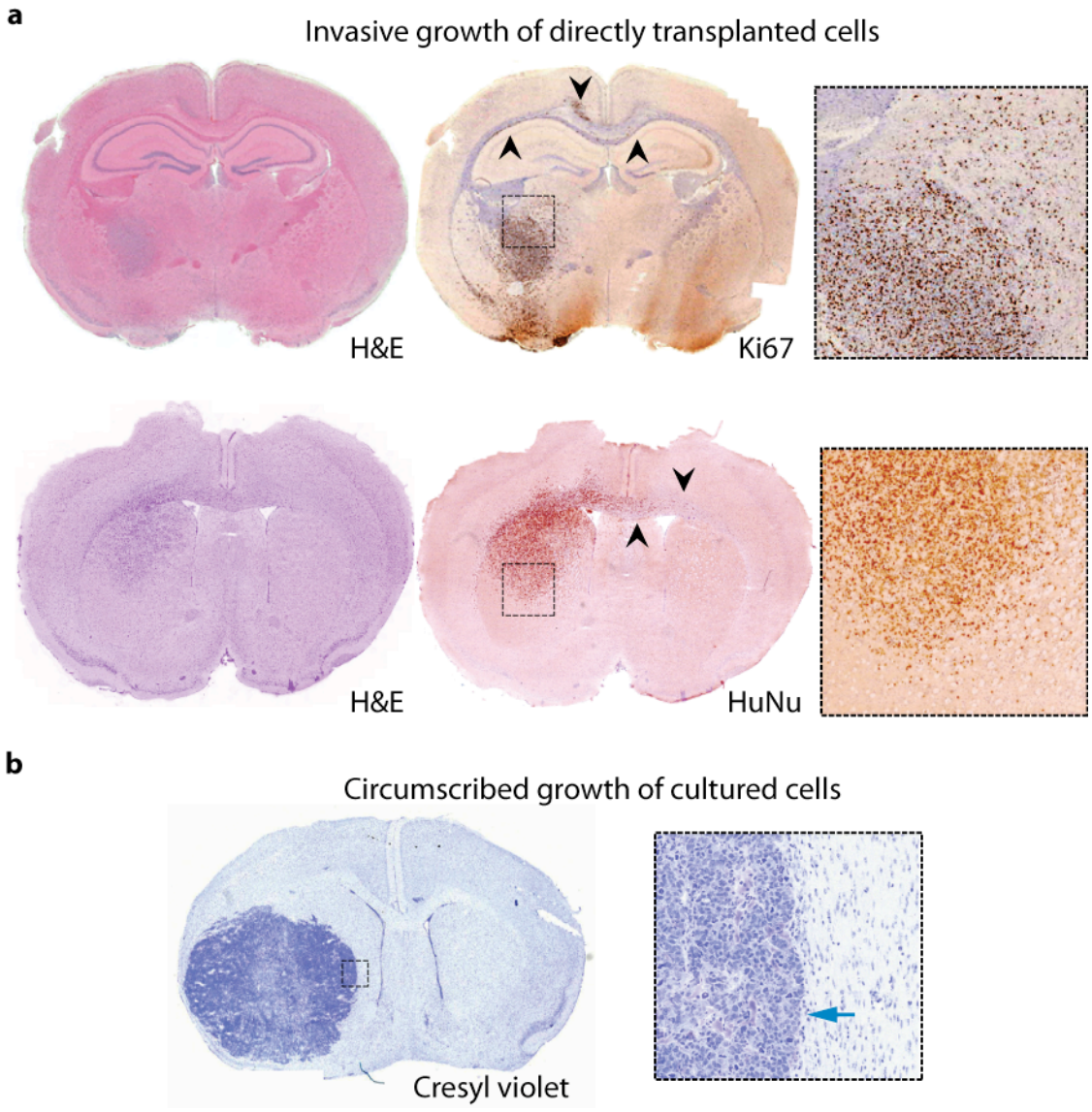

Figure 3.3. Comparision of xenotranplantation results from primary and cultured cells. (a) Direct orthotopic xenotransplantation of primary tumor cells from malignant gliomas yields tumors that display many hallmark features of patient tumor characteristics, including infiltration into the adjacent parenchyma (inset box) and migration along white matter tracts of the corpus callosum (arrowheads). Both Ki67 and HuNu are used here as markers of xenotransplanted tumor cells. (b) On the other hand, transplantation of a cultured glioma cell line, GL26, forms a well-circumscribed tumor mass with sharp borders (inset box) that does not represent the endogenous behavior of gliomas accurately (Image courtesy of Sara Frappier, Graduate Student in Richard Caprioli's Lab, Vanderbilt University).

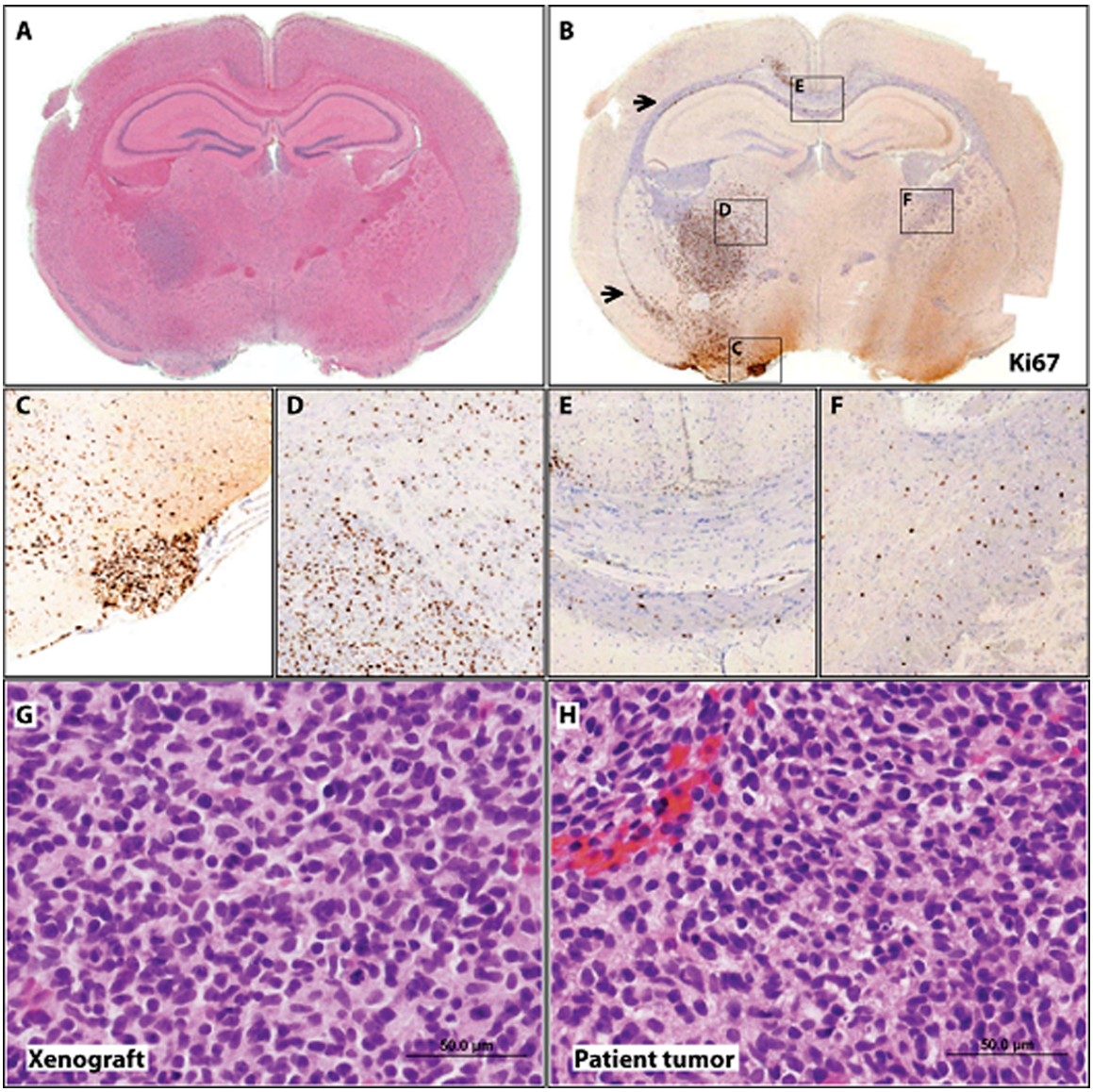

Figure 3.4. Recapitulation of disease features in primary xenografts from high grade gliomas. The panel above illustrates hallmark features obtained from primary xenograft of a 312-HGA (high grade astrocytoma). Both H&E and Ki67 staining show the location of the tumor foci in the posterior striatum (A & B). (C) shows tumor cells infiltrating and spreading through the leptomeninges. (D) Ki67+ tumor cells are seen invading into the parenchyma adjacent to the tumor injection site. (E) tumor cells can also be seen migrating along white matter tracts of the corpus callosum (arrowheads). (F) migrating tumor cells infiltrate areas on the contralateral hemisphere. (G & H) High-power magnification of H&E stained slides show histological similarities between xenograft and patient tissue including the presence of cells with atypical morphology and mitotic figures.

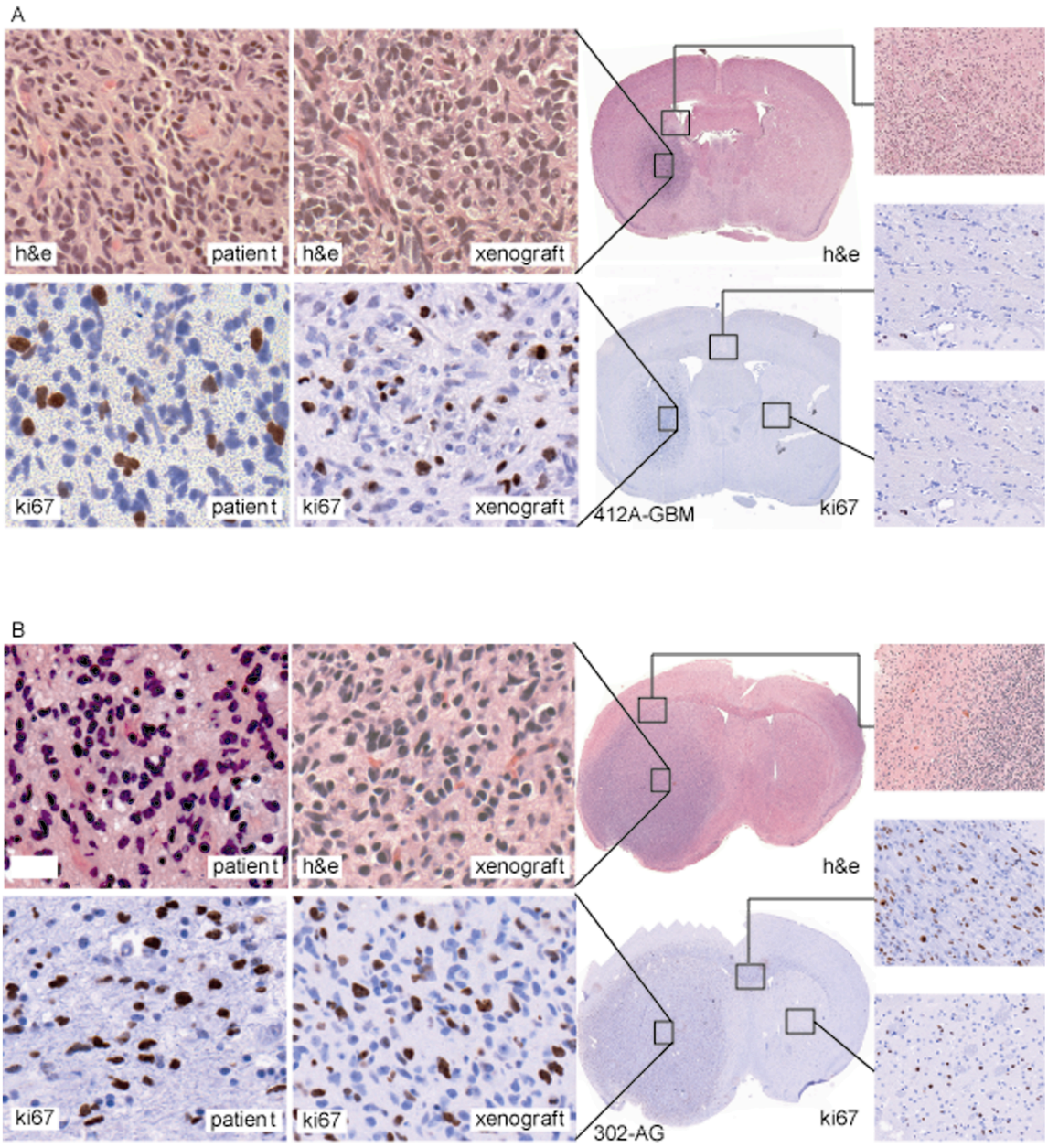

Figure 3.5. Additional high grade glioma xenograft pathology. Malignant glioma xenografts consistently displayed faithful racapitulation of patient disease pathology demonstrated by similar histological features (H&E), proliferation capcities (Ki67) and invasion through the corpus callosum towards the contralateral hemisphere (inset boxes). (A) 412A-GBM and (B) 302-AG. Abbreviations: GBM, glioblastoma multiforme, AG, anaplastic ganglioglioma.

The X-304-AOA tumor displayed extensively diffuse characteristics throughout the host brain as seen by Ki67staining (Fig 3.6) and prominent migration of tumor cells towards the SGZ and SVZ neurogenic niches. This infiltrative feature was shared in some low grade gliomas as well (Figure 3.7). Satellite cells (marked by Ki67 staining) were found in the SGZ of the dentate gyrus and SVZ of the ventricles in the X-211-O xenograft bearing brain reminiscent of transplanted stem cell migration to stem cell niche sites (Colmone et al 2008, Sipkins et al 2005).

Atypical features in low grade glioma xenografts

Surprisingly, the xenografted low grade (Grade I and II) tumors consistently displayed an aggressive phenotype *in vivo* that was uncharacteristic of these tumors compared to their behavior in patients. As revealed by H&E and Ki67 staining, all five tumors that engrafted in mice displayed a propensity to migrate towards the meninges of the brain and spread along the outer layers of the brain (Figure 3.8). Serial coronal sections of the tumor-bearing cortex revealed a range of histological phenotypes – non aggressive tumor foci (125-JPA, Fig 3.8) or an aggressive and highly malignant tumor foci (221-GG, Fig 3.8) within the brain parenchyma. As demonstrated by the H&E and GFAP staining in the 221-GG xenograft, tumor burden on the ipsilateral hemisphere near the site of implantation was extensive. The contralateral hemisphere, however, was relatively normal with no clear evidence of tumor cells present.

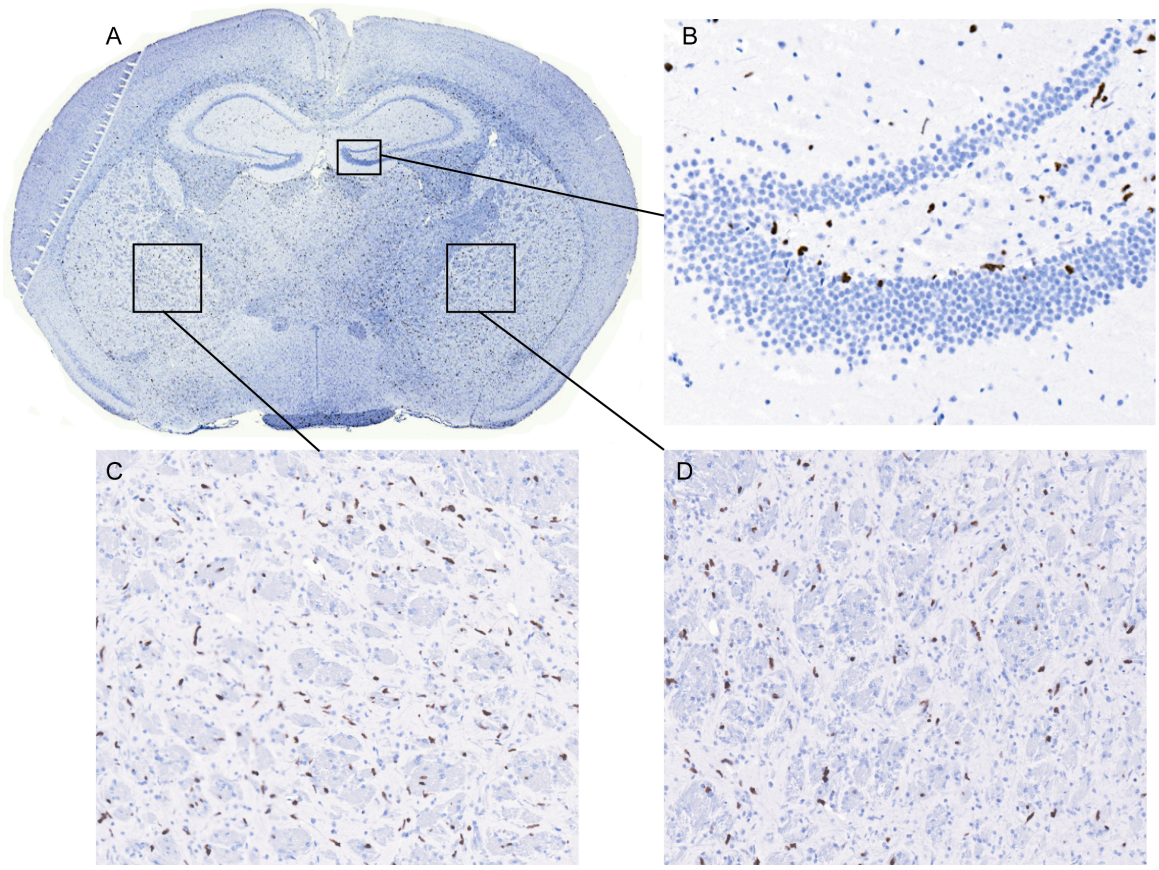

Figure 3.6. Diffuse and infiltrative characteristics of high grade glioma. The panel above shows Ki67 staining in a 304-AOA glioma. Diffuse tumor cells were located all throughout the brain of the mouse (A). High-power magnification shows Ki67+ tumor cells on both hemispheres (C & D). Ki67+ tumor cells were also found in the dentate gyrus of hippocampus suggesting a migratory response of tumor cells toward stem cells niches (B). Abbreviation: AOA, anaplastic oligoastrocytoma.

The prominent characteristic of the low grade brain tumors from this panel was their ability to migrate out of the CNS and inhabit lymph nodes within the mice. The tumors formed large growths in the lymph nodes present in the neck of the affected mice above the salivary glands (Figure 3.8). The atypical growths consisted of tightly packed tumor cells with large nucleus and small cytoplasm as revealed by H&E. Inset also shows normal lymph node structure. Moreover, the cells were highly proliferative and expressed abundant Ki67 protein. Surprisingly, although the tumor cells expressed GFAP within the tumor foci in the brain, they lost GFAP expression upon metastasizing to the lymph nodes.

Discussion

Modeling gliomas accurately in mice provides an essential tool for testing novel therapies in a relevant setting and predicting their efficacy in clinical trials. Our approach to directly xenotransplant primary tumor-initiating cells in an orthotopic site has led to the development of several mouse models that faithfully recapitulate invasive growth – a cardinal feature of infiltrative gliomas. In our high grade glioma models, tumor cells not only invade parenchyma surrounding the tumor injection site (Figures 3.4 and 3.5), but also migrate along white matter tracts of the corpus callosum and the meninges to infiltrate other areas of the brain both ipsilaterally and contralaterally. Prior to our studies, very few reports had demonstrated such extensive infiltrative behavior of glioma cells in a xenotransplantation model (Shu et al 2008). Moreover, close examination of xenograft tumor histology reveals phenotypic similarities with the corresponding

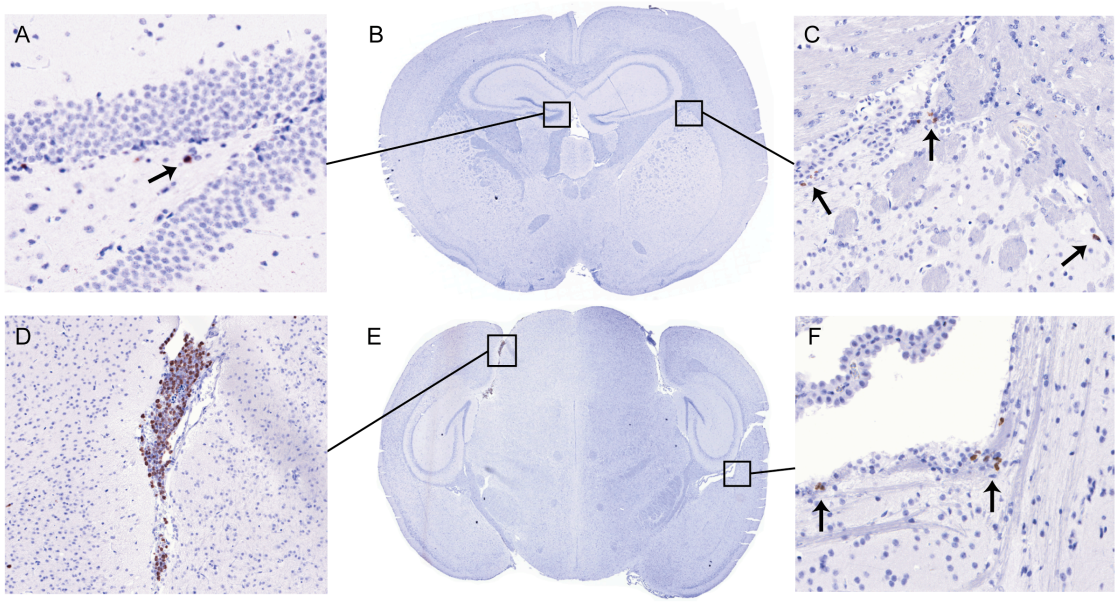

Figure 3.7. Infiltrative characteristics of low grade glioma. Diffuse and infiltrative characteristics were also seen in some low grade gliomas as illustrated by the Ki67 staining above in a 211-O xenograft. Ki67+ tumor cells can be deteced in the dentate gyrus of the hippocampus (A) and the subventricular zone (C & F). Tumor cells were also seen migrating toward the meninges of the brain (D). Abbreviations: O, oligodendroglioma.

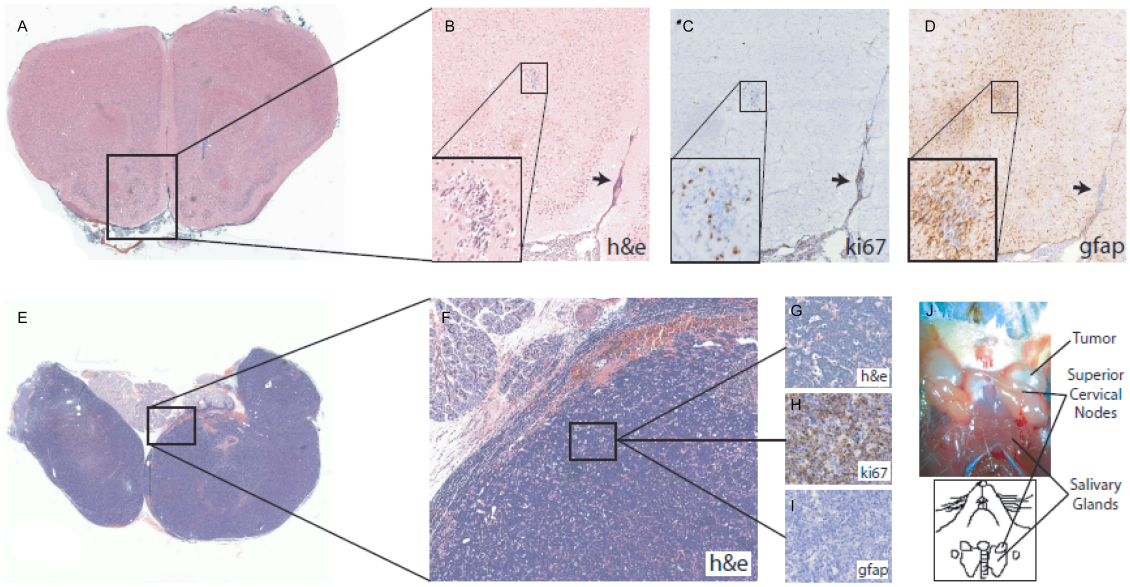

Figure 3.8. Atypical features of low grade glioma xenografts. As illustrated in the panel above from a 125-JPA xenograft, low grade tumor cells were seen not only in the brains of implanted mice (A) but also in the lymph node structures of the neck (E). Tumor foci identified by H&E (B) also expressed proliferative (C) and astrocytic (D) markers within the brain. However, the metastasized tumor component showed a different phenotype. Cells had large nucleus with very little cytoplasm (F & G). The expressed abundant Ki67 (H) suggesting active cycling of cells. But GFAP staining (I) was conspicuously absent in the metastatic component. Panel J illustrates the location of the lymph node tumors in a image and diagram of the mouse anatomy. Abbreviation: JPA, juvenile pilocytic astrocytoma.

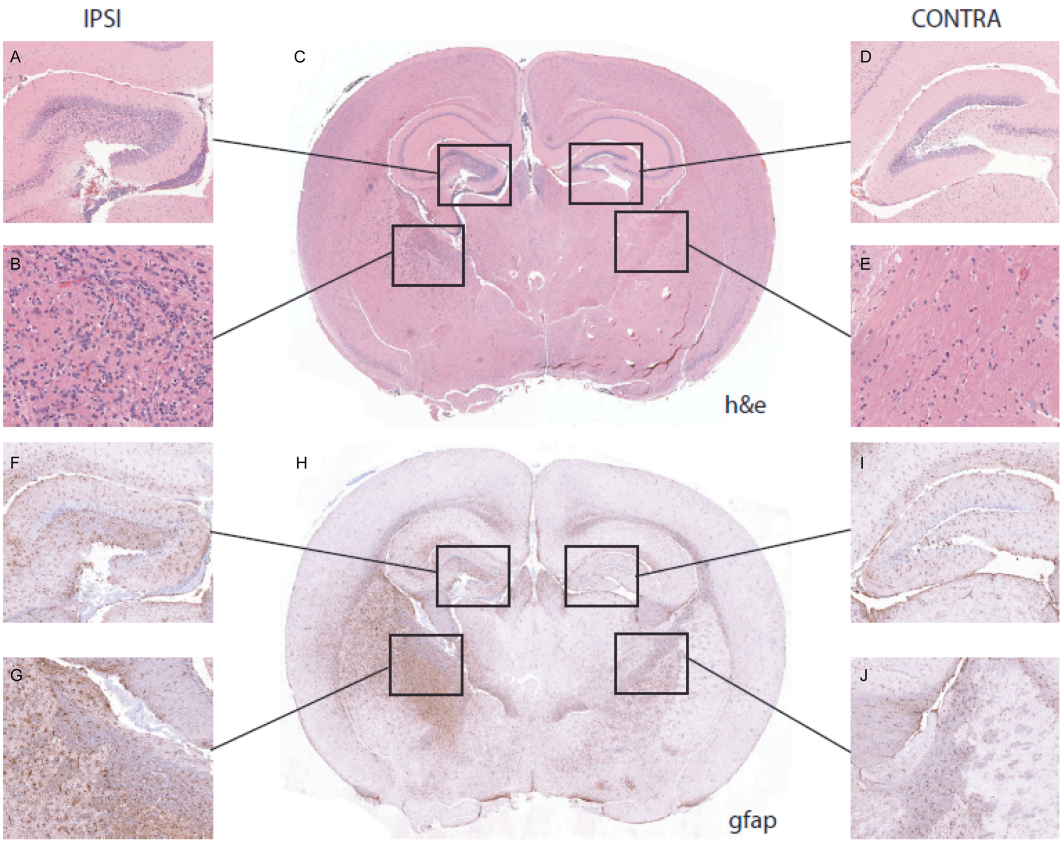

Figure 3.9. Aggressive features of low grade gliomas. Uncharacteristically aggressive features are seen in a grade II ganglioglioma (221-GG) on the ipsilateral hemisphere relative to the tumor injection site. H&E staining shows hypercellularity and atypical cellular morphology in tumor cells on the ipsilateral side (A, B, C) while the contralateral side is relatively normal (D, E). GFAP staining to mark tumor cells shows extensive staining in the ipsilateral side of the brain (F, G, H) while the corresponding contralateral side is relatively normal (I, J). Abbreviations: GG, ganglioglioma, IPSI, ipsilateral hemisphere , CONTRA, contralateral hemisphere.

patient tumor that is maintained across several passages in mice. This includes hallmark features such as cellular atypia, mitotic figures, and neo-vasculature at the tumor site.

In spite of the close similarities between our high grade glioma models and their corresponding parent tumors, a few features are lacking. One such feature that is not present in our models is necrosis (hypoxic areas surrounded by hypercellular zones called pseudopalisades) that would be expected in xenografts derived from GBM (Rong et al 2006). One possible explanation for the lack of necrosis in our model may be related to our cell selection procedure that may exclude cells responsible for the development of necrotic areas (Brat et al 2004).

The atypical characteristics observed in our low grade glioma models are interesting and suggest several possible reasons behind this phenomenon. The uncharacteristic malignant features (Fig 3.9) and metastatic growth in lymph nodes (Fig 3.8) were observed in the five low grade tumors that had successful engraftment of xenotransplanted cells. One important factor in our model that may contribute to the development of such atypical features is the use of a severly immunocompromised (NOD/SCID) host (Shultz et al 1995) that lacks both innate and adaptive immune response. Non-obese diabetic with severe combined immunodeficiency disease (NOD/SCID) mice lack function B and T cells and extremely attenuated NK cell response (McCormack et al 2005). Usage of this particular strain of mice enabled us to transplant human primary tumor cells successfully in an animal without concern for immunological rejection.

However, it is possible that low grade tumors' interaction with this particular host environment may underlie, at least in part, the aggressive and metastatic phenotype seen in the mice.

However, the aforementioned reasoning alone does not suffice to explain the atypical features since we didn't observe these characteristics in our high grade glioma models. An alternate possibility is that the low grade tumors may possess the ability or the specific cell type to develop into aggressive tumors in patients, but this phenotype is kept under control by the patient's immune surveillance system. Being transplanted into an immunocompromised host, the malignant phenotype of low grade glioma emerges. Further experiments which involve primary tumor xenotransplantation into different mouse strains that vary in the degree of immune response may provide additional insight into the biological basis for this phenomenon.

CHAPTER IV

ROLE OF THE HEDGEHOG PATHWAY IN MALIGNANT GLIOMA GROWTH

Abstract

Hedgehog pathway activity has been demonstrated in malignant glioma. However, its role in tumor growth has not been determined. Here we demonstrate that pharmacological inhibition of the Hedgehog pathway in established orthotopic malignant glioma xenografts confers a survival advantage. Pathway inhibition is measured in transplanted human tumor cells and not in host mouse brain. Correspondingly, survival benefit is observed only in tumors with an operational Hedgehog pathway. These data indicate that Hedgehog signaling regulates the growth of select malignant gliomas. We also demonstrate that Hedgehog pathway component and gene target expression segregate to CD133+ tumor initiating cells. Treated mice eventually succumb to disease, thus targeting the Hedgehog pathway in CD133+ cells produces significant, but incomplete tumor regression. Therefore, our studies suggest that more complete tumorregression may require the inclusion of other therapeutic targets, including CD133- cells.

Introduction

Malignant gliomas are characterized by invasive growth that is intractable to current therapies. One glioma cell type that confers resistance to radiation and

chemotherapy has been identified by the expression of CD133 (Prominin-1) (Bao et al 2006a, Liu et al 2006). Multipotent CD133+ cells have the capacity to initiate and passage disease in immunodeficient mice (Bao et al 2006b, Piccirillo et al 2006, Singh et al 2004b), and thus represent at least one cellular component that can maintain aggressive glioma growth. Commonly referred to as tumor-initiating or cancer stem cells, the identification of CD133+ cells in malignant glioma has prompted the characterization of regulatory molecular pathways for therapeutic strategies.

Among signaling mechanisms that regulate stem cell self-renewal and commitment (Ahn and Joyner 2005, Trowbridge et al 2006), Hedgehog (Hh) pathway activation has been demonstrated in a subset of malignant gliomas (Bar et al 2007, Clement et al 2007, Ehtesham et al 2007, Xu et al 2008). However, the role of Hh signaling in glioma growth has not been determined as prior studies involved manipulations to inhibit the Hh pathway in cultured cell lines for *in vitro* assays and prior to xenotransplantation. Glioma cells are known to undergo phenotypic and genotypic transformation in culture (Lee et al 2006). Therefore, we have initiated pathway inhibition in established glioma orthotopic xenografts from freshly resected patient specimens to test rigorously the requirement for Hedgehog signaling in tumor growth. Hh signal transduction components and small molecule modulators have been well characterized (Rohatgi and Scott 2007, Rubin and de Sauvage 2006). Smoothened, a seven-pass transmembrane domain protein that is strictly required for signal transduction (Zhang et al 2001), has been a common target of nonbiased small

molecule screens (Chen et al 2002b, Frank-Kamenetsky et al 2002). For our experiments, pharmacological inhibition was mediated by cyclopamine, a Smoothened inhibitor (Chen et al 2002a) that has been well-tolerated and effective for *in vivo* (Berman et al 2002, Karhadkar et al 2004).

Materials and Methods

Tissue procurement

Excess brain tumor specimens were obtained for research purposes from patients in accordance with a protocol approved by Vanderbilt Medical Center Institutional Review Board. Primary brain tumors were phenotyped and graded as described (Kleihues et al 1995, Kleihues et al 2002).

Immunohistochemical analysis of tumors

Immunodetection was performed for Ki67 (1:50; Dako) on paraffin-embedded sections and for anti-human nuclear epitope (1:50; Chemicon) on frozen sections as described (Ehtesham et al 2007).

CD133 immunomagnetic cell selection

Tumor samples were minced mechanically, dissociated with papain (Worthington Biochemical Corporation), and passed through a 40 μm filter. Cells were labeled with a CD133/1 (15 μg/ml; Miltenyi Biotec) antibody crosslinked to magnetic nanoparticles and subjected to immunomagnetic cell separation using the EasySep Magnetic Selection Kit (Stem Cell Technologies). Purity of the CD133-enriched population was assessed by flow cytometry after labeling enriched cells

with CD133/2-APC (Miltenyi Biotec) antibody. CD133-enriched and CD133-depleted populations were then incubated with PTCH antibody (1:200; Santa Cruz Biotechnologies, G19 Lot # J2505), followed by AlexaFluor-488 secondary antibody labeling (1:1000; Invitrogen) and analyzed by flow cytometry. Isotype-matched controls were included in the analysis to determine background signal levels. Gates thresholds were set relative to the CD133 negative-selection samples. A portion of the CD133- enriched and CD133-depleted fractions were also used for gene expression measurements using quantitative qRT-PCR.

Orthotopic xenotransplantation

10^4-10^5 CD133-enriched cells were transplanted into the striatum of NOD/SCID mice according to a protocol approved by the Vanderbilt Medical Center Institutional Animal Care and Use Committee. Mice were anesthetized with ketamine and xylazine, and securely placed on a stereotactic frame. Using aseptic surgical procedures, an incision was made in the scalp and a small burr-hole was drilled 2.5 mm lateral to the bregma. CD133-enriched cells were implanted 2.5 mm into the right striatum using a Hamilton syringe. Mice were maintained until development of neurological symptoms or signs of distress (piloerection and/or hunched posture).

Gliomasphere cell culture and Hh signaling assays

Tumor samples were dissociated (Papain, Worthington Biochemical Corporation). Cells were plated in non-treated polystyrene flasks (BD-Falcon) in

NeuroCult medium with supplements (NeuroCult® NS-A Proliferation Kit; Stem Cell Technologies), 2 g/mL heparin (Sigma), 20 ng/mL EGF (ProSpec TechnoGene), 10 ng/mL bFGF (ProSpec TechnoGene), and 1X Penicillin-Streptomycin (Invitrogen). GS were transferred to multiwell plates and cultured in triplicate for 40 hours either alone, with 50 nM SAG, or 200nM SANT1. GLI1 and GAPDH levels were measured by qRT-PCR as described below.

RNA extraction, cDNA synthesis, and qRT-PCR

Total RNA was extracted from brain tissue and GS cells with the PureLink™ RNA Mini Kit (Invitrogen). Genomic DNA was removed (RNase-Free DNase Set; QIAGEN) and purified RNA quantified (RiboGreen RNA Quantitation Kit; Invitrogen). Single-stranded cDNA was synthesized with oligo(dT) and random hexamer primers (iScript cDNA Synthesis Kit; Bio-Rad). For negative controls, reverse transcriptase was omitted from the synthesis reaction (-RT). qRT-PCR was performed in triplicate for each sample and on the corresponding –RT control with TaqMan® Fast Universal PCR Master Mix (Applied Biosystems; ABI), cDNA template, and ABI's TaqMan® Gene Expression Assay for hPTCH (Hs00970979_m1), hGLI1 (Hs00171790_m1), hGAPDH (Hs99999905_m1), hCD133 (Hs01009261_m1), hSHH (Hs00179843_m1), mGli1 (Mm00494654_m1), or mGAPDH (Mm99999915_g1). For standard curves, qRT-PCR was performed on serial dilutions of a cDNA mixture (Ehtesham et al 2007). For each amplicon, quantities were determined according to the standard curve method (User Bulletin #2, PE Applied Biosystems).

Results

Cyclopamine confers a survival benefit in established glioma xenografts

Malignant gliomas were modeled in NOD/SCID mice by orthotopic transplantation of CD133+ cells enriched from four primary tumor (PT) specimens on the day of resection (Table 1). Reflecting the heterogeneous phenotypes encompassed by WHO grades III and IV malignant glioma, the patient tumors included an anaplastic oligoastrocytoma (PT-304-AOA), a high-grade astrocytoma (PT-312-HGA), an anaplastic ganglioglioma a rare malignant glioma phenotype; PT-302-AG) and a primary GBM (PT-406-GBM). From these specimens, xenotransplanted tumors formed with variable, but generally high, rates of engraftment (69-100%) and the median length of survival ranged from 64.5-145 days.

Engraftment of transplanted cells could be visualized by hematoxylin and eosin (H&E) staining, in conjunction with immunohistochemistry for markers of cell proliferation (Ki67; Figure 4.1a, 4.1c and 4.1e; X-304-AOA, X-312-HGA, and X-406-GBM) or a panhuman nuclear epitope (anti-human nuclear; data not shown; X-302-AG) (Uchida et al 2000). Recapitulation of malignant glioma pathological features was observed and included infiltrative growth, invasion of the corpus callosum to the 5 contralateral hemisphere, and pleomorphic nuclei with mitotic figures (Figure 4.1a, 4.1c, and 4.1e). As the Hh pathway is activated in subsets of malignant glioma specimens (Bar et al 2007, Clement et al 2007, Ehtesham et al 2007, Xu et al 2008), we first sought to determine the operational status of the Hh pathway in these malignant glioma specimens.

Gliomaspheres (GS) were generated successfully from an unsorted portion for three of the four specimens (GS-304-AOA, GS-312-HGA, and GS-406-GBM) under culture conditions that are required for eliciting a Hh pathway response in glioma primary cell cultures (Ehtesham et al 2007). Addition of a Smoothened agonist (SAG, 50 nM) (Frank-Kamenetsky et al 2002) to GS-304-AOA and GS-312-HGA induced a 4-fold increase in hGLI1 mRNA expression ($p < 0.05$, Student's T-test; Figure 4.1b and 4.1d) suggesting an operational Hh pathway in these primary tumors. In contrast, GS-406- GBM cells did not respond to SAG treatment (Figure 4.1f) suggesting that this tumor lacks an operational Hh pathway. Consistent with previous Hh signaling assays in GS (Ehtesham et al 2007), basal levels of pathway activity were not reduced by treatment with a Smoothened antagonist (SANT1, 200 nM; Figure 4.1b, 4.1d and 4.1f) (Chen et al 2002b).

To determine the effect of *in vivo* Hh pathway inhibition on established tumors for which the operational status of the Hh pathway had been assayed in GS culture, X-304-AOA, X-312-HGA and X-406-GBM mice were treated with cyclopamine and assayed for survival. The survival studies were performed at initial transplantation (X-304-AOA and X-312-HGA) or first passage (X-406-GBM), depending upon adequate patient or xenograft material to generate sufficient numbers of mice. The mice were 6 randomized to receive either cyclopamine or vehicle after the first animal of a cohort became symptomatic and

Table 4.1. Clinical and pathological features of malignant gliomas

Identifier	*Pathology*	*Primary/ recurrent*	*Age*	*Gender*	*Initial Pathology*	*Prior therapy*
PT-312-HGA	High-grade astrocytoma WHO grade III	P	54	M	NA	None
PT-304-AOA	Anaplastic oligoastocytoma WHO grade III	R	44	F	Infiltrating glioma with oligodendroglial features WHO grade II	TMZ
PT-302-AG	Anaplastic ganglioglioma WHO grade III	R	28	M	Anaplastic ganglioglioma WHO grade III	Gliadel, radiation and TMZ
PY-406-GBM	Glioblastoma multiforme WHO grade IV	P	83	F	NA	None

Abbreviations: NA, not applicable; P, primary tumor; R, recurrent tumor; TMZ, temozolamide.
Shown here are the primary tumor identifier; pathology and WHO grade; age and gender of the patient; earlier therapy.

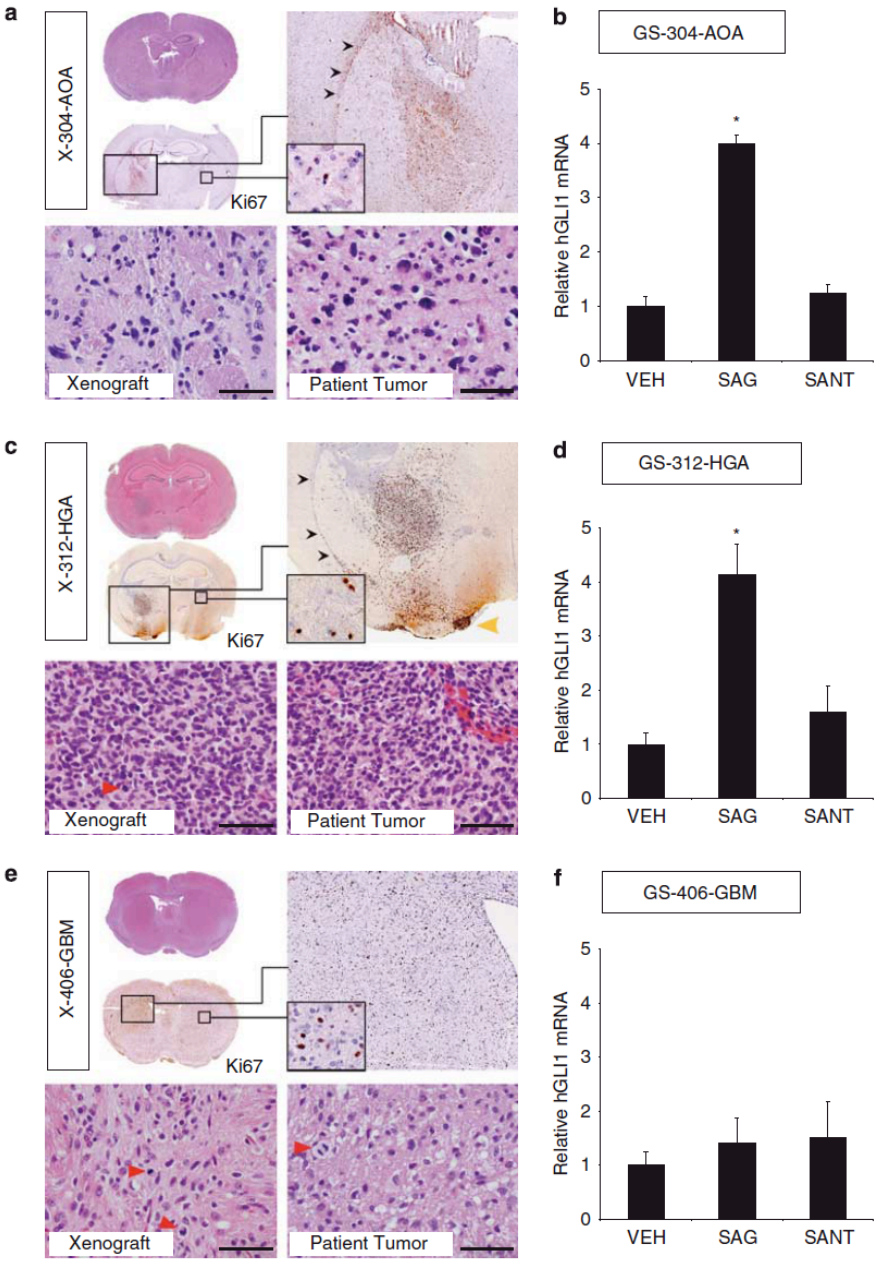

Figure 4.1. Characterization of tumor pathology in xenografts and Hedgehog (Hh) pathway responsiveness in gliomaspheres generated from malignant gliomas. Malignant glioma specimens were dissociated with papain and divided into two portions. On the day of resection, one portion was enriched for CD133þ cells by immunomagnetic selection and transplanted directly into the striatum of NOD/SCID mice. The other portion was plated in NeuroCult media with bFGF and EGF for gliomasphere (GS) culture. (a, c and e) Tumor engraftment was revealed by hematoxylin and eosin (H&E) and Ki67 staining from an anaplastic oligoastrocytoma (X-304- AOA), a high-grade astrocytoma (X-312-HGA) and a GBM (X-406-GBM). Xenotransplanted tumors recapitulated distinct features of high-grade glioma, namely infiltrative growth with invasion of the corpus callosum (black arrowheads) to involve the contralateral hemisphere (insets) and the leptomeninges (yellow arrowhead). Under high-power magnification, similar cell density and morphology was observed for each xenograft and the corresponding patient tumor (scale bar¼50 mm; red arrowheads indicate mitotic figures). (b, d and e) Hh pathway response was assayed in GS cultured for 40 h in the presence of either vehicle (VEH), a Smoothened agonist (SAG; 50 nM) or a Smoothened antagonist (SANT1; 200 nM). In triplicate cultures for each cell line and culture condition, hGLI1 levels were normalized to hGAPDH and expressed relative to vehicle-treated control GS. Relative hGLI1 mRNA levels were significantly elevated by SAG treatment in GS-304-AOA and in GS-312-HGA. In contrast, no response was elicited in GS-406-GBM. *Pp0.05.

was determined to have engraftment (Figure 4.1). Following published protocols, mice were treated by intraperitoneal injection with 25 mg/Kg/day of cyclopamine (Sanchez et al 2004, Sanchez and Ruiz i Altaba 2005). By this method, a significant survival benefit was observed only for X-304-AOA (p = 0.029, Logrank test; Figure 4.2a and data not shown). For the X-304-AOA survival study, treatment with either cyclopamine (25 mg/Kg/day; n=6) or vehicle (10% 2-Hydroxypropyl-ß-cyclodextrin; n=6) was initiated 90 days following transplantation, and was administered for 30 days. In the vehicle treatment group, 4 mice developed tumor and the median survival time as 124 days. In the cyclopamine treatment group 4 mice developed tumor and the median survival time was 190.5 days. The remaining mice (2 vehicle- and 2 cyclopamine-treated) were sacrificed 270 days after xenotransplantation and determined not to have engraftment. Thus, cyclopamine treatment conferred a median survival difference of 66.5 days (Figure 4.2a).

The lack of survival benefit in the X-312-HGA and X-406-GBM mice suggests that within these xenografts either an insufficient level or duration of pathway inhibition was achieved with daily dosing, or that the Hh pathway is not operational in these tumors. To test the first possibility, we determined the optimal dose and delivery schedule for cyclopamine. Because of limitations inherent to a direct orthotopic xenotransplantation model, namely the availability of sufficient CD133+ cells for passaging tumor in large numbers of animals and relatively slow growth kinetics, X-302-AG mice were used for dosage titration

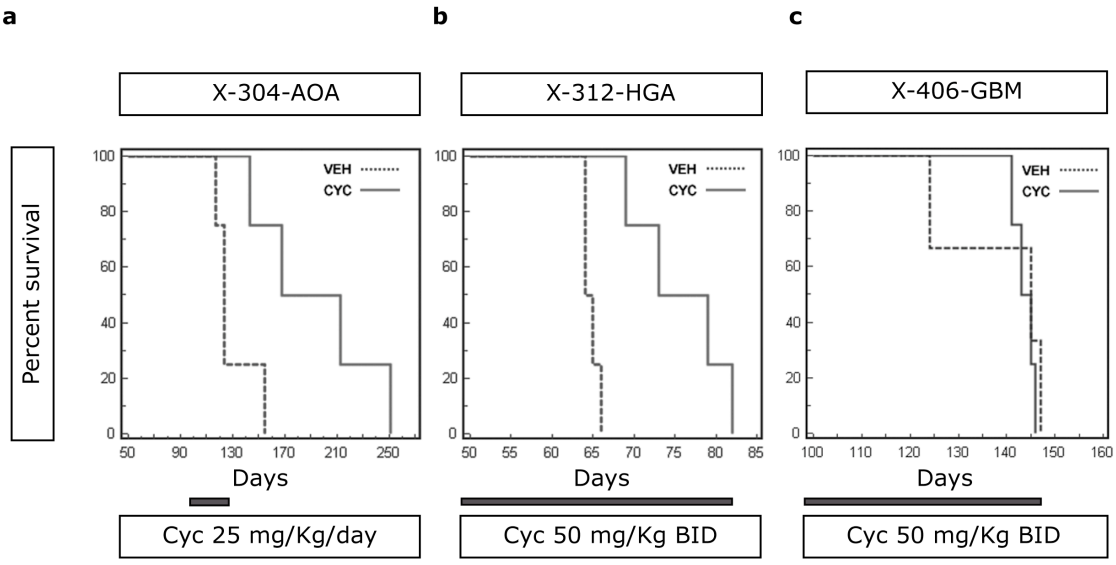

Passage	Initial		3rd		2nd	
Engraftment	67%		100%		92%	
Treatment	VEH	CYC	VEH	CYC	VEH	CYC
Sample Size	n=4	n=4	n=4	n=4	n=3	n=4
Survival (days)	124	190.5	64.5	76	145	144
Logrank test	p=0.029		p=0.0062		p=0.56	

Figure 4.2. Hedgehog (Hh) pathway inhibition confers a survival advantage. (a) 90 days after xenotransplantation, X-304-AOA mice were treated for 30 days with either cyclopamine (25 mg/kg/day) or vehicle. The median survival for cyclopamine-treated mice was 66.5 days longer than for vehicle-treated controls (P¼0.029, Logrank test). (b) Treatment was initiated in X-312-HGA mice 50 days after xenotransplantation and continued for the duration of the survival study. Cyclopamine-treated mice (50 mg/kg twice daily) had a median survival of 11.5 days longer than vehicle-treated mice (P¼0.0062, Logrank test). (c) Continuous cyclopamine treatment of X-406-GBM mice (50 mg/kg twice daily starting 100 days after xenotransplantation) did not enhance survival (P¼0.56, Logrank test). Solid gray bars indicate duration of treatment. BID, twice daily.

studies while X-312-HGA and X-406-GBM were undergoing serial passage. X-302-AG mice were injected with varying doses of 7 cyclopamine (25-100 mg/Kg) and then sacrificed at varying times after injection (1.5-16 hours). Using species-specific primers, the expression levels of human GLI1 (hGLI1) and human GAPDH (hGAPDH) were measured in a portion of the injected hemisphere by quantitative real-time PCR (qRT-PCR). We measured suppression of hGLI1 expression in X-302-AG mice treated with cyclopamine, with maximal repression at 50 mg/Kg. Furthermore, hGLI1 inhibition was transient, with maximal inhibition measured at 5 hours after injection and hGLI1 expression levels returning to baseline by 16 hours (data not shown). We therefore determined that injecting cyclopamine at 50 mg/Kg twice a day provides more complete and durable pathway inhibition than 25 mg/Kg/day. Thus to determine the operational status of the Hh pathway in X-312-HGA and X-406-GBM, mice were treated with either cyclopamine (50 mg/Kg/twice daily) or vehicle (twice daily). After one week of treatment, relative hGLI1 expression was determined by qRTPCR in vehicle (n=3 for each tumor) and cyclopamine (n=3 for each tumor) treated animals. Inhibition of hGLI1 was observed for X-312-HGA (85%, p = 0.036, Student's T-test) indicating an operational Hh pathway that can be modulated *in vivo* (Figure 4.3a). In contrast, relative hGLI1 levels were not inhibited by cyclopamine treatment in X-406-GBM (Figure 4.3a). The inability to modulate hGLI1 by small molecules in either *in vitro* (GS-406-GBM) or *in vivo* (X-406-GBM) assays (Figures 4.1f and 4.3a, respectively) suggests that the Hh pathway is not operational in this GBM.

Hh pathway activity in malignant glioma is ligand-dependant (Bar et al 2007, Clement et al 2007, Ehtesham et al 2007). Therefore, we assayed for human Shh (hSHH) mRNA expression in transplanted cells. Notably, hSHH expression can be measured in X-312-HGA, X-304-AOA and X-302-AG, but not in X-406-GBM (Figure 4.3b).

Collectively, the *in vitro* (GS-312-HGA, GS-304-AOA and GS-406-GBM), *in vivo* (X-312-HGA, X-304-AOA, X-302-AG and X-406-GBM) and hSHH expression (X-312-HGA, X-304-AOA, X-302-AG and X-406-GBM) studies identify Hh-responsive and non-responsive tumors. Furthermore, pathway activity may be directly related to active ligand production within the Hh-responsive tumors. Thus, given the evidence supporting an operational Hh pathway in X-312-HGA, we performed another survival study using more potent and durable cyclopamine dosing. By this method, continuous treatment with cyclopamine (50 mg/Kg twice daily) conferred a median survival difference of 11.5 days (p = 0.0062; Logrank test) in X-312-HGA mice (Figure 4.2b). Conversely, no difference in survival was measured in X-406-GBM mice receiving continuous treatment with a maximally inhibitory dose of cyclopamine (50 mg/Kg twice daily; Figure 4.2c).

The survival advantage from *in vivo* Hh inhibition in malignant gliomas with an operational pathway (X-304-AOA and X-312-HGA) indicates that Hh signaling regulates glioma growth. Notably, the degree of enhanced survival varies among Hh-responsive xenografts and the dosage of cyclopamine. This may relate to differences in growth kinetics of the two Hh-responsive xenografts. Survival was

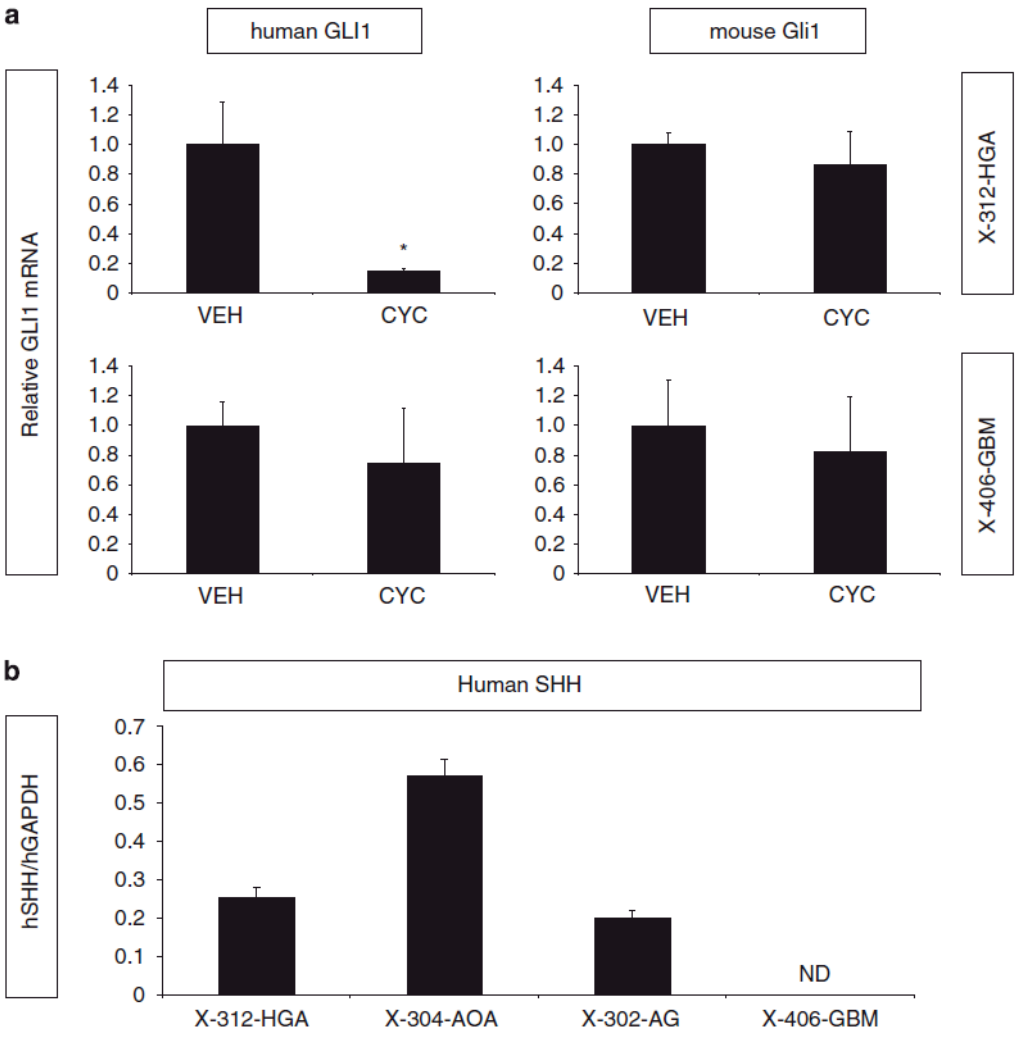

Figure 4.3. Cyclopamine treatment inhibits the Hedgehog (Hh) pathway within xenotransplanted glioma cells. (a) Mice bearing malignant glioma xenografts were treated for 1 week with either vehicle (twice daily; n¼3 for each tumor type) or cyclopamine (50mg/kg twice daily; n¼3 for each tumor type). Using species-specific primers, human GLI1 levels were normalized to hGAPDH and mouse GLi1 (mGLI1) levels were normalized to mGAPDH. Relative hGLI1 mRNA levels were significantly decreased in X-312-HGA cyclopamine-treated mice. No significant inhibition of hGLI1 was observed in X-406-GBM cyclopamine-treated mice. Relative mGLI1 mRNA levels were not altered by cyclopamine treatment in any of the malignant glioma xenografts. (b) Human Shh (hSHH) mRNA expression was detected in 6/6 X-312-HGA, 3/3 X-304-AOA, 6/6 X-302-AG and 0/6 X-406-GBM xenografts (normalized to hGAPDH and expressed as average ± s.e.m.). ND, not detected; *Pp0.05.

monitored in both treatment groups until death or endpoint criteria, and all of the mice in the cyclopamine treatment groups eventually died of disease(Figure 4.2).

Cyclopamine mediates Hedgehog pathway inhibition in transplanted human glioma cells and not in host neural parenchyma

Recent studies pertaining to epithelial-derived malignancies demonstrate that tumor-derived Shh ligand supports growth by generation of host stromal tissue (Yauch et al 2008). Using species-specific primers, we find that cyclopamine treatment modulates hGLI1 and not mGli1 expression (Figure 4.3a). These results suggest that survival benefits observed in cyclopamine- treated X-304-AOA and X-312-HGA mice are not related to Hh pathway inhibition within host neural parenchyma, but rather in transplanted glioma cells.

PTCH and GLI1 expression segregate to CD133+ cells in malignant glioma xenografts

Within malignant gliomas, expression of the Hh receptor Patched (PTCH) has been detected in cells with stem or progenitor cell features (Ehtesham et al 2007). To gain a better understanding of the glioma cellular compartments in which the Hh pathway might be operational, we evaluated PTCH expression by flow cytometry in the CD133positive- and CD133negative-selection cell populations from freshly resected tumors following immunomagnetic sorting. PTCH+ cells were highly enriched in the CD133positive-selection fraction and depleted from the CD133 negative-selection fraction from PT-312-HGA,

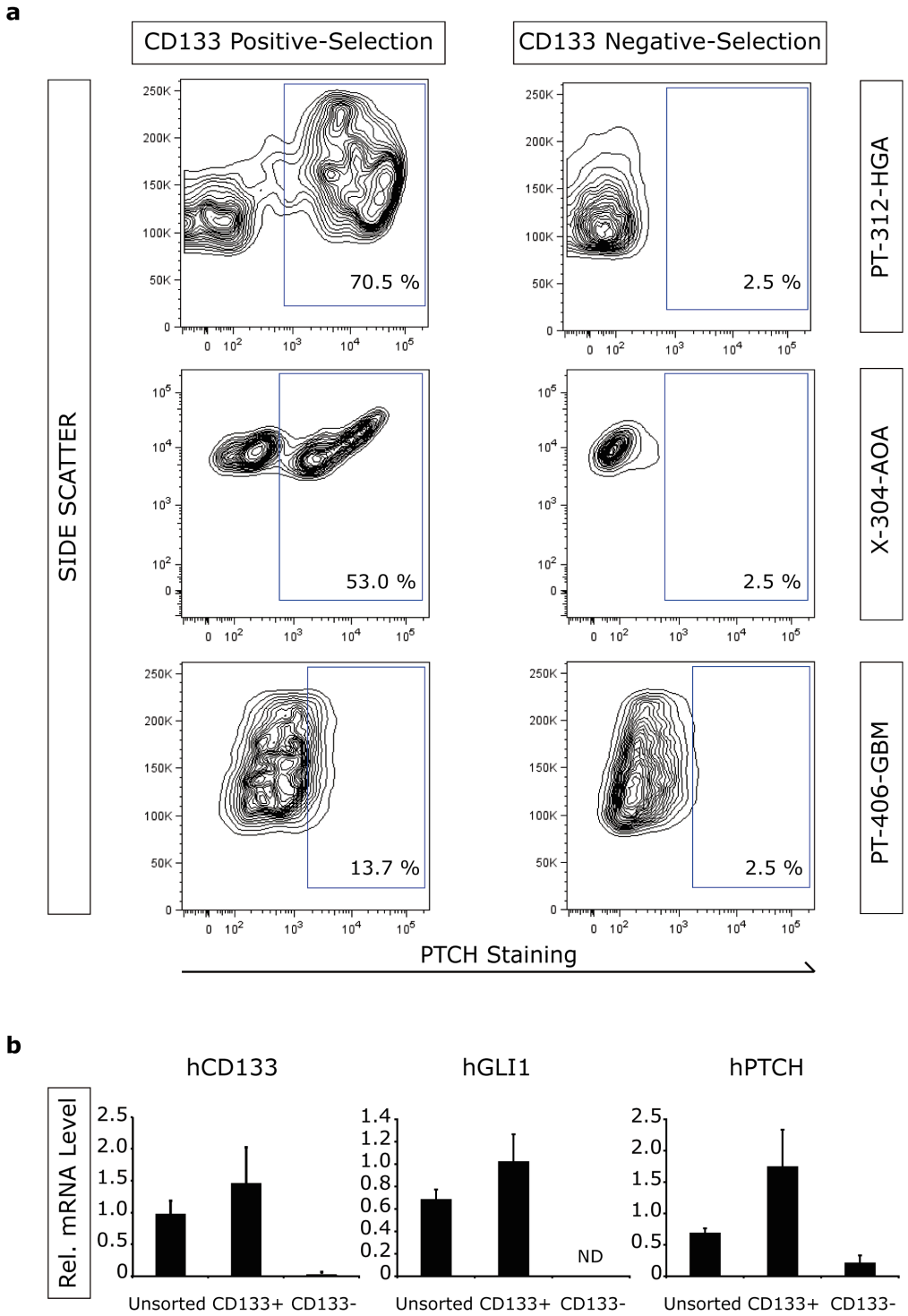

Figure 4.4. PTCH expression segregates with CD133þ cell selection within malignant glioma. (a) Expression of the Hedgehog (Hh) receptor PTCH was analysed by flow cytometry in CD133-positive and CD133-negative selection cell populations. Analysis of PT-312- HGA revealed enrichment of PTCHþ cells with CD133-positive selection, and their absence in the CD133-negative selection cell populations. Similar results were obtained with analysis of xenotransplanted tissue from X-304-AOA. In contrast, PTCH expression did not segregate with CD133-positive or -negative selection of the Hh-nonresponsive PT-406-GBM specimen. (b) Unsorted, CD133- enriched and CD133-depleted cells from X-302-AG were analysed by quantitative real-time PCR (qRT–PCR) for expression of hCD133, hGLI1, hPTCH and hGAPDH. The expression levels of hCD133, hGLI1 and hPTCH, relative to hGAPDH, were significantly elevated by CD133 positive selection. ND, not detected.

suggesting confinement of pathway responsiveness to CD133+cells (Figure 4.4a). Likewise, PTCH expression segregated with CD133+ cell selection of X-304-AOA (Figure 4.4a). In contrast, there was no significant detection or segregation of PTCH expression in CD133-selected cell populations from PT-406-GBM (Figure 4.4a), consistent with the lack of *in vitro* or *in vivo* response to pathway modulation in this tumor.

To corroborate and expand these findings, mRNA expression levels of the Hh pathway components and gene targets hPTCH and hGLI1 were measured in CD133 positive- and CD133 negative-selection cell populations following immunomagnetic sorting of X-302-AG. Compared to unsorted cells, elevated hGLI1 and hPTCH mRNA levels were detected in the CD133-enriched samples, and either not detected (hGLI1) or reduced (hPTCH) in the CD133-depleted samples (Figure 4.4b). Taken together, these data suggest pathway inhibition is mediated in CD133+ cells and that CD133- cells are not directly affected by cyclopamine treatment.

Discussion

These studies demonstrate that Hh pathway inhibition in established malignant glioma xenografts confers a significant survival advantage. Notably, survival studies performed in three xenotransplanted tumors reveal that the benefit of cyclopamine treatment is not uniform within the spectrum of malignant glioma. One key difference is the presence of an operational Hh pathway. Hh pathway activation can only be demonstrated in a subset of malignant gliomas in broad

surveys of patient samples (Bar et al 2007, Clement et al 2007, Ehtesham et al 2007, Xu et al 2008). This trend was observed in our studies of more limited sample size, by the identification of Hh responsive and non-responsive xenografts. Furthermore, and of importance for preclinical studies, the ability to modulate the Hh pathway *in vitro* has predictive value for *in vivo* modulation, as demonstrated by studies with GS-312-HGA and X-312-HGA. In support of this concept, hGLI1 levels could not be induced or suppressed in GS-406-GBM or X-406-GBM, respectively.

Another example of nonuniformity in cyclopamine response was observed between the two Hh-responsive xenografts. A longer survival benefit was measured for X-304-AOA mice with a lower dose and duration of cyclopamine treatment than for X-312-HGA. Many factors may have influenced this difference including prior treatment in the patient, tumor engraftment rate and growth kinetics, or cell selection pressures of tumor passage. With regard to tumor growth kinetics, in this study cyclopamine treatment was initiated after the first animal of a cohort developed symptoms. Thus for the more slow-growing X-304-AOA, treatment was initiated earlier in the course of disease (day 90 with a median survival of 124 days in control animals). In contrast, X-312-HGA displayed faster growth kinetics as all mice bearing the initial xenotransplant died or met criteria for sacrifice within a span of 7 days following initiation of treatment with cyclopamine at 25 mg/Kg/day. These observations suggest a greater survival benefit may be obtained with initiation of pathway inhibition earlier in the course of tumor growth. Future studies to address these differences in

cyclopamine response would benefit from the use of small-animal imaging to establish tumor engraftment and thus enable earlier treatment initiation.

Prior studies pertaining to Hh signaling and ligand-independent growth of medulloblastoma have utilized systemic doses of cyclopamine as low as 10 mg/Kg very other day to achieve meaningful pathway inhibition in the cerebellum (Sanchez and Ruiz i Altaba 2005). Our results indicate that much higher doses of cyclopamine are required for inhibiting the growth of gliomas with ligand-dependent Hh pathway activation. This difference in sensitivity is consistent with the hypothesis of “oncogene-addiction” (Weinstein and Joe 2008), such that lower doses of cyclopamine are sufficient for medulloblastoma in which tumor initiation and growth are associated with constitutive activation of the Hh pathway by loss of PTCH function (Berman et al 2002).

With regard to Hh-dependant tumor growth, signaling within either tumor cells or host tissue has been demonstrated, depending upon the tumor type (Berman et al 2002, Yauch et al 2008). Our studies indicate that in the case of malignant glioma, cyclopamine inhibits the Hh pathway in xenotransplanted cells and not in host cerebrum.

In this context, our observation that a survival advantage can be demonstrated only in mice xenotransplanted with Hh-responsive gliomas argues strongly that this benefit is a result of cyclopamine-mediated Hh pathway inhibition and not due to off-target effects. We have previously demonstrated a requirement for the addition of exogenous Hh ligand to induce a pathway response in primary GS cultures (Ehtesham et al 2007). Furthermore, the Hh

pathway in GS appears to be at a basal level as the addition of SANT1 does not reduce relative hGLI1 levels. Thus the finding from our *in vivo* model that transplanted cells generate hSHH transcript, indicates that Shh production is not maintained under these GS culture conditions. Notably, hSHH transcript is detected only in Hh-responsive xenografts and suggests that tumor cells may be a source of ligand. Whether this underlies autocrine or paracrine signaling among glioma cells has not been addressed in these studies.

Within solid and hematologic cancers, the frequency and phenotypes of tumorigenic cells in transplantation models remain to be fully characterized (Kelly et al 2007, Quintana et al 2008). However, to date CD133 is the best characterized surface marker for prospective isolation of tumor-initiating cells from malignant glioma. Despite several caveats, the concept of tumor-initiating cells provides a framework for conceptualizing the cellular heterogeneity of tumors, with a hierarchical arrangement of multipotent tumor cells giving rise to transient amplifying progenitor and ultimately postmitotic cells (Barker et al 2009, Clarke et al 2006, Zhu et al 2009). The segregation of Hh pathway components and gene targets, PTCH and GLI1, to CD133+ cells suggests that CD133- cell behavior is not subject to Hh pathway regulation. Thus, CD133- transient amplifying cells (Ligon et al 2007) might contribute to tumor growth in spite of cyclopamine treatment. Additionally, the CD133- compartment may contain other Hh-unresponsive tumor-initiating cells, as CD133- cells isolated directly from malignant gliomas have been shown to engraft in nude rats (Ogden et al 2008). Therefore, greater tumor regression might be achieved by combining Hh pathway

inhibition with therapies directed at other glioma cell types such as CD133- transient amplifying cells or other tumor-propagating cells.

Common approaches for modeling human cancer in mice include germ-line genetic modification or xenotranplantation (Fomchenko and Holland 2006, Gutmann et al 2006, Shu et al 2008, Suggitt and Bibby 2005). In these studies, a direct orthotopic glioma xenotransplantation model was utilized to reduce the potential for cell transformation in culture (Lee et al 2006). Inherent limitations of this model include availability of adequate patient material and initial engraftment rate, the number of CD133+ cells available for initial transplantation and subsequent passage and relatively slow growth kinetics. Importantly though, it has afforded the opportunity to: (i) define the presence or absence of an operational Hh pathway in an array of malignant glioma specimens; (ii) determine the optimal inhibitory dose and delivery schedule for cyclopamine; (iii) identify the glioma cell type in which Hh signaling occurs; and (iv) demonstrate enhanced survival by pharmacological inhibition of Hh signaling. These findings indicate that Hh signaling regulates the growth of select malignant gliomas, and the utility of targeting this pathway in a preclinical model.

CHAPTER V

CONCLUSIONS

Understanding mechanisms that regulate glioma growth is crucial to the development of targeted therapies. Our studies demonstrate that Hh signaling within gliomas represents an important mechanism that supports tumor growth. An important aspect of our work demonstrates that the Hh pathway is activated and operational only in distinct glioma subtypes (summarized in Figure 5.1). This distinction will be of fundamental value in designing clinical trials to investigate the use of Hh pathway inhibitiors in primary brain tumors. Furthermore, we have found that the pathway is operational in stem-like cells within specific glioma subtypes. An essential accomplishment in our studies pertaining to the biological role of Hh signaling in glioma growth was the development of a relevant preclinical model. In the process of creating direct orthotopic xenotransplantation models, we made an interesting observation. Malignant glioma primary xenografts faithfully recapitulated hallmark features of patient pathology. In contrast, low grade glioma primary xenografts demonstrated atypical features after xenotransplantation that raised interesting questions regarding the tumor-host interaction within these gliomas and illustrated a limitation of our model – namely, the use of severely immunocompromised mice that does not fully represent the immune response of host to the tumor tissue.

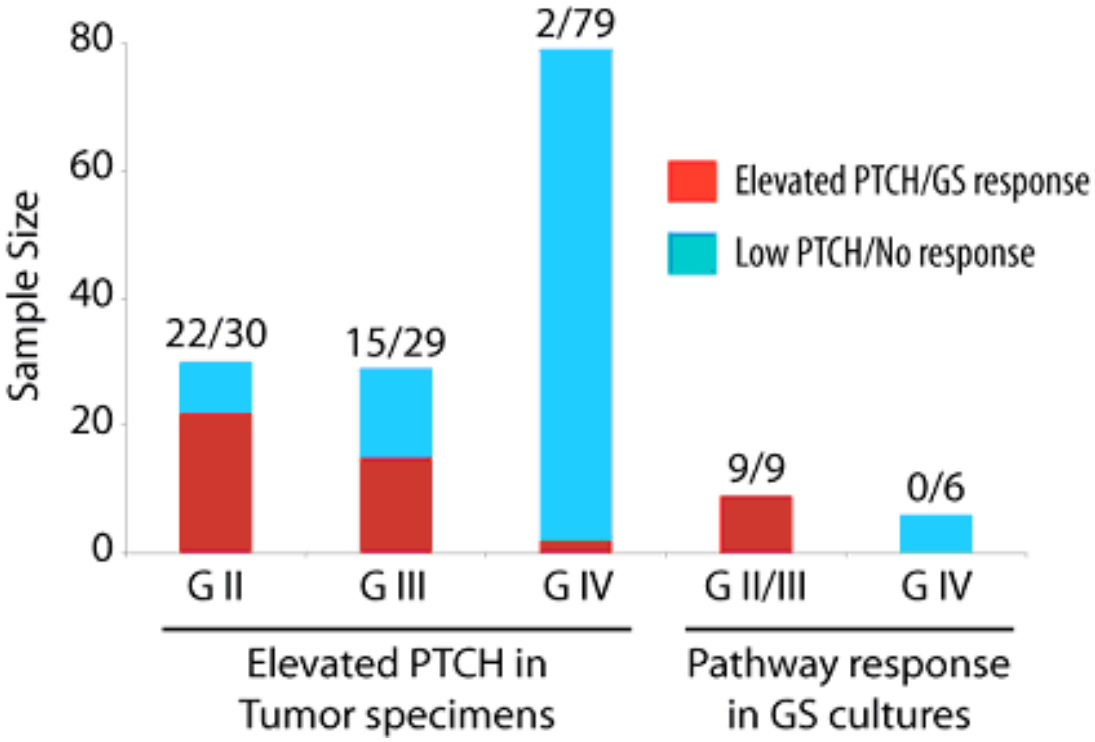

Figure 5.1. Survey of Hh pathway in malignant gliomas. PTCH mRNA expression levels in malignant glioma specimens were expressed as the fold-difference relative to control human brain tissues. On the left half of the graph are the numbers of specimens with ≥ 3-fold (red) and < 3-fold (blue) differences. To assay Hh pathway activity in primary gliomaspheres (GS), PTCH and GLI1 mRNA levels were measured following culture in the presence or absence of purified Shh protein or pathway-specific small molecule modulators. On the right half of the graph are the numbers of primary cell lines in which a significant pathway response was present (red) or absent (blue). These findings demonstrate that many WHO grade II and III gliomas contain an operational Hh pathway.

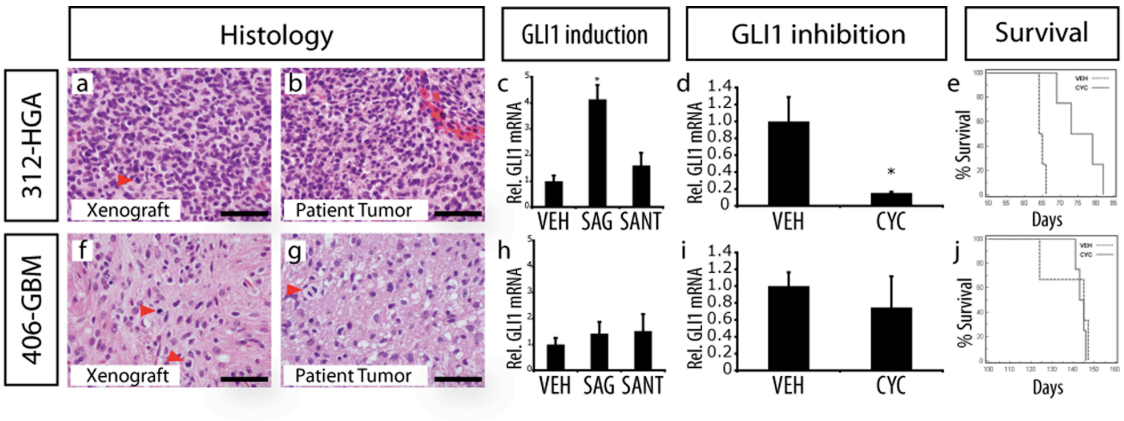

Figure 5.2. Characterization of the Hedgehog pathway in malignant gliomas. (a-j) On the day of resection, a high-grade astrocytoma (312-HGA) and a glioblastoma (406-GBM) specimen were dissociated with papain. One portion was transplanted directly into NOD/SCID mice and the other portion was plated in gliomasphere culture conditions. Similar histological features were observed for each xenograft (a and f) and the corresponding patient tumor (b and g; scale bar = 50 μm; red arrowheads indicate mitotic figures). An *in vitro* Hedgehog pathway response (GLI1 induction) was measured in gliomaspheres cultured in the presence of either vehicle (VEH), a Smoothened agonist (SAG, 50 nM) or a Smoothened antagonist (SANT1, 200 nM) for 312-HGA (c), but not for 406-GBM (h). An *in vivo* Hedgehog response (human GLI1 inhibition) was measured in mice bearing malignant glioma xenografts treated for one week with either vehicle or cyclopamine (a Smoothened antagonist; 50 mg/Kg twice daily), for 312-HGA mice (d). No significant inhibition of human GLI1 was observed in X-406-GBM mice (i). Hedgehog pathway inhibition (cyclopamine 50 mg/Kg twice daily for 30 days) confers a survival advantage for 312-HGA mice (e; p = 0.0062, Logrank test). Continuous cyclopamine treatment of X-406-GBM mice does not enhance survival (j; p = 0.56, Logrank test).

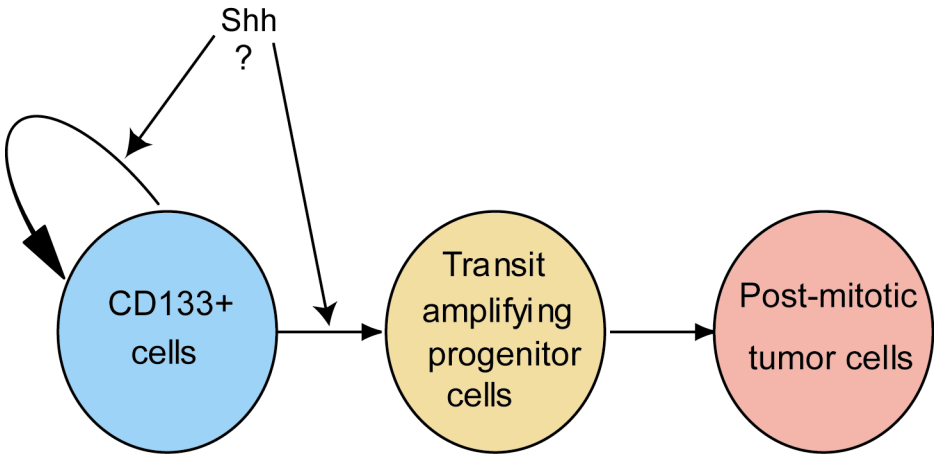

Figure 5.3. Schematic diagram of the role of Hh signaling in gliomas. The diagram illustrates that Shh signaling regulates glioma growth by acting on CD133+ cells. Its specific role in regulation CD133+ cell self-renewal or commitment mechanisms needs further investigation.

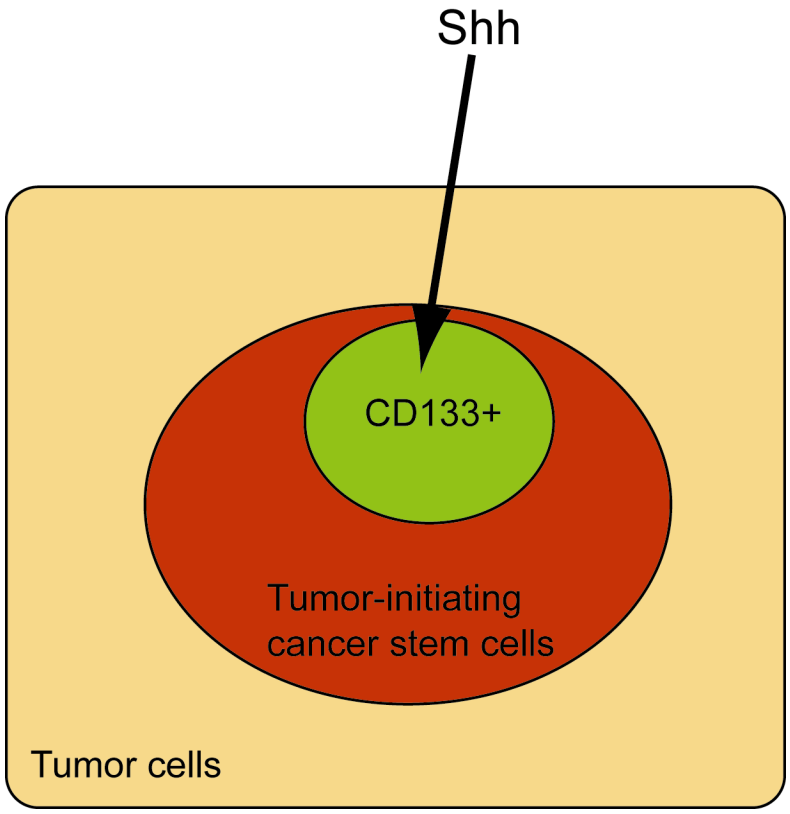

Figure 5.4. Schematic diagram of the cell type that Hh signaling regulates. The diagram illustrates that Shh signaling regulates glioma growth by acting on CD133+ cells. These cells may be part of a larger group of tumor-initiating cancer stem cells that initiates and maintains growth of tumor cells within gliomas.

One important question to consider in our studies is the reason behind the differential status of Hedgehog signaling in glioma subtypes. Our results indicate that the pathway does not play an operational role in *de novo* GBMs. This was confirmed by gene and protein expression analysis (Figure 5.1), *in vitro* signaling assays and, to a limited extent, *in vivo* preclinical studies (summarized in Figure 5.2). However, one potential alternative explanation for the disparity could be sampling variability in tissue selection. Since GBMs are known to be extremely heterogeneous in tissue histology, it is possible that the portions of tissue selected for individual experiments, analysis and xenotransplantation varied in their Hh pathway activation profile. However, this possibility seems unlikely owing to the consistent trend that was observed across several GBM samples. Additional preclinical studies using several GBM xenograft models can further support our hypothesis that the Hh pathway does not play an operational role in GBMs.

Our results suggest that regulation of CD133+ cells, and subsequently tumor growth, within GBMs could be driven by molecular mechanisms independent of the Hh pathway. For example, the EGF signaling pathway components are known to be over-expressed in GBMs suggesting the prominent role of tyrosine-receptor-kinase (TRK) signaling in GBM growth. It is possible that GBM growth relies on one or more TRK signaling mechanisms and circumvents the involvement of the Hh pathway. If so, then treatment with the Hh pathway inhibitors may have no direct effect in GBMs as suggested by our preclinical studies. However, two interesting avenues of research emerge from our data. Hh

signaling may play an early role in regulating CD133+ cells that is suppressed, or inactivated, later in the development of GBMs. This could explain the results from our data, which relies on analysis from fully established GBM patient samples. To test this question, we can use transgenic animal models that faithfully recapitulate the development stages of GBM, thus allowing us to study the kinetics of pathway activation if the Hh pathway does play a role at specific periods of GBM development. Another interesting question to explore will be the role of the pathway in the development of secondary GBM, which are a clinically and molecularly distinct entity, compared to primary GBM. As alluded to in Chapter 2, access to larger number of secondary GBM patient samples will allow us to more carefully evaluate the role of the Hh pathway in this particular glioma subtype.

Another interesting question that merits investigation relates to the specific biological role that the Hh pathway plays in regulating CD133+ cells. As illustrated in Figure 5.3, it remains to be seen whether the pathway specifically regulates the self-renewal mechanism of CD133+ cells or the commitment phase to transit-amplifying progenitor cells. Based on studies related to the pathway's role in adult neural stem cell maintenance (Ahn and Joyner 2005) one would expect the pathway to control self-renewal of CD133+ cells. However, an intriguing possibility could emerge if Hh pathway is found to regulate CD133+ cell commitment. If so, this may suggest that blocking the pathway could lead to a relative increase in the number of CD133+ cells as they continue to self-renew without transitioning towards lineage commitment. If this blockade of commitment

underlies the reason behind the survival advantage in our glioma models, then we can infer that continuous inhibition of the Hh pathway would be necessary to prevent regrowth of tumor from the accumulated CD133+ cells upon release from pathway inhibition. Moreover, this suggests that blocking CD133+ cell commitment may slowly deplete tumors from a continuous source of rapidly-dividing progenitor cells.

Additionally, our results suggest that enhanced anti-tumor benefit can be achieved by a method of combination therapy using Hh pathway inhibitors that could take many forms. For example, targeting both CD133+ and CD133- cells could ensure that all cellular components of a tumor are eliminated. Owing to the elevated multi-drug resistance mechanisms of cancer stem cells, it is possible that enhanced benefit can be achieved by pairing Hh pathway inhibitors with multi-drug transport inhibitors that can increase retention of drugs within cancer stem cells. Alternately, combining Hh pathway inhibitors with known chemotherapeutic drug regimens could eliminate the highly proliferative component of the tumor along with effects on CD133+ cells. Further elucidation of parallel molecular signaling pathways that can regulate both CD133+ and CD133- cells will allow us to explore combination therapies that exploit the dependency of tumor cells on Hh and other pathways.

Another intriguing model, illustrated in Figure 5.4, may also predict treatment success based on Hh pathway inhibition. The model suggests that CD133+ cells may form one compartment of a larger group of tumor-initiating cancer stem cell population. Cancer stem cells, as defined by their shared

properties of self-renewal, multi-potency and tumor-initiation, may consist of subgroups of cells that express different phenotypic markers and exhibit different functional characteristics. CD133 is thus far the best-characterized marker for cancer stem cells, although it may identify only one subgroup of cancer stem cells. Whether other subgroups within the cancer stem cell population respond to Hh pathway inhibition is uncertain at this point. Also unknown is the possibility that CD133+ cells are themselves progeny of these multi-potent subgroups. This raises the possibility that the incomplete tumor regression and eventual death of our cyclopamine treated mice may depend upon the inability of Hh pathway inhibition to block the growth of these other cell types. Discovering unique markers that can identify these various cell types can help us define more accurately the hierarchy that governs CD133+ cells.

In our studies, we demonstrated that the Hh pathway can be inhibited *in vivo* and leads to significant survival advantage only in treated mice bearing Hh-responsive tumors. Taken together, the results of our studies do not support the "one size fits all" hypothesis for the role of Hedgehog signaling in gliomas purported in previous reports. Our hope is that rigorous design of clinical trials based on Hedgehog pathway inhibitors will take into account this significant distinction.

REFERENCES

(2004). Cancer facts and figures. *American Cancer Society*.

Ahn S, Joyner AL (2005). In vivo analysis of quiescent adult neural stem cells responding to Sonic hedgehog. *Nature* **437:** 894-897.

Azzarelli B, Miravalle L, Vidal R (2004). Immunolocalization of the oligodendrocyte transcription factor 1 (Olig1) in brain tumors. *J Neuropathol Exp Neurol* **63:** 170-179.

Bao S, Wu Q, McLendon RE, Hao Y, Shi Q, Hjelmeland AB *et al* (2006a). Glioma stem cells promote radioresistance by preferential activation of the DNA damage response. *Nature* **444:** 756-760.

Bao S, Wu Q, Sathornsumetee S, Hao Y, Li Z, Hjelmeland AB *et al* (2006b). Stem Cell-like Glioma Cells Promote Tumor Angiogenesis through Vascular Endothelial Growth Factor. *Cancer Res* **66:** 7843-7848.

Bar EE, Chaudhry A, Lin A, Fan X, Schreck K, Matsui W *et al* (2007). Cyclopamine-mediated hedgehog pathway inhibition depletes stem-like cancer cells in glioblastoma. *Stem Cells* **25:** 2524-2533.

Barker N, Ridgway RA, van Es JH, van de Wetering M, Begthel H, van den Born M *et al* (2009). Crypt stem cells as the cells-of-origin of intestinal cancer. *Nature* **457:** 608-611.

Beachy PA, Cooper MK, Young KE, von Kessler DP, Park WJ, Hall TM *et al* (1997). Multiple roles of cholesterol in hedgehog protein biogenesis and signaling. *Cold Spring Harb Symp Quant Biol* **62:** 191-204.

Beachy PA, Karhadkar SS, Berman DM (2004). Tissue repair and stem cell renewal in carcinogenesis. *Nature* **432:** 324-331.

Becher MW, Kotzuk JA, Sharp AH, Davies SW, Bates GP, Price DL *et al* (1998). Intranuclear neuronal inclusions in Huntington's disease and dentatorubral and pallidoluysian atrophy: correlation between the density of inclusions and IT15 CAG triplet repeat length. *Neurobiol Dis* **4:** 387-397.

Berman DM, Karhadkar SS, Hallahan AR, Pritchard JI, Eberhart CG, Watkins DN *et al* (2002). Medulloblastoma growth inhibition by hedgehog pathway blockade. *Science* **297:** 1559-1561.

Berman DM, Karhadkar SS, Maitra A, Montes De Oca R, Gerstenblith MR, Briggs K *et al* (2003). Widespread requirement for Hedgehog ligand stimulation in growth of digestive tract tumours. *Nature* **425:** 846-851.

Bitgood MJ, Shen L, McMahon AP (1996). Sertoli cell signaling by Desert hedgehog regulates the male germline. *Curr Biol* **6:** 298-304.

Blanco Calvo M, Bolos Fernandez V, Medina Villaamil V, Aparicio Gallego G, Diaz Prado S, Grande Pulido E (2009). Biology of BMP signalling and cancer. *Clin Transl Oncol* **11:** 126-137.

Bleehen NM, Stenning SP (1991). A Medical Research Council trial of two radiotherapy doses in the treatment of grades 3 and 4 astrocytoma. The Medical Research Council Brain Tumour Working Party. *Br J Cancer* **64:** 769-774.

Brat DJ, Castellano-Sanchez AA, Hunter SB, Pecot M, Cohen C, Hammond EH *et al* (2004). Pseudopalisades in glioblastoma are hypoxic, express extracellular matrix proteases, and are formed by an actively migrating cell population. *Cancer Res* **64:** 920-927.

Calabrese C, Poppleton H, Kocak M, Hogg TL, Fuller C, Hamner B *et al* (2007). A perivascular niche for brain tumor stem cells. *Cancer Cell* **11:** 69-82.

Calcutt NA, Allendoerfer KL, Mizisin AP, Middlemas A, Freshwater JD, Burgers M *et al* (2003). Therapeutic efficacy of sonic hedgehog protein in experimental diabetic neuropathy. *J Clin Invest* **111:** 507-514.

Chen JK, Taipale J, Cooper MK, Beachy PA (2002a). Inhibition of Hedgehog signaling by direct binding of cyclopamine to Smoothened. *Genes Dev* **16:** 2743-2748.

Chen JK, Taipale J, Young KE, Maiti T, Beachy PA (2002b). Small molecule modulation of Smoothened activity. *Proc Natl Acad Sci U S A* **99:** 14071-14076.

Chen Y, Struhl G (1996). Dual roles for patched in sequestering and transducing Hedgehog. *Cell* **87:** 553-563.

Chiang C, Litingtung Y, Lee E, Young KE, Corden JL, Westphal H *et al* (1996). Cyclopia and defective axial patterning in mice lacking Sonic hedgehog gene function. *Nature* **383:** 407-413.

Chidambaram A, Goldstein AM, Gailani MR, Gerrard B, Bale SJ, DiGiovanna JJ *et al* (1996). Mutations in the human homologue of the Drosophila patched gene in Caucasian and African-American nevoid basal cell carcinoma syndrome patients. *Cancer Res* **56:** 4599-4601.

Clarke MF, Dick JE, Dirks PB, Eaves CJ, Jamieson CH, Jones DL *et al* (2006). Cancer stem cells--perspectives on current status and future directions: AACR Workshop on cancer stem cells. *Cancer Res* **66:** 9339-9344.

Clement V, Sanchez P, de Tribolet N, Radovanovic I, Ruiz i Altaba A (2007). HEDGEHOG-GLI1 signaling regulates human glioma growth, cancer stem cell self-renewal, and tumorigenicity. *Curr Biol* **17:** 165-172.

Colmone A, Amorim M, Pontier AL, Wang S, Jablonski E, Sipkins DA (2008). Leukemic cells create bone marrow niches that disrupt the behavior of normal hematopoietic progenitor cells. *Science* **322:** 1861-1865.

Cooper MK, Porter JA, Young KE, Beachy PA (1998). Teratogen-mediated inhibition of target tissue response to Shh signaling. *Science* **280:** 1603-1607.

Dahmane N, Ruiz i Altaba A (1999). Sonic hedgehog regulates the growth and patterning of the cerebellum. *Development* **126:** 3089-3100.

Dahmane N, Sanchez P, Gitton Y, Palma V, Sun T, Beyna M *et al* (2001). The Sonic Hedgehog-Gli pathway regulates dorsal brain growth and tumorigenesis. *Development* **128:** 5201-5212.

Daniel VC, Marchionni L, Hierman JS, Rhodes JT, Devereux WL, Rudin CM *et al* (2009). A primary xenograft model of small-cell lung cancer reveals irreversible changes in gene expression imposed by culture in vitro. *Cancer Res* **69:** 3364-3373.

De Witt Hamer PC, Van Tilborg AA, Eijk PP, Sminia P, Troost D, Van Noorden CJ *et al* (2008). The genomic profile of human malignant glioma is altered early in primary cell culture and preserved in spheroids. *Oncogene* **27:** 2091-2096.

Deleyrolle LP, Reynolds BA (2009). Isolation, expansion, and differentiation of adult Mammalian neural stem and progenitor cells using the neurosphere assay. *Methods Mol Biol* **549:** 91-101.

Ding H, Shannon P, Lau N, Wu X, Roncari L, Baldwin RL *et al* (2003). Oligodendrogliomas result from the expression of an activated mutant epidermal growth factor receptor in a RAS transgenic mouse astrocytoma model. *Cancer Res* **63:** 1106-1113.

Echelard Y, Epstein DJ, St-Jacques B, Shen L, Mohler J, McMahon JA *et al* (1993). Sonic hedgehog, a member of a family of putative signaling molecules, is implicated in the regulation of CNS polarity. *Cell* **75:** 1417-1430.

Ehtesham M, Sarangi A, Valadez JG, Chanthaphaychith S, Becher MW, Abel TW *et al* (2007). Ligand-dependent activation of the hedgehog pathway in glioma progenitor cells. *Oncogene*.

El-Jawahri A, Patel D, Zhang M, Mladkova N, Chakravarti A (2008). Biomarkers of clinical responsiveness in brain tumor patients : progress and potential. *Mol Diagn Ther* **12:** 199-208.

Fan L, Pepicelli CV, Dibble CC, Catbagan W, Zarycki JL, Laciak R *et al* (2004). Hedgehog signaling promotes prostate xenograft tumor growth. *Endocrinology* **145:** 3961-3970.

Fomchenko EI, Holland EC (2006). Mouse models of brain tumors and their applications in preclinical trials. *Clin Cancer Res* **12:** 5288-5297.

Frank-Kamenetsky M, Zhang XM, Bottega S, Guicherit O, Wichterle H, Dudek H *et al* (2002). Small-molecule modulators of Hedgehog signaling: identification and characterization of Smoothened agonists and antagonists. *J Biol* **1:** 10.

Friedman HS, McLendon RE, Kerby T, Dugan M, Bigner SH, Henry AJ *et al* (1998). DNA mismatch repair and O6-alkylguanine-DNA alkyltransferase analysis and response to Temodal in newly diagnosed malignant glioma. *J Clin Oncol* **16:** 3851-3857.

Frosina G (2009). DNA repair and resistance of gliomas to chemotherapy and radiotherapy. *Mol Cancer Res* **7:** 989-999.

Galli R, Binda E, Orfanelli U, Cipelletti B, Gritti A, De Vitis S *et al* (2004). Isolation and characterization of tumorigenic, stem-like neural precursors from human glioblastoma. *Cancer Res* **64:** 7011-7021.

Gutmann DH, Maher EA, Van Dyke T (2006). Mouse Models of Human Cancers Consortium Workshop on Nervous System Tumors. *Cancer Res* **66:** 10-13.

Hegi ME, Diserens AC, Gorlia T, Hamou MF, de Tribolet N, Weller M *et al* (2005). MGMT gene silencing and benefit from temozolomide in glioblastoma. *N Engl J Med* **352:** 997-1003.

Hemmati HD, Nakano I, Lazareff JA, Masterman-Smith M, Geschwind DH, Bronner-Fraser M *et al* (2003). Cancerous stem cells can arise from pediatric brain tumors. *Proc Natl Acad Sci U S A* **100:** 15178-15183.

Hermann PC, Huber SL, Herrler T, Aicher A, Ellwart JW, Guba M *et al* (2007). Distinct populations of cancer stem cells determine tumor growth and metastatic activity in human pancreatic cancer. *Cell Stem Cell* **1:** 313-323.

Hillier WF, Jr. (1954). Total left cerebral hemispherectomy for malignant glioma. *Neurology* **4:** 718-721.

Holland EC, Celestino J, Dai C, Schaefer L, Sawaya RE, Fuller GN (2000). Combined activation of Ras and Akt in neural progenitors induces glioblastoma formation in mice. *Nat Genet* **25:** 55-57.

Holland EC (2001). Gliomagenesis: genetic alterations and mouse models. *Nat Rev Genet* **2:** 120-129.

Horowitz ME, Etcubanas E, Christensen ML, Houghton JA, George SL, Green AA *et al* (1988). Phase II testing of melphalan in children with newly diagnosed rhabdomyosarcoma: a model for anticancer drug development. *J Clin Oncol* **6:** 308-314.

Huse JT, Holland EC (2009). Genetically engineered mouse models of brain cancer and the promise of preclinical testing. *Brain Pathol* **19:** 132-143.

Ingham PW, McMahon AP (2001). Hedgehog signaling in animal development: paradigms and principles. *Genes Dev* **15:** 3059-3087.

Johnson JI, Decker S, Zaharevitz D, Rubinstein LV, Venditti JM, Schepartz S *et al* (2001). Relationships between drug activity in NCI preclinical in vitro and in vivo models and early clinical trials. *Br J Cancer* **84:** 1424-1431.

Johnson RL, Rothman AL, Xie J, Goodrich LV, Bare JW, Bonifas JM *et al* (1996). Human homolog of patched, a candidate gene for the basal cell nevus syndrome. *Science* **272:** 1668-1671.

Jordan CT, Guzman ML, Noble M (2006). Cancer stem cells. *N Engl J Med* **355:** 1253-1261.

Karhadkar SS, Bova GS, Abdallah N, Dhara S, Gardner D, Maitra A *et al* (2004). Hedgehog signalling in prostate regeneration, neoplasia and metastasis. *Nature* **431:** 707-712.

Karpel-Massler G, Schmidt U, Unterberg A, Halatsch ME (2009). Therapeutic inhibition of the epidermal growth factor receptor in high-grade gliomas: where do we stand? *Mol Cancer Res* **7:** 1000-1012.

Katayam M, Yoshida K, Ishimori H, Katayama M, Kawase T, Motoyama J *et al* (2002). Patched and smoothened mRNA expression in human astrocytic tumors inversely correlates with histological malignancy. *J Neurooncol* **59:** 107-115.

Keime-Guibert F, Chinot O, Taillandier L, Cartalat-Carel S, Frenay M, Kantor G *et al* (2007). Radiotherapy for glioblastoma in the elderly. *N Engl J Med* **356:** 1527-1535.

Kelly PN, Dakic A, Adams JM, Nutt SL, Strasser A (2007). Tumor growth need not be driven by rare cancer stem cells. *Science* **317:** 337.

Kerbel RS (2003). Human tumor xenografts as predictive preclinical models for anticancer drug activity in humans: better than commonly perceived-but they can be improved. *Cancer Biol Ther* **2:** S134-139.

Kita M, Okawa T, Tanaka M, Ikeda M (1989). [Radiotherapy of malignant glioma--prospective randomized clinical study of whole brain vs local irradiation]. *Gan No Rinsho* **35:** 1289-1294.

Kleihues P, Soylemezoglu F, Schauble B, Scheithauer BW, Burger PC (1995). Histopathology, classification, and grading of gliomas. *Glia* **15:** 211-221.

Kleihues P, Louis DN, Scheithauer BW, Rorke LB, Reifenberger G, Burger PC *et al* (2002). The WHO classification of tumors of the nervous system. *J Neuropathol Exp Neurol* **61:** 215-225; discussion 226-219.

Klement G, Baruchel S, Rak J, Man S, Clark K, Hicklin DJ *et al* (2000). Continuous low-dose therapy with vinblastine and VEGF receptor-2 antibody induces sustained tumor regression without overt toxicity. *J Clin Invest* **105:** R15-24.

Kreisl TN (2009). Chemotherapy for malignant gliomas. *Semin Radiat Oncol* **19:** 150-154.

Kristiansen K, Hagen S, Kollevold T, Torvik A, Holme I, Nesbakken R *et al* (1981). Combined modality therapy of operated astrocytomas grade III and IV. Confirmation of the value of postoperative irradiation and lack of potentiation of bleomycin on survival time: a prospective multicenter trial of the Scandinavian Glioblastoma Study Group. *Cancer* **47:** 649-652.

Lacroix M, Abi-Said D, Fourney DR, Gokaslan ZL, Shi W, DeMonte F *et al* (2001). A multivariate analysis of 416 patients with glioblastoma multiforme: prognosis, extent of resection, and survival. *J Neurosurg* **95:** 190-198.

Lai K, Kaspar BK, Gage FH, Schaffer DV (2003). Sonic hedgehog regulates adult neural progenitor proliferation in vitro and in vivo. *Nat Neurosci* **6:** 21-27.

Laperriere N, Zuraw L, Cairncross G (2002). Radiotherapy for newly diagnosed malignant glioma in adults: a systematic review. *Radiother Oncol* **64:** 259-273.

Lee J, Kotliarova S, Kotliarov Y, Li A, Su Q, Donin NM *et al* (2006). Tumor stem cells derived from glioblastomas cultured in bFGF and EGF more closely mirror the phenotype and genotype of primary tumors than do serum-cultured cell lines. *Cancer Cell* **9:** 391-403.

Ligon KL, Fancy SP, Franklin RJ, Rowitch DH (2006). Olig gene function in CNS development and disease. *Glia* **54:** 1-10.

Ligon KL, Huillard E, Mehta S, Kesari S, Liu H, Alberta JA *et al* (2007). Olig2-regulated lineage-restricted pathway controls replication competence in neural stem cells and malignant glioma. *Neuron* **53:** 503-517.

Liu S, Dontu G, Mantle ID, Patel S, Ahn NS, Jackson KW *et al* (2006). Hedgehog signaling and Bmi-1 regulate self-renewal of normal and malignant human mammary stem cells. *Cancer Res* **66:** 6063-6071.

Machold R, Hayashi S, Rutlin M, Muzumdar MD, Nery S, Corbin JG *et al* (2003). Sonic hedgehog is required for progenitor cell maintenance in telencephalic stem cell niches. *Neuron* **39:** 937-950.

Maher EA, Brennan C, Wen PY, Durso L, Ligon KL, Richardson A *et al* (2006). Marked genomic differences characterize primary and secondary glioblastoma subtypes and identify two distinct molecular and clinical secondary glioblastoma entities. *Cancer Res* **66:** 11502-11513.

Maruo K, Ueyama Y, Inaba M, Emura R, Ohnishi Y, Nakamura O *et al* (1990). Responsiveness of subcutaneous human glioma xenografts to various antitumor agents. *Anticancer Res* **10:** 209-212.

Mason WP, Cairncross JG (2008). Invited article: the expanding impact of molecular biology on the diagnosis and treatment of gliomas. *Neurology* **71:** 365-373.

McCormack E, Bruserud O, Gjertsen BT (2005). Animal models of acute myelogenous leukaemia - development, application and future perspectives. *Leukemia* **19:** 687-706.

McGirt MJ, Than KD, Weingart JD, Chaichana KL, Attenello FJ, Olivi A *et al* (2009). Gliadel (BCNU) wafer plus concomitant temozolomide therapy after primary resection of glioblastoma multiforme. *J Neurosurg* **110:** 583-588.

Mikheev AM, Stoll EA, Mikheeva SA, Maxwell JP, Jankowski PP, Ray S *et al* (2009). A syngeneic glioma model to assess the impact of neural progenitor target cell age on tumor malignancy. *Aging Cell* **8:** 499-501.

Mokhtari K, Paris S, Aguirre-Cruz L, Privat N, Criniere E, Marie Y *et al* (2005). Olig2 expression, GFAP, p53 and 1p loss analysis contribute to glioma subclassification. *Neuropathol Appl Neurobiol* **31:** 62-69.

Nieder C, Mehta MP, Jalali R (2009). Combined Radio- and Chemotherapy of Brain Tumours in Adult Patients. *Clin Oncol (R Coll Radiol)*.

Norden AD, Drappatz J, Wen PY (2008). Novel anti-angiogenic therapies for malignant gliomas. *Lancet Neurol* **7:** 1152-1160.

Nusslein-Volhard C, Wieschaus E (1980). Mutations affecting segment number and polarity in Drosophila. *Nature* **287:** 795-801.

Ogden AT, Waziri AE, Lochhead RA, Fusco D, Lopez K, Ellis JA *et al* (2008). Identification of A2B5+CD133- tumor-initiating cells in adult human gliomas. *Neurosurgery* **62:** 505-514; discussion 514-505.

Oh S, Huang X, Chiang C (2005). Specific requirements of sonic hedgehog signaling during oligodendrocyte development. *Dev Dyn* **234:** 489-496.

Ohgaki H, Dessen P, Jourde B, Horstmann S, Nishikawa T, Di Patre PL *et al* (2004). Genetic pathways to glioblastoma: a population-based study. *Cancer Res* **64:** 6892-6899.

Palma V, Lim DA, Dahmane N, Sanchez P, Brionne TC, Herzberg CD *et al* (2005). Sonic hedgehog controls stem cell behavior in the postnatal and adult brain. *Development* **132:** 335-344.

Pandita A, Aldape KD, Zadeh G, Guha A, James CD (2004). Contrasting in vivo and in vitro fates of glioblastoma cell subpopulations with amplified EGFR. *Genes Chromosomes Cancer* **39:** 29-36.

Pang BC, Wan WH, Lee CK, Khu KJ, Ng WH (2007). The role of surgery in high-grade glioma--is surgical resection justified? A review of the current knowledge. *Ann Acad Med Singapore* **36:** 358-363.

Park CY, Tseng D, Weissman IL (2009). Cancer stem cell-directed therapies: recent data from the laboratory and clinic. *Mol Ther* **17:** 219-230.

Pathi S, Pagan-Westphal S, Baker DP, Garber EA, Rayhorn P, Bumcrot D *et al* (2001). Comparative biological responses to human Sonic, Indian, and Desert hedgehog. *Mech Dev* **106:** 107-117.

Pepinsky RB, Zeng C, Wen D, Rayhorn P, Baker DP, Williams KP *et al* (1998). Identification of a palmitic acid-modified form of human Sonic hedgehog. *J Biol Chem* **273:** 14037-14045.

Piccirillo SG, Reynolds BA, Zanetti N, Lamorte G, Binda E, Broggi G *et al* (2006). Bone morphogenetic proteins inhibit the tumorigenic potential of human brain tumour-initiating cells. *Nature* **444:** 761-765.

Porter JA, Ekker SC, Park WJ, von Kessler DP, Young KE, Chen CH *et al* (1996a). Hedgehog patterning activity: role of a lipophilic modification mediated by the carboxy-terminal autoprocessing domain. *Cell* **86:** 21-34.

Porter JA, Young KE, Beachy PA (1996b). Cholesterol modification of hedgehog signaling proteins in animal development. *Science* **274:** 255-259.

Puglisi MA, Sgambato A, Saulnier N, Rafanelli F, Barba M, Boninsegna A *et al* (2009). Isolation and characterization of CD133+ cell population within human primary and metastatic colon cancer. *Eur Rev Med Pharmacol Sci* **13 Suppl 1:** 55-62.

Quintana E, Shackleton M, Sabel MS, Fullen DR, Johnson TM, Morrison SJ (2008). Efficient tumour formation by single human melanoma cells. *Nature* **456:** 593-598.

Reifenberger J, Reifenberger G, Liu L, James CD, Wechsler W, Collins VP (1994). Molecular genetic analysis of oligodendroglial tumors shows preferential allelic deletions on 19q and 1p. *Am J Pathol* **145:** 1175-1190.

Reifenberger J, Wolter M, Weber RG, Megahed M, Ruzicka T, Lichter P *et al* (1998). Missense mutations in SMOH in sporadic basal cell carcinomas of the skin and primitive neuroectodermal tumors of the central nervous system. *Cancer Res* **58:** 1798-1803.

Reynolds BA, Weiss S (1992). Generation of neurons and astrocytes from isolated cells of the adult mammalian central nervous system. *Science* **255:** 1707-1710.

Roessler E, Belloni E, Gaudenz K, Jay P, Berta P, Scherer SW *et al* (1996). Mutations in the human Sonic Hedgehog gene cause holoprosencephaly. *Nat Genet* **14:** 357-360.

Rohatgi R, Scott MP (2007). Patching the gaps in Hedgehog signalling. *Nat Cell Biol* **9:** 1005-1009.

Rong Y, Durden DL, Van Meir EG, Brat DJ (2006). 'Pseudopalisading' necrosis in glioblastoma: a familiar morphologic feature that links vascular pathology, hypoxia, and angiogenesis. *J Neuropathol Exp Neurol* **65:** 529-539.

Rowitch DH (2004). Glial specification in the vertebrate neural tube. *Nat Rev Neurosci* **5:** 409-419.

Rubin LL, de Sauvage FJ (2006). Targeting the Hedgehog pathway in cancer. *Nat Rev Drug Discov* **5:** 1026-1033.

Sanai N, Alvarez-Buylla A, Berger MS (2005). Neural stem cells and the origin of gliomas. *N Engl J Med* **353:** 811-822.

Sanai N, Berger MS (2008). Glioma extent of resection and its impact on patient outcome. *Neurosurgery* **62:** 753-764; discussion 264-756.

Sanchez P, Hernandez AM, Stecca B, Kahler AJ, DeGueme AM, Barrett A *et al* (2004). Inhibition of prostate cancer proliferation by interference with SONIC HEDGEHOG-GLI1 signaling. *Proc Natl Acad Sci U S A* **101:** 12561-12566.

Sanchez P, Ruiz i Altaba A (2005). In vivo inhibition of endogenous brain tumors through systemic interference of Hedgehog signaling in mice. *Mech Dev* **122:** 223-230.

Sarangi A, Valadez JG, Rush S, Abel TW, Thompson RC, Cooper MK (2009). Targeted inhibition of the Hedgehog pathway in established malignant glioma xenografts enhances survival. *Oncogene*.

Sasai K, Romer JT, Lee Y, Finkelstein D, Fuller C, McKinnon PJ *et al* (2006). Shh pathway activity is down-regulated in cultured medulloblastoma cells: implications for preclinical studies. *Cancer Res* **66:** 4215-4222.

Shapiro WR, Basler GA, Chernik NL, Posner JB (1979). Human brain tumor transplantation into nude mice. *J Natl Cancer Inst* **62:** 447-453.

Sharpless NE, Depinho RA (2006). The mighty mouse: genetically engineered mouse models in cancer drug development. *Nat Rev Drug Discov* **5:** 741-754.

Shu Q, Wong KK, Su JM, Adesina AM, Yu LT, Tsang YT *et al* (2008). Direct orthotopic transplantation of fresh surgical specimen preserves CD133+ tumor cells in clinically relevant mouse models of medulloblastoma and glioma. *Stem Cells* **26:** 1414-1424.

Shultz LD, Schweitzer PA, Christianson SW, Gott B, Schweitzer IB, Tennent B *et al* (1995). Multiple defects in innate and adaptive immunologic function in NOD/LtSz-scid mice. *J Immunol* **154:** 180-191.

Singh SK, Clarke ID, Terasaki M, Bonn VE, Hawkins C, Squire J *et al* (2003). Identification of a cancer stem cell in human brain tumors. *Cancer Res* **63:** 5821-5828.

Singh SK, Clarke ID, Hide T, Dirks PB (2004a). Cancer stem cells in nervous system tumors. *Oncogene* **23:** 7267-7273.

Singh SK, Hawkins C, Clarke ID, Squire JA, Bayani J, Hide T *et al* (2004b). Identification of human brain tumour initiating cells. *Nature* **432:** 396-401.

Sipkins DA, Wei X, Wu JW, Runnels JM, Cote D, Means TK *et al* (2005). In vivo imaging of specialized bone marrow endothelial microdomains for tumour engraftment. *Nature* **435:** 969-973.

St-Jacques B, Hammerschmidt M, McMahon AP (1999). Indian hedgehog signaling regulates proliferation and differentiation of chondrocytes and is essential for bone formation. *Genes Dev* **13:** 2072-2086.

Stupp R, Mason WP, van den Bent MJ, Weller M, Fisher B, Taphoorn MJ *et al* (2005). Radiotherapy plus concomitant and adjuvant temozolomide for glioblastoma. *N Engl J Med* **352:** 987-996.

Stupp R, Hegi ME, Mason WP, van den Bent MJ, Taphoorn MJ, Janzer RC *et al* (2009). Effects of radiotherapy with concomitant and adjuvant temozolomide versus radiotherapy alone on survival in glioblastoma in a randomised phase III study: 5-year analysis of the EORTC-NCIC trial. *Lancet Oncol* **10:** 459-466.

Suggitt M, Bibby MC (2005). 50 years of preclinical anticancer drug screening: empirical to target-driven approaches. *Clin Cancer Res* **11:** 971-981.

Taipale J, Chen JK, Cooper MK, Wang B, Mann RK, Milenkovic L *et al* (2000). Effects of oncogenic mutations in Smoothened and Patched can be reversed by cyclopamine. *Nature* **406:** 1005-1009.

Takimoto CH (2001). Why drugs fail: of mice and men revisited. *Clin Cancer Res* **7:** 229-230.

Taylor MD, Liu L, Raffel C, Hui CC, Mainprize TG, Zhang X *et al* (2002). Mutations in SUFU predispose to medulloblastoma. *Nat Genet* **31:** 306-310.

Thayer SP, di Magliano MP, Heiser PW, Nielsen CM, Roberts DJ, Lauwers GY *et al* (2003). Hedgehog is an early and late mediator of pancreatic cancer tumorigenesis. *Nature* **425:** 851-856.

Theunissen JW, de Sauvage FJ (2009). Paracrine Hedgehog signaling in cancer. *Cancer Res* **69:** 6007-6010.

Trowbridge JJ, Scott MP, Bhatia M (2006). Hedgehog modulates cell cycle regulators in stem cells to control hematopoietic regeneration. *Proc Natl Acad Sci U S A* **103:** 14134-14139.

Uchida N, Buck DW, He D, Reitsma MJ, Masek M, Phan TV *et al* (2000). Direct isolation of human central nervous system stem cells. *Proc Natl Acad Sci U S A* **97:** 14720-14725.

Unden AB, Holmberg E, Lundh-Rozell B, Stahle-Backdahl M, Zaphiropoulos PG, Toftgard R *et al* (1996). Mutations in the human homologue of Drosophila patched (PTCH) in basal cell carcinomas and the Gorlin syndrome: different in vivo mechanisms of PTCH inactivation. *Cancer Res* **56:** 4562-4565.

Vescovi AL, Galli R, Reynolds BA (2006). Brain tumour stem cells. *Nat Rev Cancer* **6:** 425-436.

Villano JL, Seery TE, Bressler LR (2009). Temozolomide in malignant gliomas: current use and future targets. *Cancer Chemother Pharmacol* **64:** 647-655.

Walker MD, Green SB, Byar DP, Alexander E, Jr., Batzdorf U, Brooks WH *et al* (1980). Randomized comparisons of radiotherapy and nitrosoureas for the treatment of malignant glioma after surgery. *N Engl J Med* **303:** 1323-1329.

Watanabe T, Nobusawa S, Kleihues P, Ohgaki H (2009). IDH1 mutations are early events in the development of astrocytomas and oligodendrogliomas. *Am J Pathol* **174:** 1149-1153.

Watkins DN, Berman DM, Burkholder SG, Wang B, Beachy PA, Baylin SB (2003). Hedgehog signalling within airway epithelial progenitors and in small-cell lung cancer. *Nature* **422:** 313-317.

Wechsler-Reya RJ, Scott MP (1999). Control of neuronal precursor proliferation in the cerebellum by Sonic Hedgehog. *Neuron* **22:** 103-114.

Weinstein IB, Joe A (2008). Oncogene addiction. *Cancer Res* **68:** 3077-3080; discussion 3080.

Wendler F, Franch-Marro X, Vincent JP (2006). How does cholesterol affect the way Hedgehog works? *Development* **133:** 3055-3061.

Wetmore C, Eberhart DE, Curran T (2001). Loss of p53 but not ARF accelerates medulloblastoma in mice heterozygous for patched. *Cancer Res* **61:** 513-516.

Xu Q, Yuan X, Liu G, Black KL, Yu JS (2008). Hedgehog signaling regulates brain tumor-initiating cell proliferation and portends shorter survival for patients with PTEN-coexpressing glioblastomas. *Stem Cells* **26:** 3018-3026.

Yan H, Parsons DW, Jin G, McLendon R, Rasheed BA, Yuan W *et al* (2009). IDH1 and IDH2 mutations in gliomas. *N Engl J Med* **360:** 765-773.

Yauch RL, Gould SE, Scales SJ, Tang T, Tian H, Ahn CP *et al* (2008). A paracrine requirement for hedgehog signalling in cancer. *Nature* **455:** 406-410.

Yin AH, Miraglia S, Zanjani ED, Almeida-Porada G, Ogawa M, Leary AG *et al* (1997). AC133, a novel marker for human hematopoietic stem and progenitor cells. *Blood* **90:** 5002-5012.

Zhang XM, Ramalho-Santos M, McMahon AP (2001). Smoothened mutants reveal redundant roles for Shh and Ihh signaling including regulation of L/R asymmetry by the mouse node. *Cell* **105:** 781-792.

Zhou YH, Hu Y, Mayes D, Siegel E, Kim JG, Mathews MS *et al* (2009). PAX6 suppression of glioma angiogenesis and the expression of vascular endothelial growth factor A. *J Neurooncol*.

Zhu L, Gibson P, Currle DS, Tong Y, Richardson RJ, Bayazitov IT *et al* (2009). Prominin 1 marks intestinal stem cells that are susceptible to neoplastic transformation. *Nature* **457:** 603-607.